Biomechanical Consequences of Gait Impairment at the Ankle and Foot: Injury, Malalignment, and Co-contraction

By

Ruoli Wang

May 2012
Technical Report
Royal Institute of Technology
Department of Mechanics
SE-100 44 Stockholm, Sweden



To my grandparents 致我的祖父母们

Biomechanical consequences of gait impairment at the ankle and foot: injury, malalignment, and co-contraction

Ruoli Wang

Department of Mechanics, Royal Institute of Technology (KTH) SE-100 44 Stockholm, Sweden

ABSTRACT

The human foot contributes significantly to the function of the whole lower extremity during standing and locomotion. Nevertheless, the foot and ankle often suffer injuries and are affected by many musculoskeletal and neurological pathologies. The overall aim of this thesis was to evaluate gait parameters and muscle function changes due to foot and ankle injury, malalignment and co-contraction. Using 3D gait analysis, analytical analyses and computational simulations, biomechanical consequences of gait impairment at the ankle and foot were explored in ablebodied persons and in patient groups with disorders affecting walking.

We have characterized gait patterns of subjects with ankle fractures with a modified multi-segment foot model. The inter-segmental foot kinematics were determined during gait in 18 subjects one year after surgically-treated ankle fractures. Gait data were compared to an age- and gender-matched control group and the correlations between functional ankle score and gait parameters were determined. It was observed that even with fairly good clinical results, restricted range of motion and malalignment at and around the injured area were found in the injured limb.

Moment-angle relationship (dynamic joint stiffness) - the relationship between changes in joint moment and changes in joint angle - is useful for demonstrating interaction of kinematics and kinetics during gait. Ankle dynamic joint stiffness during the stance phase of gait was analyzed and decomposed into three components in thirty able-bodied children, eight children with juvenile idiopathic arthritis and eight children with idiopathic toe-walking. Compared to controls, the component associated with changes of ground reaction moment was the source of highest deviation in both pathological groups. Specifically, ankle dynamic joint stiffness differences can be further identified via two subcomponents of this component which are based on magnitudes and rates of change of the ground reaction force and of its moment arm. And differences between the two patient groups and controls were most evident and interpretable here.

Computational simulations using 3D musculoskeltal models can be powerful in investigating movement mechanisms, which are not otherwise possible or ethical to measure experimentally. We have quantified the effect of subtalar malalignment on the potential dynamic function of the main ankle dorsiflexors and plantarflexors: the gastrocnemius, soleus and tibialis anterior. Induced acceleration analysis was used to compute muscle-induced joint angular and body center of mass accelerations. A three-dimensional subject-specific linkage model was configured by gait data and driven by 1 Newton of individual muscle force. The excessive subtalar inversion or eversion was modified by offsetting up to ±20° from the normal subtalar angle while other configurations remain unaltered. We confirmed that in normal gait, muscles generally acted as their anatomical definitions, and that muscles can create motion in many joints, even those not spanned by the muscles. Excessive subtalar eversion was found to enlarge the plantarflexors' and tibialis anterior's function.

In order to ascertain the reliability of muscle function computed from simulations, we have also performed a parametric study on eight healthy adults to evaluate how sensitive the muscle-induced joints' accelerations are to the parameters of rigid foot-ground contact model. We quantified accelerations induced by the gastrocnemius, soleus and tibialis anterior on the lower limb joints. Two types of models, a 'fixed joint' model with three fixed joints under the foot and a 'moving joint' model with one joint located along the moving center of pressure were evaluated. The influences of different foot-ground contact joint constraints and locations of center of pressure were also investigated. Our findings indicate that both joint locations and prescribed degrees-of-freedom of models affect the predicted potential muscle function, wherein the joint locations are most influential. The pronounced influences can be observed in the non-sagittal plane.

Excessive muscle co-contraction is a cause of inefficient or abnormal movement in some neuromuscular pathologies. We have identified the necessary compensation strategies to overcome excessive antagonistic muscle co-contraction at the ankle joint and retain a normal walking pattern. Muscle-actuated simulation of normal walking and induced acceleration analysis were performed to quantify compensatory mechanisms of the primary ankle and knee muscles in the presence of normal, medium and high levels of co-contraction of two antagonistic pairs (gastrocnemius-tibialis anterior and soleus-tibialis anterior). The study showed that if the co-contraction level increases, the nearby synergistic muscles can contribute most to compensation in the gastrocnemius-tibialis anterior pair. In contrast, with the soleus-tibialis anterior co-contraction, the sartorius and hamstrings can provide important compensatory roles in knee accelerations

This dissertation documented a broad range of gait mechanisms and muscle functions in the foot and ankle area employing both experiments and computational simulations. The strategies and mechanisms in which altered gait and muscles activation are used to compensate for impairment can be regarded as references for evaluation of future patients and for dynamic muscle functions during gait.

Keywords: muscle function, gait analysis, induced acceleration, foot kinematics, dynamic joint stiffness

PREFACE

This thesis is based on the following publications that will be referred to by their roman numerals:

- Ι Ruoli Wang, Charlotte K.Thur, Elena M. Gutierrez-Farewik, Per Wretenberg, Eva Broström
 - One year follow-up after operative ankle fractures: a prospective gait analysis study with multi-segment foot model. Gait and Posture 2010; 31(2): 234-40.
- Π Ruoli Wang, Eva W. Broström, Anna-Clara Esbjörnsson, Elena M. Gutierrez-Farewik
 - Analytical decomposition can help to interpret ankle joint moment-angle relationship. Accepted in Journal of Electromyography and Kinesiology
- Ш Ruoli Wang, Elena M. Gutierrez-Farewik
 - The effect of subtalar inversion/eversion on the dynamic function of the tibialis anterior, soleus, and gastrocnemius during the stance phase. Gait and Posture 2011; 34(1):29-35.
- IV Ruoli Wang, Elena M. Gutierrez-Farewik
 - A parametric study of the rigid foot-ground contact model: effects on induced accelerations of the lower limb joints in the stance-phase. Submitted
- V Ruoli Wang, Elena M. Gutierrez-Farewik
 - Compensatory strategies in response to excessive muscle co-contraction at the ankle joint during walking. Submitted

Division of work between authors

The research project was initiated by Dr. Elena Gutierrez-Farewik (EGF) and Dr. Eva W. Broström (EWB), where EGF was the main supervisor and co-author in Paper I, II, III, IV and V. EWB acted as co-supervisor and was advisor of the work resulting in Paper I and II. Dr. Charlotte K. Thur (CKT) and Dr. Per Wretenberg (PW) were clinical advisors and co-authors in Paper I. Anna-Clara Esbjörnsson (ACE) was co-authors in paper II. Ruoli Wang (RW) continuously discussed the progress throughout the work with EGF and EWB.

Paper I

The experimental data was collected by EWB and RW. The data processing and statistical analysis were done by RW with input from EGF and EWB. 90% of the paper was written by RW and 10% by CKT with input from EWB, EGF and PW.

Paper II

The analytical and statistical analyses were done by RW and the experimental data was collected by ACE, EWB and EGF. The paper was written by RW with input from EGF, ACE and EWB.

Paper III

The simulations were done by RW and the experimental data was collected by RW and EGF. The paper was written by RW with input from EGF.

Paper IV

The simulations were done by RW and the experimental data was collected by RW and EGF. The paper was written by RW with input from EGF.

Paper V

The simulations were done by RW and the experimental data was collected by RW and EGF. The paper was written by RW with input from EGF.

LIST OF ABBREVIATIONS

ANOVA Analysis of Variance ANCOVA Analysis of Covariance

COM Center of Mass COP Center of Pressure

CMC Computed Muscle Control

CI Co-contraction Index DJS **Dynamic Joint Stiffness DOF** Degree-of-freedom DP **Descending Phase EMG** Electromyography **ERP** Early Rising Phase **FGC** Foot-ground Contact

IC **Initial Contact**

GRF

Induced Acceleration Analysis IAA

ITW Idiopathic Toe-walking ΙK **Inverse Kinematics** ID **Inverse Dynamics**

ILAR International League of Association for Rheumatology

Ground Reaction Force

JIA Juvenile Idiopathic Arthritis

Late Rising Phase LRP MTP Metatarsophalangeal

MIA Muscle Induced Acceleration

RMS Root Mean Square **ROM** Range of Motion

RRA Residual Reduction Algorithm

SDP **Short Descending Phase**

3D Three-dimensions/dimensional

TABLE OF CONTENTS

ABSTRACT	V
PREFACE	VII
LIST OF ABBREVIATIONS	XI
INTRODUCTION	1
RELATED FUNCTIONAL ANATOMY OF THE ANKLE AND FOOT BIOMECHANICS OF NORMAL GAIT GAIT AND MOTION ANALYSIS RELATED PATHOLOGIES AND DISORDERS COMPUTATIONAL METHODS IN MUSCULOSKELETAL COORDINATION	1 4 7 9 11
SPECIFIC AIMS	15
MATERIALS AND METHODS	17
SUBJECTS GAIT ANALYSIS DYNAMIC JOINT STIFFNESS (STUDY II) INDUCED ACCELERATION ANALYSIS (STUDIES III-V) MUSCULOSKELETAL MODEL SIMULATION PROCEDURE DATA ANALYSIS	17 18 19 20 21 22 24
RESULTS AND DISCUSSION	27
MULTI-SEGMENT FOOT KINEMATICS (STUDY I) DYNAMIC JOIONT STIFFNESS AND ITS SUB-COMPONENTS (STUDY II) INDUCED JOINT ANGULAR ACCELERATIONS AND BODY CENTER OF MASS ACC (STUDY III-V) GENERAL DISCUSSIONS	27 28 CELERATIONS 30 31
CONCLUSIONS AND FUTURE WORK	35
SUMMARY OF PAPERS	37
PAPER II PAPER III PAPER IV PAPER V	37 37 37 37 37

Ruoli Wang

ACKNOWLEDGEMENT	39
REFERENCE LIST	41
APPENDIX	51
PAPER I-V	

INTRODUCTION

The study of human gait can be traced back thousands of years and Aristotle was attributed with the earliest recorded comments about human walking (Harris et al., 2006). It was not until the renaissance that further progress was made through the experiments and theorizing of Giovanni Borelli (Borelli, 1989). During the later part of the 18th century and early part of 19th century, a series of French physiologists made observations of human walking. They, however, only addressed the understanding of human walking either in mechanics or in physiology (Baker, 2007). Weber brothers (1836) were the pioneers who addressed both mechanics and physiology problems and first published foot temporal and stride parameters using experimental measurements (Basmajian and Licht, 1978). Eadweard Muybridge (1925) and Leland Stanford used an array of sequenced cameras attempt to settle a bet to whether horses have a period of 'double float' while galloping. Braune and Fischer (1987) further developed the first 3D movement analysis and Amar (1916) first used a pneumatic system to develop a three-component forceplate. Since then, studies using motion analysis have become numerous; a current PubMed search using keywords movement analysis, motion analysis or gait analysis returns over 149,000 items. The focus in this thesis is on the foot and ankle during gait.

The human foot, the only part of the body that acts on an external surface in upright, unsupported positions, supports and balances the body during gait. With muscle coordination, the foot can be compliant to cope with uneven ground surfaces to achieve a smooth motion and maintain dynamic stability. Ankle injuries, foot pain and muscle dysfunctions are common and stem from the large impact forces and rotational moments during weight-bearing activities (Smith, 1996). As the distal end of the lower extremity, its position or movement can influence the position, movement or loading at the knee or hip of either limb and the back (Hamill and Knutzen, 2006). This thesis includes three major parts: Part I (Study II) is the experimental gait analysis of foot kinematics in patients with ankle fractures. Part II (Study II) is the analytical decomposition analysis of ankle dynamic joint stiffness (moment-angle relationship) in able-bodied children and children with juvenile idiopathic arthritis and idiopathic toe-walking. Part III (Studies III, IV and V) studies the influence of abnormal foot kinematics and ankle antagonistic muscle pair co-contraction on individual muscle functions during walking using simulation.

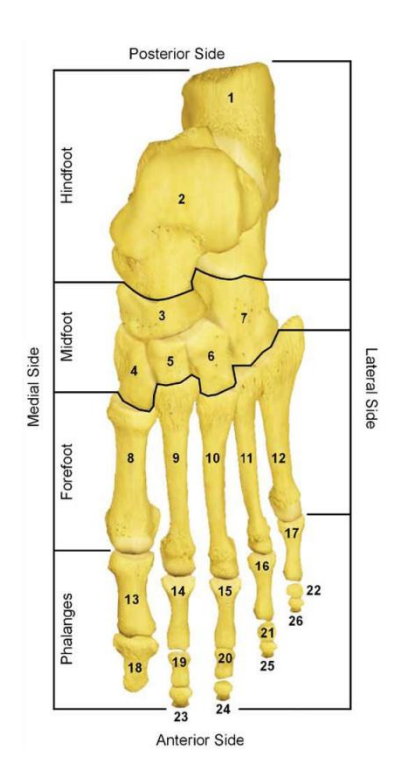
RELATED FUNCTIONAL ANATOMY OF THE ANKLE AND FOOT

The foot and ankle make up a complex anatomical structure consisting of 26 irregularly shaped bones, 30 synovial joints, and more than 100 ligaments, tendons, and muscles acting on the segments (Hamill and Knutzen, 2006). The foot is considered to have four subdivisions: the hindfoot, midfoot, forefoot, and phalanges (Fig 1). Other than the talocrural joint (ankle), most of the motion in walking occurs at three of the synovial joints: the subtalar, midtarsal, and metatarsophalangeal joints (MTP) (Perry and Burnfield, 2010).

Talocrural joint

The ankle or talocrural joint is comprised of 3 bones: tibia, fibula and talus (Fig 2). The articulations of this joint complex are between the dome of the talus and the tibia plafond, the medial facet of the talus and the medial malleolus, and the lateral facet of the talus and the lateral malleolus respectively. Although the ankle joint is commonly considered as a hinged synovial joint allowing only dorsiflexion/plantarflexion movement, the anatomical axis of the joint has been demonstrated horizontal and oblique to the frontal plane of the foot due to outward rotation of the lower end of the tibia (Wright et al., 1964). Moreover, movement of the foot at the ankle joint rarely occurs alone; it is invariably combined with motion about the subtalar and midtarsal joints (Palastanga et al., 2006). The lateral and deltoid ligaments have important roles in maintaining stability in the articular motions.

1



Index	Name	Segment	Index	Name	Segment
1	Calcaneus	Hindfoot	9	Second metatarsal	Forefoot
2	Talus	Hindfoot	10	Third metatarsal	Forefoot
3	Navicular	Midfoot	11	Fourth metatarsal	Forefoot
4	Medial cuneiform	Midfoot	12	Fifth metatarsal	Forefoot
5	Intermediate cuneiform	Midfoot	13-17	Proximal phalanges	Phalanges
6	Lateral cuneiform	Midfoot	18	Distal phalanges	Phalanges
7	Cuboid	Midfoot	19-22	Middle phalanges	Phalanges
8	First metatarsal	Forefoot	23-26	Distal phalanges	Phalanges

Figure 1: Bones in the foot, modified from Abboud (Abboud, 2002)

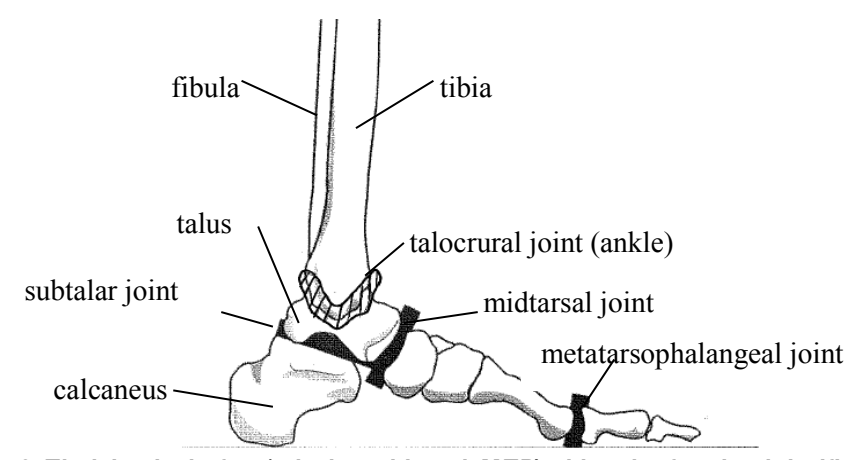


Figure 2: The joints in the foot (subtalar, midtarsal, MTP) with major functional significance during walking, modified from Perry and Burnfield (2010)

Subtalar joint

The subtalar joint is situated between the talus and the calcaneus (Fig 2). With the ankle joint, the oblique orientation of the subtalar joint axis (from the posterior lateral plantar surface to the anterior dorsal medial surface of the talus (Fig 3) allows the foot to move relative to the tibia in a complex manner (Czerniecki, 1988), which is usually defined as pronation and supination. The prime function of the subtalar joint is to absorb the rotation of the lower extremity during the support phase of gait (Hamill and Knutzen, 2006).

Midtarsal and metatarsophalangeal joints

The midtarsal joint is the junction of the hindfoot and forefoot and contributes to the shock absorption of forefoot contact (Fig 2). The MTP joint is the toe break, which allows the foot to roll over the metatarsal heads rather than the tips of the toes. The five metatarsal heads provide a broad area of support across the forefoot (Perry and Burnfield, 2010).

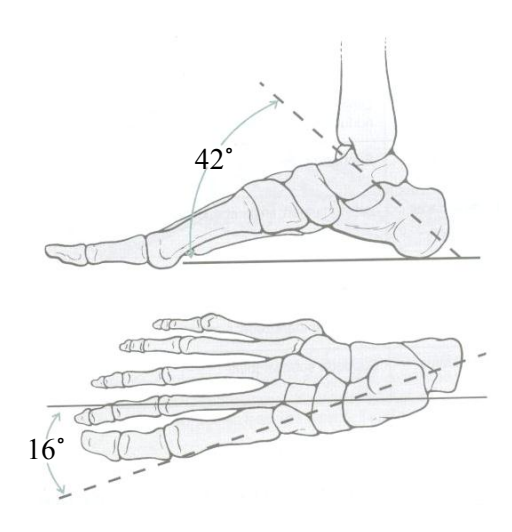


Figure 3: The axis of the subtalar joint, modified from Hamill and Knutzen (2006)

Ankle dorsiflexors and plantarflexors

Twenty-three muscles act on the ankle and the foot (Fig 4), and play important roles in sustaining impacts of very high magnitude, and in generating (contracting concentrically) and absorbing energy (contracting eccentrically) during movement (Hamill and Knutzen, 2006). Ankle plantarflexors refer to the muscles which can extend the ankle resulting in the forefoot moving away from the body, while ankle dorsiflexors can flex the ankle resulting in the forefoot moving towards the body. The gastrocnemius together with the soleus are the chief plantarflexors of the ankle joint. The gastrocnemius spans the knee joint, so it is also a powerful knee flexor. The other plantarflexor muscles produce only 7% of the remaining plantarflexor force (DiStefano, 2009). The most medial dorsiflexor is the tibialis anterior, whose tendon is farthest from the joint, thus giving it a significant mechanical advantage as a powerful dorsiflexor (DiStefano, 2009). Previous studies reported that the gastrocnemius, soleus and tibialis anterior also have inversion leverage of the subtalar joint (Czerniecki, 1988; Hamill and Knutzen, 2006).

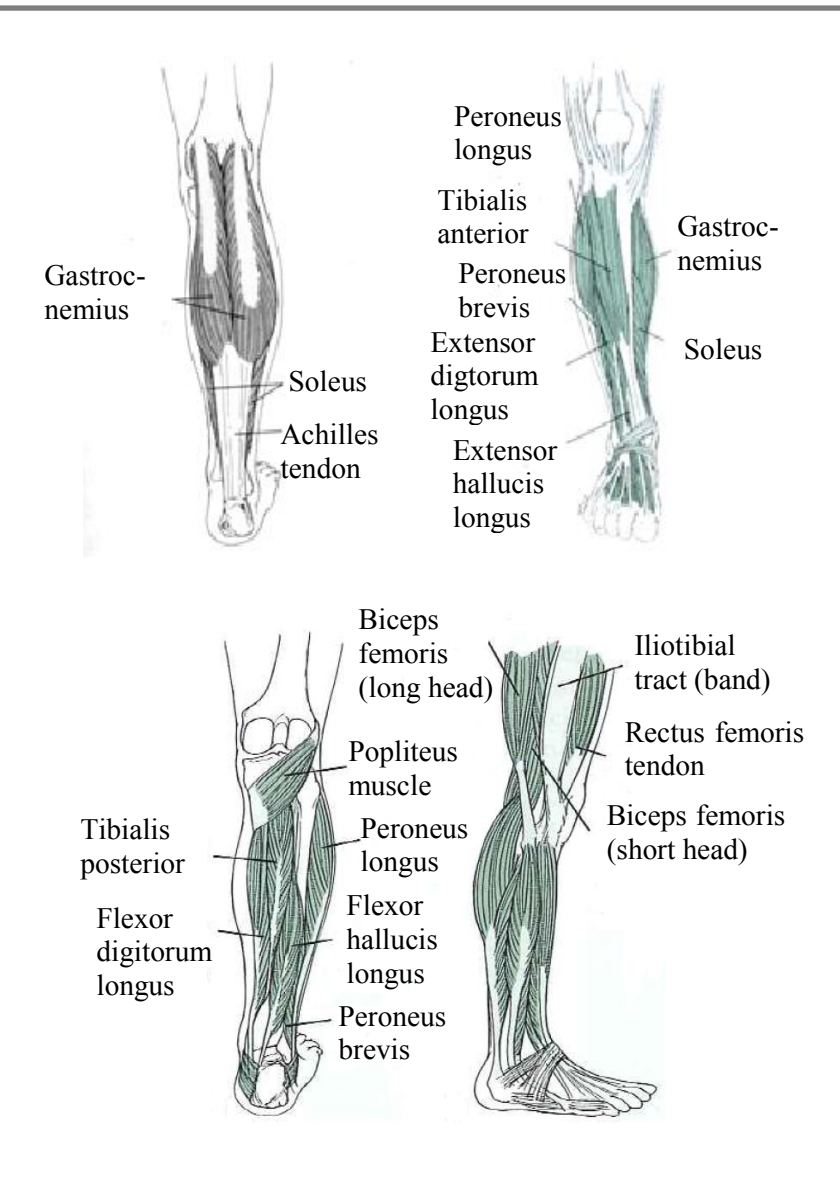


Figure 4: The ankle and knee muscles, modified from Hamill and Knutzen (2006)

BIOMECHANICS OF NORMAL GAIT

Normal gait cycle can be divided into stance and swing phases. The stance phase is approximately the first 60% of the gait cycle and starts with initial contact (IC) when foot touches the floor. Loading response (0-10% of gait cycle) is the initial double stance which ends when the contralateral foot is lifted for swing (Perry and Burnfield, 2010). Following loading response is mid-stance (10-30% of gait cycle) and terminal stance (30-50% of gait cycle), which are the single-limb support intervals. The final phase (50-60% of gait cycle) of stance is pre-swing, the second double support in the stance phase.

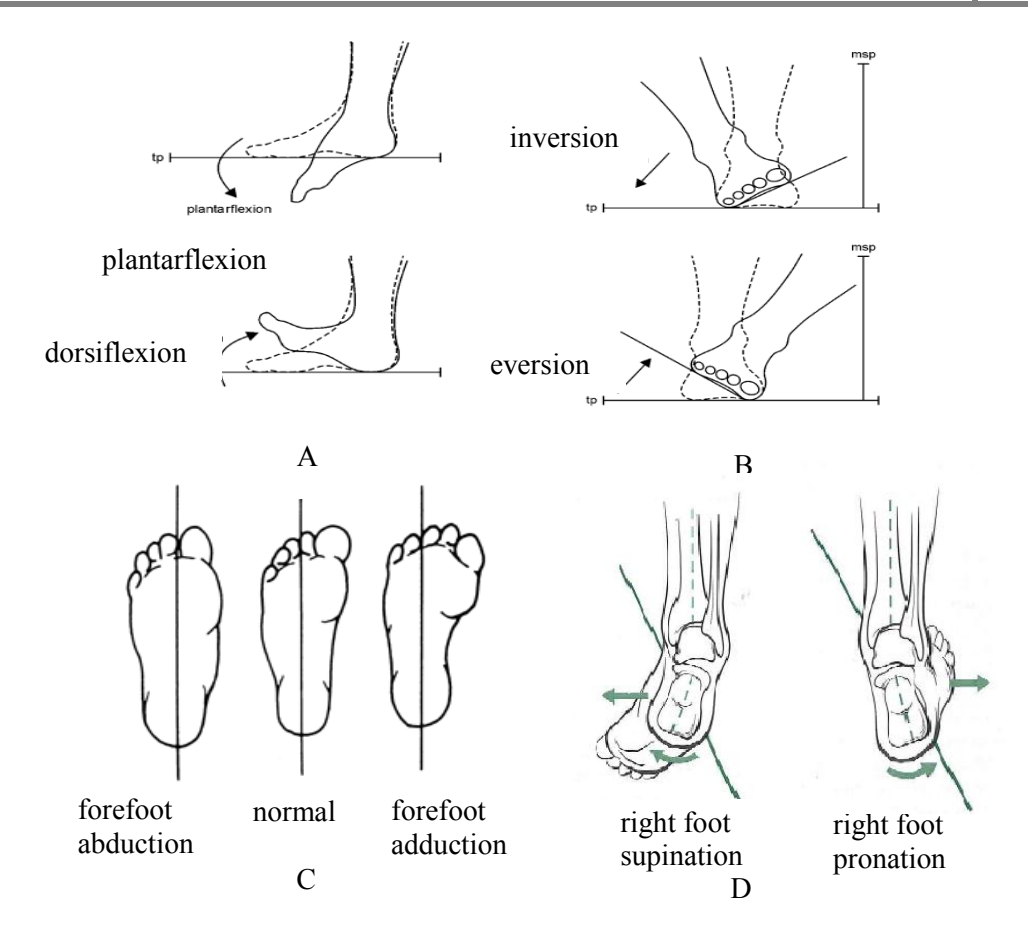


Figure 5: Foot motion definition: (A) plantarflexion-dorsiflexion (B) inversion-eversion (C) forefoot adduction-abduction (D) supination-pronation (A, B, C modified from Abboud 2002, D modified from Hamill and K nutzen 2006)

Motion definition

Conventionally, human movements are described based on three cardinal planes of the body. The sagittal plane bisects the body into right and left; the frontal plane bisects the body into anterior and posterior; the transverse plane bisects the body into superior and inferior. Six basic movements occur in varying combinations in the joints of the body. Flexion/extension is the bending/straightening movement in the sagittal plane, in which the relative angle of the joint between two adjacent segments decreases/increases. Abduction is the movement away from the midline of the body or segment and adduction is the return movement back toward the midline of the body or segment in the frontal plane. Internal rotation is the rotating movement of a segment's anterior surface toward the midline of the body and external rotation, the opposite movement in which a segment's anterior surface moves away from the midline. Although several specialized movement names are assigned to the foot movement, they are still generally regarded in the basic planes (Fig 5). Plantarflexion is the movement when the distal aspect of the foot is angled downwards in the sagittal plane away from the tibia, and dorsiflexion is the movement when the distal aspect is angled towards the tibia in the sagittal plane. Hindfoot inversion takes place in the frontal plane when the medial border of the foot lifts so that the sole of the foot faces towards the other foot. Hindfoot eversion is the opposite movement of the hindfoot. Forefoot adduction is the movement when the distal aspect of the forefoot is angled towards the midline of the body in the transverse plane. Forefoot abduction is the movement when the distal aspect is angled away from the midline of the body. In orthopedics, a varus deformity is a term for the inward angulation of the distal segment of a bone or joint. The opposite of varus is called valgus. Common confusion exists over the use of the terms inversion and eversion with pronation and supination. Foot pronation consists of a combination of ankle dorsiflexion, calcaneal eversion, and forefoot abduction.

Foot supination is the opposite of pronation, with ankle plantarflexion, calcaneal inversion, and forefoot adduction (Hamill and Knutzen, 2006).

The foot's movement during the stance phase

At IC, the ankle is almost neutral or slightly plantarflexed and the subtalar joint is inverted. In a short period afterwards, the foot is passively plantarflexed in a smooth, regulated manner such that the ankle joint plantarflexion is stopped synchronously with the forefoot making contact with the ground (Root et al., 1977). During the loading-response, only the lateral side of the foot makes contact with the ground so to transfer weight to the forefoot. The effect of the ground reaction force (GRF) on the lateral side of the forefoot tends to evert the forefoot (Schwartz et al., 1964). The ankle changes its direction towards dorsiflexion after foot-flat and the tibia becomes the moving segment. Ankle dorsiflexion continues throughout mid-stance and reaches its maximum in terminal stance. At the same time, the forefoot gradually moves towards inversion. The subtalar joint slowly reverses eversion toward inversion throughout the terminal stance, particularly during toe-rise and reaches its peak in pre-swing (Wright et al., 1964). There is a rapid ankle plantarflexion following terminal double support which reaches the maximum at the end of the stance phase (Perry and Burnfield, 2010).

Brief muscle roles in stance

As described by Perry and Burnfield (2010), during the stance phase, the muscle functions are primarily for providing weight-bearing stability, shock absorption, and progression over the supporting foot. In particular, the progression of gait is assisted by four foot rockers: heel rocker, ankle rocker, forefoot rocker and toe rocker (Fig 6).

Ankle Muscles: After IC, in response to the large external plantarflexion moment generated by the GRF, ankle dorsiflexors (tibialis anterior, extensor digitorum longus, and extensor hallucis longus) decelerate the ankle plantarflexion. This dynamic response also contributes to limb progression, as the tibia actively advances while the forefoot descends. Following the forefoot floor contact, the GRF advances forward along the foot so to create a large external dorsiflexion moment. The plantarflexors (soleus and gastrocnemius primarily) react eccentrically to restrain the rate of ankle dorsiflexion. In the toe-rocker, the soleus and gastrocnemius' contractions reduce rapidly with the rapid decline of GRF since the body weight transfers to the other limb. The tibialis anterior and toe extensors begin to activate at the end of the toe-rocker to decelerate the ankle plantarflexion and prepare for foot lifting in initial swing.

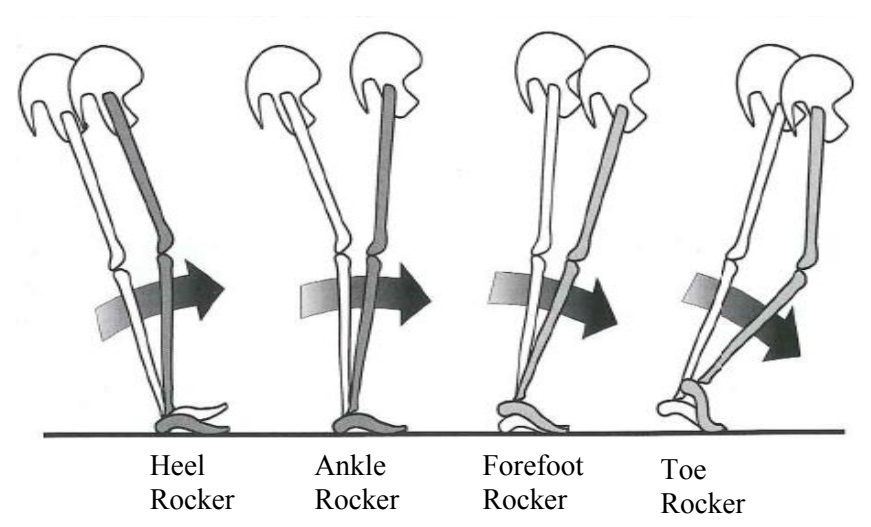


Figure 6: Four rockers in stance phase. The arrow indicates the direction of motion, modified from Perry and Burnfield (2010).

Knee Muscles: The vasti muscles (knee extensors) activate eccentrically during heel-rocker to decelerate knee flexion and absorb shock while also maintaining knee stability. The vasti activity ceases by the middle of mid-stance when the primary responsibility of limb control transfers to the ankle plantarflexors. The knee flexors (hamstrings) act mainly to protect potential knee hyperextension with declining activity levels.

Hip Muscles: The hip extensors (adductor magnus and lower gluteus maximus) contract intensively to control hip flexion, and the hip abductors (upper gluteus maximus and gluteus medius) activate to enhance pelvis stability during heel-rocker. The hip muscles are otherwise largely inactive during the rest of the stance phase.

Using musculoskeletal modeling and dynamic simulations, comprehensive muscles' functions can be quantified during walking. Muscles generally function according to their anatomical definition. Ankle dorsiflexors were found to support the body while slowing forward progression during heel-rocker. Hip and knee extensors (vasti and gluteus maximus) were found to provide much of the body's vertical support while slowing forward progression in the first half of the gait cycle (Pandy, 2001; Neptune et al., 2004; Liu et al., 2006; Kepple et al., 1997). Ankle plantarflexors were identified as primary contributors of support and forward progression during the late half of stance (Gottschall and Kram, 2003; Kepple et al., 1997; Pandy, 2001; Neptune et al., 2004). Fewer studies have focused on the muscle contributions in planes other than sagittal, probably since peak forces in these planes are much smaller than in the vertical and fore-aft directions. Pandy *et al.* reported that muscles that generate vertical support and forward progression (vasti, soleus and gastrocnemius) also accelerate body center of mass (COM) laterally, along with hip adductors (adductor magnus, adductor longus and adductor brevis) and ankle evertors (peroneus brevis and peroneus longus). The hip abductors and ankle invertors (tibialis posterior, flexor digitorum longus and flexor hallucis longus) control the medial-lateral balance by accelerating the COM laterally (Pandy et al., 2010).

Studies have also shown that the influence of muscle force is not isolated to the joints it crosses - the influence on remote joints must also be considered. This was referred to as dynamic coupling – a muscle can accelerate a joint which it does not cross (Zajac and Gordon, 1989). For example, considerable contributions to hip extension have been found from the tibialis anterior, soleus and gastrocnemius (Jonkers et al., 2003). Moreover, analysis of muscle contributions has also indicated that synergistic muscles can function differently over different joints. For instance, the gastrocnemius and soleus have been shown to function synergistically at the ankle joint, but with opposite effects at the knee in toe-rocker. The soleus can generate knee extension acceleration while the gastrocnemius can accelerate knee flexion (Fox and Delp, 2010a; Goldberg et al., 2003; Neptune et al., 2001).

GAIT AND MOTION ANALYSIS

Contemporary gait analyses focus primarily on the measurement of joint kinematics and kinetics, electromyography (EMG), oxygen consumption and foot plantar pressures. Gait analysis has been very helpful in diagnostic evaluations of some motion disorders and can provide important complementary information prior to invasive treatment. Gait analysis used in this thesis involves markers placed on specific anatomic landmarks. The markers are covered in a retro-reflective material which can reflect the light from infrared cameras to sensors mounted on the camera. The marker positions are used to describe the three-dimensional positions and movements of body segments and joints. The assumption of this method is that the surface-mounted markers reflect the motion of the underlying bones or structures. Measurement errors introduced with soft tissue deformations have been estimated in studies comparing surface-mounted marker movement to intra-cortical pin-mounted markers. The least error has been reported in the sagittal plane and larger error in the frontal and transverse planes of the knee motion (Reinschmidt et al., 1997; Benoit et al., 2006). Westblad *et al.* (2002) reported skin movement artifact for movement of the calcaneus relative to the tibia during stance phase, where root mean

Ruoli Wang

square (RMS) was small at 2.5° (inversion/eversion), 1.7° (plantarflexion/dorsiflexion) and 2.8° (adduction/abduction). Nester *et al.* (2007) compared kinematic data from a four-segment foot model to the kinematics of the foot bones comprising four segments. They found differences were greatest for motion of the combined navicular/cuboid relative to calcaneus and the medial forefoot segment relative to the navicular/cuboid. RMS error of commercially-available capture systems in calculating the distance of two markers in a volume with a length of 2.0-4.6 m was reported between 0.6 mm and 1.7 mm (Ehara et al., 1997). Dynamic motion capture with more cameras resulted in higher error, and error in calculating a known angle between markers on a rotating plate were between 1.4° and 4.2° (Richards, 1999), though camera technology has vastly improved since then.

Dynamic joint stiffness: joint angle-moment relationship

Human walking patterns are typically characterized by plotting single joint kinematics and kinetics curves as a function of time or percentage of gait cycle. Researchers have introduced a new parameter 'dynamic joint stiffness (DJS)', which may help to clarify some dynamic effects by examining pairs of kinematics and kinetic variables together and assessing the correlations among them (Crenna and Frigo, 2011). DJS was defined as the resistance that a joint (i.e. the active muscles and other passive soft tissue structures that cross the joint) offers during gait response to an applied moment, which can be quantified as the slope of the joint moment plotted as a function of the joint angle (Davis and DeLuca, 1996). Studies have shown that DJS is helpful in analyzing, at a joint level, how the motor task is coordinated and how stable the joint is. A previous study has showed that ankle DJS was a repeatable and approximately constant parameter in the ankle and forefoot (Perry and Burnfield, 2010) in normal walking. The potential clinical utilization of DJS was illustrated by examining 2nd rocker stiffness and the graphic description of the angle-moment contour after different interventions, i.e. selective dorsal rhizotomy (Peacock et al., 1987), Baker-type lengthening of the gastrocnemius muscle (Baker, 1956) in children with cerebral palsy (Davis and DeLuca, 1996). The angle – moment contour can describe the absorption and production of mechanical energy in walking (Crenna and Frigo, 2011; Gabriel et al., 2008), e.g. at the ankle joint, increasing internal plantarflexor moment with ankle dorsiflexing means energy absorption. DJS was also found to be associated with many factors, e.g. walking speed, gender. age etc. Walking speed was found to have a different influence on different lower limb joints as well as in the different sub-phases (Frigo et al., 1996). Compared to a young adult group, an elderly group had slightly higher ankle DJS for most of the stance phase (Crenna and Frigo, 2011). Gabriel et al. found that the lower ankle stiffness in females than in males is associated with an increased risk of ankle sprain or common injuries associated with lack of joint stability (2008).

Characterization of the quasi-linear (nearly linear) behavior of the joint angle-moment relationship has also shown its possibility as a quantitative diagnostic approach to the motor control behavior and as a treatment evaluation in subjects with motion disorders. DJS was found significantly higher in patients with bilateral arthroplasty than in healthy controls, and the authors suggested that it is an important factor in assessing relationships between hip impairments and dynamics in other joints (Tateuchi et al., 2011). Persons with advanced stages of knee osteoarthritis were found to have higher knee DJS irrespective of walking speed, which may be a strategy to overcome knee instability, often found in this population (Zeni Jr and Higginson, 2009).

Although studies have used DJS to quantify motor control behavior at joints, there are some assumptions and uncertainties. DJS (as the concept 'quasi-stiffness'), describes the ability of the system to resist externally imposed displacements regardless of the time course of the displacement, which is not necessarily related to the ability of the system to deform or to store elastic energy.

RELATED PATHOLOGIES AND DISORDERS

Ankle Fracture

Ankle fracture in this thesis refers to malleolar fractures. It is one of most common lower limb fractures, and the frequency has been increasing over the past few decades, especially in elderly women (Bengner et al., 1986; Kannus et al., 1996). According to previous epidemiological studies, the incidence of ankle fractures is between 107 and 184 per 100,000 persons per year (Bengner et al., 1986; Court-Brown et al., 1998; Daly et al., 1987; Jensen et al., 1998). Another study had shown that this rise has continued during the entire 1980s and 1990s (Kannus et al., 1996). In the United States, ankle fractures have been reported to occur in as many as 8.3 per 1000 medical-care recipients, a figure that appears to be rising steadily (Koval et al., 2005).

In order to describe fractures and help physicians determine appropriate treatment, two classification schemes based on radiographic presentation, called Danis-Weber and Lauge-Hansen, are widely used. Lauge-Hansen's classification, first reported in 1950 (Lauge-Hansen, 1950), takes the posture of the foot at the moment of injury and the direction of deforming force into consideration, and subsequently divides ankle fractures into five types. While it provides a better understanding of injury mechanisms, resulting in improved technique in closed treatment of unstable fractures (Lindsjö, 1985), it is complicated and difficult to apply. Weber's classification divides ankle fractures into 3 types (A, B, C) on the basis of the anatomy of the fracture of the lateral malleolus (Müller et al., 1991). It is easy to use and requires few clinical details, but its weakness of ignoring the biomechanical aspect of the medial injury makes the evaluation of results difficult. Another commonly used classification scheme for ankle fractures is the simple anatomic division into uni-, bi- and trimalleolar fractures. Some authors have advocated modifications to the existing schemes to achieve more biomechanical and clinical relevance (Pettrone et al., 1983).

Juvenile idiopathic arthritis

Juvenile idiopathic arthritis (JIA) is an umbrella term for a group of persistent inflammatory disease in childhood (aged 0-16 yrs) with arthritides with unknown etiology lasting more than six weeks (Petty et al., 2004). In this thesis, the subjects with JIA were classified according to ILAR criteria (International League of Association for Rheumatology). JIA affects around 1500 children in Sweden and influences many aspects of daily activities (Gäre et al., 1987; Berntson et al., 2001). A population-based epidemiological study in Nordic countries of JIA reported an incidence of 15/100000 children per year (Berntson et al., 2003). JIA in girls predominates over JIA in boys with a ratio of 3:2 (Cassidy, 2002).

Depending on the type of JIA, the clinical symptoms may vary; nevertheless, the most profound symptoms include joint inflammation and stiffness, pain, fatigue, and reduced physical ability (Cassidy, 2002; Giannini et al., 1992; Klepper et al., 1992; Schneider and Passo, 2002). Joint stiffness is usually more evident in the morning and in both affected and non-affected joints. The inflamed joints are tender and painful, and pain can be particularly bothersome at night (Broström, 2004). Apart from articular symptoms, weight loss and fatigue may occur in all types of JIA (Cassidy, 2002; Giannini et al., 1992; Klepper et al., 1992; Schneider and Passo, 2002). Long duration of an active disease may be associated with a reduction in height, discrepancy in leg length, and shortening of muscles and tendons, which may cause flexion contractures (permanent shortening of a muscle) (Cassidy, 2002; Giannini et al., 1992; Bacon et al., 1990; Fan et al., 1998; Lindehammar and Backman, 1995; Vostrejs and Hollister, 1988). Children with JIA have also been reported as having great limitations in physical activity, lower aerobic endurance, decreased muscle strength and a restriction of joint motion, which most often affects extremities (Henderson et al., 1995; Singsen, 1995; Giannini and Protas, 1991; Klepper, 1999). The kinematics and kinetics of children with JIA differ from healthy children, and include significantly lower walking velocity and step length, more anteriorly tilted pelvis,

Ruoli Wang

reduced hip extension, reduced knee extension during single-support phase, reduced plantarflexion in pre-swing, reduced peaks of ankle moments and power, and reduced peaks in the vertical GRF (Broström, 2004; Hartmann et al., 2010).

Idiopathic toe-walking

Toe walking is defined as lack of heel floor contact at the onset of stance during gait. Idiopathic toe-walking (ITW) is a term used to describe the condition in which children walk on their toes in the absence of any known cause (Sala et al., 1999). ITW is a diagnosis made by exclusion and for a person who is otherwise neurologically normal and possesses normal muscle strength and selective motor control. Persistent equinus (plantarflexed) positioning can result in a plantarflexion contracture, eventually with permanent shortening of the gastrocnemius/soleus muscle complex. The incidence of ITW has been reported to be 7% to 24% of the childhood population (Furrer and Deonna, 1982).

Studies have been performed to evaluate characteristic gait patterns in ITW, which include variable heel strike (the incidence of spontaneous heel-contact is variant) (Crenna et al., 2005; Hicks et al., 1988), a short period of dorsiflexion with progressive plantarflexion until toe-off (Armand et al., 2006), premature onset of triceps surae (gastrocnemius and soleus) activation and excessive overlapping of gastrocnemius and tibialis anterior activity (Sala et al., 1999). Decreased ankle range of motion (ROM) due to limited dorsiflexion was also presented in a majority of children with ITW, and as a distinction from other toe-walking populations (Engelbert et al., 2011). Management of children with ITW is controversial. Treatments consist of physiotherapy, serial casting, and open or percutaneous lengthening of the Achilles tendons. Recently, botulinum toxin (BTX) injection, which was used to treat muscular hyperactivity, has also been reported to positively affect the gait in some children with ITW (Engström et al., 2010).

Muscle co-contraction

Muscle co-contraction has been defined as the concurrent activation of agonist (prime mover) and antagonist (primer stabilizer) muscles across the same joint (Falconer and Winter, 1985). From a purely mechanical point of view, the muscles contract simultaneously with little contributions to the useful muscular work output, which is one of the major causes of mechanical inefficiency during movement (Winter, 2009). Co-contraction has sometimes been found in infancy and childhood when the reciprocal inhibition (the agonist contracts, the antagonist is simultaneously inhibited (Sherrington, 1940)) is lower than in adults with more predictable movements, and may usually decline during development (Myklebust et al., 1986; Gatev, 1972). In normal gait, antagonistic muscle pairs at each lower extremity joint contract in an alternating pattern with low durations of concurrent activity, to generate sufficient joint moment. Despite of the greater energy expenditure, possible advantages of muscle co-contraction in providing joint stabilization (stiffness) and protection (Hagood et al., 1990), increasing precision (Karst and Hasan, 1987; Humphrey and Reed, 1983), and increasing ability to compensate for unexpected load (Damiano, 1993) have been observed. One possible explanation for co-contraction could be that the central nervous system (CNS) modulates the impedence of muscles – the static and dynamic relationship between muscle force and imposed stretches - through cocontraction of antagonist muscles to adapt to the environment. The antagonist muscles would add impedence while the torque from opposing muscles would subtract (Hogan, 1984).

Excessive muscle co-contraction has been observed in neuromuscular pathologies and is even associated with normal aging. Notably co-contraction accompanies spastic gait, e.g. due to hemiplegia, paraparesis, or cerebellar syndromes (Dierick et al., 2002), but it can also accompany postural instability or weakness in persons with normal levels of muscle tone (Brooks, 1986).

COMPUTATIONAL METHODS IN MUSCULOSKELETAL COORDINATION

In biomechanics, we can either input the muscle forces to predict the displacement of the body segments, or compute joint moments and forces from a combination of measured external forces, segment kinematics, and anthropometric data. The first technique is referred to as a forward dynamics approach, and the latter, as an inverse dynamics approach.

The inverse dynamics method is commonly employed in clinical gait analysis to compute the net joint moments, and net joint powers (Winter et al., 1990). The foot, shank and thigh are considered to be rigid segments connected by joint articulations. The measured ground reaction force and estimated segmental accelerations are inserted into the Newton-Euler equations of motion, starting at the most distal segment (e.g. foot) and solving for the proximal joint force and moments (e.g. ankle) (Zajac et al., 2002). One limitation of the traditional Newton-Euler inverse dynamics method is its inability to identify the roles of individual muscles in coordinating the body segments (Zajac et al., 2002). In order to understand the individual muscle contributions to the movement, additional methodologies are needed to decompose the net joint moments or joint forces, which can be estimated directly from the inverse dynamics, into individual muscle moment or muscle forces. Static optimization is one method, but is not entirely reliable to study muscle coordination because of the uncertainty in the optimization criterion inherent in this approach (Marshall et al., 1989; Herzog, 1996). EMG activity is often recorded in gait studies, but its relationship with certain muscle force is still debatable (Perry, 1998; Inman et al., 1981).

Various methods can be used to find muscle or joint moment contributions with forward dynamics. One method is to use the net joint moments computed from traditional inverse dynamics as input to a forward dynamical model (Kepple et al., 1997). One of the most difficult aspects of generating muscle-driven dynamical simulations compatible with experimental observation is finding an appropriate muscle activation pattern. Optimization theory and a dynamical model to iteratively find the muscle excitations are usually applied, but the conventional approaches usually require inordinate amounts of time (Zajac, 1993; Anderson and Pandy, 2001; Neptune et al., 2001). A recently introduced algorithm - computed muscle control (CMC) - employs feedforward and feedback control to determine muscle excitations which can track experimental kinematics more efficiently using only a single integration of the state equations (Thelen and Anderson, 2006).

Induced acceleration analysis (IAA) is an approach which lies conceptually at the intersection of the field of forward dynamics and inverse dynamics, and which may serve as an enhancement to the conventional inverse dynamical approach. The basis of the analysis is the identification of the instantaneous contribution of a particular muscle (e.g. gastrocnemius) or muscle group (e.g. ankle plantarflexors) to an outcome measurement (e.g. acceleration of the center-of-mass of the body). Zajac and Gordon (1989) first introduced IAA as a tool to demonstrate that the gastrocnemius, anatomically a knee flexor and ankle plantarflexor can in certain circumstances act as a knee extensor. Mechanical analysis of the whole musculoskeletal system revealed that muscle groups crossing a joint would generally act to accelerate all joints of the body (Zajac and Gordon, 1989). In recent years, researchers using this approach have expanded our understanding of how individual muscles or muscle groups control body motion, e.g. contribution to the vertical GRF in gait (Anderson and Pandy, 2003), the body COM in running (Hamner et al., 2010), the energetics of the body segment during the normal gait (Neptune et al., 2004) and the influences of different walking velocities on muscle contributions to swing initiation (Fox and Delp, 2010b). Clinical IAA studies have demonstrated that excessive external tibial rotation, a transverse plane misalignment of the lower leg, can reduce the lower limb muscles' capacity to extend the hip and knee during single-limb stance, and may be contribute to crouch gait (Schwartz and Lakin, 2003; Hicks et al., 2007). IAA analysis of stiff-legged gait studies indicated that variable causes of the stiff-legged gait were highly related to patients' specific impairments (Riley and Kerrigan, 1999). However, it should be noted that IAA is a snapshot in time of

Ruoli Wang

contributions of individual forces acting on the body segments without regard to the cumulative effects of past muscle and gravity force trajectories on the system behavior (Zajac et al., 2002).

Musculoskeletal model

Whether in forward or inverse dynamics, one must employ an anatomical model of the musculoskeletal system. In gait analysis using surface-mounted markers, a model is required to infer the position of the body segments from the measurement positions of the markers. In forward simulations, a musculoskeletal model containing accurate three-dimensional (3D) geometry of each muscle is often used to comprehend the dynamic function of individual muscles.

Kinematic model in gait analysis

The most widely used whole-body gait models consist of 15 rigid body segments (head, torso, upper arms, lower arms, hands, pelvis, thighs, shanks, and feet). However, representing the foot as a single rigid body with a revolute ankle joint is inadequate to demonstrate the true 3D foot motion. During the last few years, many noteworthy biomechanical foot models which include multiple segments have been developed (Stebbins et al., 2006; Khazzam et al., 2006; Woodburn et al., 2004; Saraswat et al., 2011; Simon et al., 2006).

There are some consensuses in these models. Since the number of segments that can be tracked is limited when using the typical camera configuration for a full body motion analysis, most foot models contain three or four segments and express angular relationship as Euler angles (Kidder et al., 1996; Myers et al., 2004). Most models reference their dynamic angles to a standard zero position, where static joint angles are defined to be zero (Leardini et al., 1999; Moseley et al., 1996), which contributed to the reduction of the possible variations from marker placement. However, there are some inconsistencies in segment definitions. For instance, the group from Marquette University defined the forefoot segment with cuneiform, cuboid and metatarsal bones (Myers et al., 2004). The Oxford foot model defined forefoot segments rigorously only with metatarsal bones, and the midfoot segment was considered as a mechanism transmitting joint between the forefoot and hindfoot segment (Stebbins et al., 2006).

Muscle models

Early muscle model studies have led to databases of origins and insertions of lower extremity muscles based on cadaver studies (Brand et al., 1982; White et al., 1989). However, these databases had limitations of small sample sizes, lack of gender, and wrapping points allowing muscle lines-of-action to pass through bones (Kepple et al., 1998). For many muscles, the origin and insertion points are enough. However, for muscles such as the quadriceps, addition landmarks wrapping around bones are needed while the body is in many postures. Kepple et al. created a new musculoskeletal database using a large number of specimens and allowing for comparisons of gender and racial variation, but still faced problems of software implementation (Kepple et al., 1998). In order to remedy the limitations associated with the earlier databases, Delp et al. (1990) created a standard implementation musculoskeletal database with the muscle-tendon actuator model proposed by Zajac and Gordon (1989). This is a generic model which can be scaled based on the recorded markers placed on anatomical landmarks to fit a specific subject. It is worth noting that the musculoskeletal system is very intricate and large anatomical variations exist among individuals. Using modern medical imaging techniques, e.g. magnetic resonance image or computer tomography, to construct a subject-specific musculoskeletal model can generate more accurate and representative analyses (Arnold et al., 2000), particularly in persons with deformities. However, the disadvantages of time required and lack of standard imaging protocols have largely limited its application.

Foot -ground contact

An appropriate ground contact model determines how the interaction of the foot and ground will be defined during the stance phase, which has often been a challenge in computational simulation. In IAA, this was especially substantial for decomposing GRF arising from certain muscles. If assuming the biomechanical system to be in rigid contact with the environment, performing the decomposition is a relatively straightforward procedure. For example, one can simulate foot-flat phase by fixing the foot to the ground, and the corresponding GRF made by an individual muscle force equals the enforcement of the kinematic constraints of the fixing joint. The contact point assumptions have varied, from a single point located at the center of pressure (COP) (Hamner et al., 2010; Kepple et al., 1997) to multiple points distributed over the sole of the foot (Anderson and Pandy, 2003; Pandy et al., 2010). When foot contact with the environment was modeled using spring-damping units under the sole, the decomposition was more complex. Anderson et al. employed five spring-damping units on each foot, whose forces were always on but varied exponentially with displacement (Anderson and Pandy, 1999). In a study by Neptune et al. (2001), the contact between the foot and the ground was modeled as 30 independent visco-elastic elements with Coulomb friction in order to include the mechanical properties of a shoe and underlying soft tissues. Different foot-ground contact (FGC) models and kinematic constraints applied on the points may influence the computed the muscle functions, which is not directly measurable. A theoretical principle of 'superposition' – that the sum of the contributions of all forces (e.g. muscles, gravity and centrifugal forces) to the GRF must be equal to the overall GRF measured in an experimental motion analysis – has been suggested, in order to gain confidence in the computed muscle function (Anderson and Pandy, 2003; Hamner et al., 2010; Pandy et al., 2010). However, a recent study has evaluated 3 single and 3 multiple point contact models and stated that lower superposition errors do not necessarily imply greater validity in the prediction of muscle functions (Dorn et al., 2011).

SPECIFIC AIMS

The scope of the thesis is in the biomechanical consequences of gait impairment at the foot and ankle joint. **Study I** aimed to quantify post-operating foot motion in subjects with treated ankle injury (i.e. ankle fractures); **Study II** aimed to investigate the biomechanical contributors to the ankle anglemoment relationship in healthy and patient groups; **Study III** aimed to identify the lower limb muscle functions in the presence of foot malalignment (i.e. hindfoot inversion or eversion); **Study IV** aimed to study the influence of the foot-ground contact model - kinematic constraints and locations of the COP - on the dynamic muscle functions; **Study V** aimed to identify the necessary compensatory mechanisms to overcome excessive co-contraction of ankle muscles and retain a normal walking pattern. The specific aims were:

Study I

- 1. To determine whether ankle fractures resulted in kinematic deviations at or around the injured area.
- 2. To identify the secondary effects caused by unilateral ankle fractures, i.e. motion between other segments in bilateral limbs.
- 3. To explore whether the clinical ankle function score Olerud/Molander Ankle Score (OMAS) was associated with kinematics parameters.

Study II

- 1. To decompose ankle DJS into individual dynamic components
- 2. To explore the hypothesis that the deviations found in DJS compared to normal in two different patient groups, juvenile idiopathic arthritis and idiopathic toe walking, can be better interpreted through examination of individual components.

Study III

- 1. To study the effect of subtalar alignment on the dynamic function of the tibialis anterior, gastrocnemius and soleus to accelerate the subtalar, ankle, knee and hip joints.
- 2. To compute the forward (propulsion) and vertical (support) acceleration of the body center of mass (COM) induced by three muscles and study the effect of the subtalar angle on the muscle induced propulsion and support accelerations of COM.

Study I V

- 1. To compare the influence of a fixed joint ground contact model and a moving joint model on potential dynamic functions of the gastrocnemius, soleus and tibialis anterior in accelerating the lower limb joints.
- 2. To analyze the effects of contact joint constraints on potential muscle functions in accelerating the lower limb joints.
- 3. To determine the influences of a medial and lateral shift of the COP on potential muscle functions in accelerating the lower limb joints.

Study V

1. To perform muscle-actuated simulations of normal walking in the presence of normal, medium and high levels of co-contraction of two ankle antagonistic pairs — pair 1: gastrocnemius-tibialis anterior and pair 2: soleus — tibialis anterior.

Ruoli Wang

2. To identify compensatory mechanisms of ankle and knee muscles to retain normal walking in the presence of excessive ankle muscle co-contraction, by computing induced angular accelerations of knee and hip muscles.

MATERIALS AND METHODS

Detailed description of all the materials and methods used in this thesis are given in the original studies. A summary of these methods are presented here. Subject participation was voluntary. Ethical approval for this study was obtained from the local ethics committee.

SUBJECTS

Study I

Eighteen patients with ankle fractures who were treated with open reduction and internal fixation at Karolinska University Hospital participated in a follow-up study using clinical gait analysis including a multi-segment foot model. Twelve patients had a lateral malleolar fracture and 6 patients had a trimalleolar fracture. An age- and gender-matched control group was gathered from a cohort of healthy adults without musculoskeletal disease or history of lower-extremity injury (Table 1).

Study II

Thirty healthy children without history of neurological or orthopedic disease, 8 children with JIA and 8 children with ITW were examined in this retrospective study. All subjects were selected from the database at the Gait Analysis Laboratory at Karolinska University Hospital. Children with JIA were selected with exclusion criteria of 1) history of lower limb surgery and 2) having undergone treatment within 4 weeks prior to data collection. Children with ITW were selected with exclusion criteria of having undergone any surgical or spasticity-reducing treatment before the data collection (Table 1).

Study III+IV

Eight healthy adult controls without musculoskeletal disease or history of lower-extremity injury participated in these studies (Table 1).

Study V

Nine healthy adult controls without musculoskeletal disease or history of lower-extremity injury participated in the study (Table 1).

Table 1: Subjects demography in the Studies I-V

	Stu	dy I	Study II		Study III + IV	Study V	
	Ankle fracture	Control	JIA ³	ITW ⁴	Control	Control	Control
Number of subjects	18	18	8	8	30	8	9
Age ¹ (yrs)	39	40	15	7	10	32	29
	(17 to 64)	(19 to 64)	(7 to 17)	(6 to 12)	(7 to 14)	(23 to 60)	(27 to 39)
Male/Female	10/8	10/8	2/6	3/5	17/13	3/5	4/5
Height ² (cm)	173 (7)	173 (7)	150 (24)	136 (15)	144 (14)	171 (7)	168 (9)
Body weight ² (kg)	76 (15)	72 (12)	40 (20)	35 (14)	38 (11)	63(12)	64 (11)

¹ Median(range)

GAIT ANALYSIS

Procedure (Studies I - V)

Subjects were tested in 3D gait analysis along a 10m walkway using an 8-camera motion analysis system (Vicon MX 40, Oxford, UK). Retro-reflective markers were placed on bony landmarks or specific anatomical positions as required by the kinematics models. The subjects walked barefoot at a self-selected pace. A series of walking trials were collected to achieve three left and three right trials yielding complete data sets in **Studies I-II**, and one representative trial was used as normal input configuration in **Studies III-V**. In **Study V**, surface electromyographic (EMG) data (Motion Laboratory Systems, Baton Rouge, LA, USA) were recorded for the biceps femoris long head (BFLH), rectus femoris (RF), medial gastrocnemius (GAS), soleus (SOL) and tibialis anterior (TA) bilaterally according to standardized electrode placement (www.seniam.org)¹.

Model

Study I

All subjects were examined using a modified version of the Oxford foot model (Stebbins et al., 2006). The model simplified the foot structure to three rigid segments (tibia, hindfoot, and forefoot) and one vector (hallux). The midfoot was regarded as a mechanism transmitting motion between the hindfoot and forefoot. All inter-segment motions except the hallux were free of constraints, i.e. six degrees of freedom. A set of 18 markers (9 mm) was placed on body landmarks on each side in a static trial, of which four were then removed for the dynamic trials (Appendix A).

² Mean (S.D.)

³ Juvenile idiopathic arthritis

⁴ Idiopathic toe walking

¹ The detailed description of post-processing of EMG data can be found in Paper V, section 2.2.

A modified method based on a spherical rotation coordinate system (Cheng, 2000) was adopted to obtain frontal plane hallux varus/valgus relative to forefoot. A unit vector was used to represent the long axis of the hallux segment and the rotation was determined in a reference coordinate XYZ, which was assumed to be fixed and aligned to the forefoot segment. Thus hallux varus/valgus can be measured as an angle (θ) between the unit vector (r) of the hallux and its projection on the sagittal plane of the forefoot (XZ plane, Fig 7).

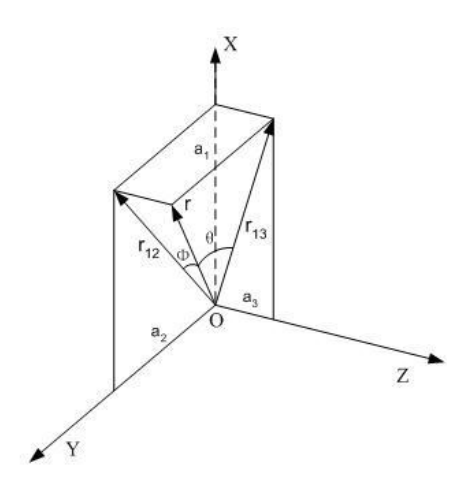


Figure 7: Hallux/Forefoot varus or valgus angle

Study II

All subjects were tested with a conventional full-body or lower body marker set (Appendix B).

Studies III-V

All subjects were tested with a conventional full-body marker set, plus the modified Oxford foot model marker set (Appendix A).

DYNAMIC JOINT STIFFNESS (STUDY II)

Analytical decomposition

The ankle DJS q is defined as

$$q = \frac{dM_{ax}}{d\theta_a} \tag{1}$$

where θ_a is the sagittal plane ankle angle and, due to the chain rule, Eq. (1) can be represented as:

$$q = \frac{dM_{ax}}{d\theta_a} = \frac{\frac{dM_{ax}}{dt}}{\frac{d\theta_a}{dt}} \tag{2}$$

Internal dorsi/plantarflexion ankle moment was derived based on the equilibrium equations of inverse dynamics (Appendix C and D), can be written as:

$$M_{ax} = M_{GRFAx} + M_{FAx} + M_{GAx} \tag{3}$$

where M_{FAx} is moment about ankle due to the accelerations (linear and angular), M_{GAx} , is moment about ankle due to the segment mass, M_{GRFAx} is moment about ankle due to ground reaction force, all in the sagittal plane. From Eqs. (2-3), ankle DJS can be decomposed into **three components**:

$$q = \frac{\frac{dM_{GRFAx}}{dt}}{\frac{d\theta_a}{dt}} + \frac{\frac{dM_{FAx}}{dt}}{\frac{d\theta_a}{dt}} + \frac{\frac{dM_{GAx}}{dt}}{\frac{d\theta_a}{dt}}$$
Component 1 Component 2 Component 3 (4)

Component 1 represents the ratio of changes in GRF moment to changes in ankle angle; Component 2 represents the ratio of changes in moment due to foot accelerations to changes in ankle angle; Component 3 represents the ratio of changes in moment due to foot mass to changes in ankle angle.

Component 1 was subsequently decomposed further into Eq. (5)

$$\frac{dM_{GRFAx}}{\frac{dd}{dt}} = \frac{\frac{d}{dt}(\vec{L} \times \vec{GRF})_x}{\frac{d\theta_a}{dt}} = \frac{\frac{d}{dt}(\vec{L} \times \vec{GRF})_x}{\frac{d\theta_a}{dt}} = \frac{(\frac{d\vec{L}}{dt} \times \vec{GRF})_x + (\vec{L} \times \frac{d\vec{GRF}}{dt})_x}{\frac{d\theta_a}{dt}} \xrightarrow{\text{of component 1}} \frac{1}{dt} \xrightarrow{\text{of component 1}} \frac{1}{dt$$

(5)

where \vec{L} is the moment arm of the ground reaction force vector \vec{GRF} .

Component 1A represents the changes of GRF moment arm times the GRF, and Component 1B represents the GRF's moment arm times the change in GRF.

Linear regression

The stance phase was divided into three sub-phases according to (Crenna and Frigo, 2011): early rising phase (ERP), late rising phase (LRP), and descending phase (DP)ⁱⁱ. For each sub-phases, a linear regression line, minimizing the least square distance between the data points and the line was computed to quantify the slope of the curve (Frigo et al., 1996).

INDUCED ACCELERATION ANALYSIS (STUDIES III-V)

The generalized equations-of-motion of a multi-articulated body system (Zajac and Gordon, 1989) can be written as:

 $^{^{\}mathrm{ii}}$ The detailed description of sub-phase definition can be found in Paper II, section 2.4 $20\,$

$$[M]\ddot{\vec{q}} = [R]\vec{F}_m + \vec{G}(\vec{q}) + \vec{V}(\vec{q}, \dot{\vec{q}}^2) + \vec{F}_E$$
(6)

where $\vec{q}, \dot{\vec{q}}, \ddot{\vec{q}}$ are the vectors of generalized coordinates, velocities and accelerations; [M] the system mass matrix; \vec{F}_m the vector of muscle forces; [R] the matrix of muscle moment arms; $\vec{G}(\vec{q})$ the vector of gravitational force; $\vec{V}(\vec{q}, \dot{\vec{q}}^2)$ the vector of velocity-related forces (i.e. centripetal and Coriolis forces), \vec{F}_E the vector of external force (i.e. \overline{GRF} in this thesis).

Thus the accelerations $\ddot{\vec{q}}$ are:

$$\ddot{\vec{q}} = [M]^{-1} ([R] \vec{F}_m + \vec{G}(\vec{q}) + \vec{V}(\vec{q}, \dot{\vec{q}}^2) + \vec{F}_E)$$
(7)

Since $[M]^{-1}$ is non-diagonal, any one muscle force $\vec{F}_{m,i}$, contributes instantaneously to any acceleration \ddot{q}_k in \ddot{q} , and thus to all segmental and joint linear and angular accelerations (Zajac et al., 2002).

The contribution of an individual muscle force $\vec{F}_{m,i}$ to the accelerations of the segments $\ddot{\vec{q}}$ at a certain instant is presumed to be the summed contribution arising from $\vec{F}_{m,i}$ at that instant, and the \overline{GRF} due to the immediately previous trajectory of $\vec{F}_{m,i}$ (Zajac et al., 2003),

To analyze the role of the individual muscles, gravitational force and force terms arising from angular velocities were set to zero. The acceleration produced solely by muscle forces can be acquired:

$$\ddot{\vec{q}} = [M]^{-1} ([R]\vec{F}_m + \vec{F}_E)$$
(8)

Depending on the explicit constraints described in the section Ground-foot contact model, the term of \vec{F}_E can be rewritten as:

$$\vec{F}_E = [C]^T \lambda \tag{9}$$

where [C] is the constraint matrix, which maps the constraint forces λ to system generalized forces. Meanwhile, λ is solved to fulfill the defined ground foot contact constraints.

MUSCULOSKELETAL MODEL

In **Studies III+IV**, a 3D linkage model with 28 segments (including head+neck, torso, arms, pelvis, thighs, shanks, patellas, taluses, feet and toes), 30 joints and 88 musculoskeletal actuators was developed, based on Delp's model (1990).

In **Study V**, a generic model (Arnold et al., 2010) with 14 segments (head+torso, pelvis, femurs, tibias, patellas, taluses, calcaneus, toes), 23 DOFs and 96 musculotendon actuators was used.

Foot-ground contact model

There were two types of foot-ground contact models, 'fixed joint' and 'moving joint' models, used in this thesis as summarized in Table 2.

Fixed joint model

Three foot-ground joints were added – at the posterior inferior point of the heel ('GFH'), the distal end of the third metatarsal ('GFM'), and the distal end of the hallux ('GFT'). 'Simple DOF' and 'Multiple DOF' referred to varying rotational DOFsⁱⁱⁱ allowed in each joint.

In **Study !!!**, location of the FGC joints was modified to take into account excessive subtalar inversion or eversion^{iv}.

Moving joint model

One moving joint was added, which was moved instantaneously along the COP. 'Point' referred to the joint with 3 rotational DOFs. 'RollingOnSurface' referred to the constraint on a rolling body (foot) that is in contact with a plane defined on another body (ground), where no penetration, no slipping and no twisting were allowed (Hamner et al., 2010).

Table 2: Foot-ground contact models

Foot-Ground Contact Model	Constraints	Study III	Study IV	Study V
Fixed Joint	Simple DOF	Х	Х	
	Multiple DOF		Х	
Moving Joint	Point ^v		Х	
	RollingOnSurface			Х

SIMULATION PROCEDURE

Study III

The simulation consisted of 3 major steps, including model scaling (A), inverse kinematics and IAA. The analyses were performed using SIMM Dynamic Pipeline and SD/FAST (Symbolic Dynamics, Inc. Mountain View, CA). The pipeline is illustrated in Appendix E. In order to simulate the mal-alignment of the subtalar joint, excessive subtalar inversion or eversion was modeled by offsetting up to ±20° from the normal subtalar angle and moving the contact joint accordingly while other configurations remain unaltered.

Model Scaling (A)

The dimensions of each segment were scaled by the segment's scale factor, which was based on the distance between the joint centers. The joint center was determined by the locations of the 'critical' markers from the static trial (MusculoGraphics Inc., 2004). The optimal fiber length and tendon slack length of each muscle were scaled to preserve the force generating properties of the generic model. The mass of the model were scaled to match each subject's recorded mass.

22

iii The detailed definition of 'Simple DOF' and 'Multiple DOF' can be found in Paper IV, section 2.4.1

^{iv} The detailed modification of the location of the foot-ground contact can be found in Paper III, section 2.3

^v In Paper IV, the 'Point' FGC model was referred as 'moving joint'.

Study IV+V

The simulation consisted of 6 major steps, including model scaling (B), inverse kinematics (IK), inverse dynamics (ID), residual reduction algorithm (RRA), computed muscle control (CMC), and IAA, which were performed in OpenSim 2.4 (Delp et al., 1990). The simulation pipeline of **Study V** is illustrated in Appendix F.

Model Scaling (B)

The generic musculoskeletal model was used to generate scaled subject-specific models. The dimensions of each segment were scaled by the segment's scale factor, which was based on the relative distance between experimentally placed marker pairs and marker pairs attached to the model. The optimal fiber length and tendon slack length of each muscle were scaled to preserve the force generating properties of the generic model. The mass of the model was scaled to match each subject's recorded mass.

Inverse Kinematics

IK is the process of determining the generalized coordinates for the model that best match the experimental kinematics recorded for the subject. At each time frame, IK computes generalized coordinate values using a weighted least squares optimization problem by minimizing the sum of the squared differences between experimental and model markers.

Inverse Dynamics

ID determines the generalized forces (e.g. net forces and torques) at each joint of a multibody linkage system based on the known joint kinematics, inertial properties and external loads (e.g. GRF). The mechanical behavior of the multibody linkage is governed by equations of motion derived using Newton's 2nd law.

Residual Reduction Algorithm

Due to the errors from modeling assumptions and marker data processing, the kinematics are not completely consistent with the measured GRF. The residual forces and moments between the most proximal segment (i.e. pelvis) and the ground are needed to drive the model to track the given kinematics. The residuals are computed and averaged over the duration of the movement. The COM of the model's torso is then altered by a small amount to reduce the residuals. RRA is then applied to alter the kinematics slightly to further reduce the residuals by applying a control algorithm. In other words, each generalized coordinate of the model is controlled by an idealized actuator. For instance, six DOFs between model and ground are actuated by six residuals, and each joint DOF is actuated by an idealized joint moment. RRA runs forward in time to compute the actuator forces to solve a optimization problem that will cause the model to move from its current configuration toward its desired (Anderson et al., 2006).

Computed Muscle Control

CMC was used to generate a set of muscle excitations that produce a coordinated muscle-driven simulation of the subjects' movement. First, CMC uses a proportional-derivative control to compute a set of desired accelerations which can drive the model toward the experimentally derived coordinates. The next step was to solve a static optimization problem by minimizing the sum of the muscle activations to compute actuator controls achieving the desired accelerations from the first step, while

accounting for muscle activation and contraction dynamics. The final step was to use the computed controls to perform a standard forward dynamic simulation.

Induced Acceleration Analysis

IAA was used to compute accelerations caused by individual forces acting on a model, e.g. induced ankle angular accelerations or translational COM accelerations by the gastrocnemius. There are two options in performing IAA; one is to use predicted muscle forces (i.e. in **Study V**) to compute actual induced accelerations, another is to quantify the potential contributions of muscles by applying only 1N of muscle force (i.e. in **Study III**).

Co-contraction (Study V)

Identification of agonist and antagonist muscle was performed according to Falconer and Winter (Falconer and Winter, 1985). Three co-contractions levels (normal, medium, and high) of two ankle joint antagonist pairs (pair 1: GAS – TA, pair 2: SOL - TA) were simulated according to Eq (10). At the normal level, the excitations of antagonistic pairs were computed in CMC with experimental EMG constraints. The excitation of co-contracted muscle was defined according to Eq. (10).

$$Excitation_{cocontr,ant} = Excitation_{normal,ant} + \gamma(Excitation_{normal.ago} - Excitation_{normal.ant})$$

$$(10)$$

where $Excitation_{cocontr,ant}$ is excitation of the antagonist muscle under medium or high level co-contraction, $Excitation_{normal,ant}$ is excitation of the antagonist muscle under normal co-contraction, γ is the co-contraction ratio, $Excitation_{normal.ago}$ is excitation of the agonist muscle under normal co-contraction, and $Excitation_{normal.ant}$ is excitation of the antagonist muscle under normal co-contraction. A medium level of co-contraction was defined as $\gamma = 0.3$, and a high level as $\gamma = 0.6$, and were simulated by increasing the antagonist activity (see Fig 1 in Paper V).

The co-contraction index (CI) vi was also calculated in normal, medium and high levels of co-contraction using the computed excitations (Falconer and Winter, 1985).

DATA ANALYSIS

All statistical tests in the thesis were performed using SPSS v14 software (Chicago, IL, USA). The significance was determined at the p < 0.05 level.

Kinematics (Study I)

Discrete kinematics and temporal-spatial parameters were calculated for each gait cycle, and the average from the three left and three right gait cycles were used for further statistical analysis. The kinematics were represented as relative angles and are summarized in Table 3.

Kinematics and temporal-spatial parameters were analyzed using a two-way repeated measures analysis of variance (ANOVA) with side (injured side and non-injured side) as within-group factor and group (ankle fractures and control group) as the between-group factor (Campbell et al., 2007). The

vi The definition of CI can be found in Paper V, section 2.5.

Spearman's rank correlation coefficient was used to identify associations between OMAS and the inter-segment foot kinematics parameter.

Table 3: Kinematic parameters in Study I

	Stance and Swing phase								
	Hindfoot/Tibia angle	Forefoot/Hindfoot angle	Forefoot/Tibia angle	Hallux/Forefoot angle					
Sagittal plane	Max dorsiflexion, Max plantarflexion, range of motion								
Frontal plane	Max inversion, Max eversion, average	Max supination, Min supination, average	Max supination, Max pronation, average						
Transverse plane	Max internal rotation, Max external rotation, ROM	Max adduction, Max abduction, range of motion	Max adduction, Min adduction, range of motion	Max varus, Max valgus, average					

Max: maximum Min: minimum

Dynamic joint stiffness (Study II)

Both the analytical decomposition and linear regression were applied to three individual trials per subject (left and right sides separately) and a mean value for each side was calculated for each subject in each sub-phase. All values were multiplied by 100 for more convenient numerical representation. The intraclass correlation coefficient (ICC 2) was determined to test the assumption of agreement in ankle DJS computed from linear regression and from analytical decomposition. Data (ankle DJS and each component) were analyzed using a two-way repeated measures ANOVA with side as the withingroup factor and group (control group or JIAs, and control group or ITWs) as between-group factor. The differences in ankle DJS and its components were also analyzed with an individual one-way analysis of covariance (ANCOVA) with walking speed as a covariance to determine whether the walking speed influenced the differences between groups.

Induced joint angular and body center of mass accelerations (Studies III-V)

Study III

The GAS, SOL and TA's potential contributions to the hip, knee, ankle and subtalar joint angular acceleration and linear acceleration of body COM were calculated in five subtalar configurations (Inversion 20°, Inversion 10°, Normal, Eversion 10°, Eversion 20°).

Study IV

In each comparison of FGC models, the GAS, SOL and TA's potential contributions to the hip, knee, ankle and subtalar joint angular accelerations were averaged throughout each sub-phase. The absolute

mean differences of comparison 3 (medial and lateral shift of COP) were also quantified for each subject and averaged across all the subjects to obtain a mean difference in each sub-phase^{vii}.

Study V

Contributions from the primary ankle dorsiflexors and plantarflexors (GAS, SOL, TA, TP: tibialis posterior; PL: peroneus longus; EDL: extensor digitorum longus; EHL: extensor hallucis longus) and knee flexors and extensors (HAMS: semimembranosus, semitendinosus and BFLH combined; BFSH: biceps femoris short head; GRC: gracilis; SART: Sartorius; VAS: vastus medialis, vastus intermedius, and vastus lateralis combined; RF: rectus femoris) to knee and ankle angular accelerations were averaged throughout each sub-phase viii.

vii The definition of the sub-phase was identical as in Study III, detailed in Paper III, section 2.2.

The definition of the sub-phase was detailed described in Paper III, section 2.6.

RESULTS AND DISCUSSION

MULTI-SEGMENT FOOT KINEMATICS (STUDY I)

The main contribution from this study is that it describes characteristic multi-segmental foot motions in patients with ankle fractures one year post-operatively (see Table 4 and Fig 1 in Paper I), which was difficult to evaluate clinically. Still, very few gait studies have focused on the ankle joint (see Paper I) and this is the first study we know of evaluating post-operative ankle fractures with a multi-segment foot model.

Table 4: Results summery in Study I: inter-segmental kinematics (ROM: range of motion).

Inter-segmental foot kinematics	Ankle fracture group Vs. Control group (Injured side)	Injured side Vs. Non-injured side (Ankle fracture Group)
Hindfoot/Tibia		less max plantarflexion (Swing) less sagittal ROM (Swing)
Forefoot/Hindfoot	less transverse ROM (stance+swing)	less transverse ROM (swing+stance)
Forefoot/Tibia	less Max plantarflexion (swing) less sagittal ROM (swing) less Max adduction (swing)	less Max plantarflexion (swing) less sagittal ROM(swing) less Max adduction(swing) less transverse ROM (stance+swing)
Hallux/Forefoot		less Max dorsiflexion less ROM (Swing)

The finding in this thesis of a smaller ROM in the injured talocrural joint corresponded to previous findings and were attributed to stiffness, pain and swelling (Nilsson et al., 2003). Our findings of smaller transverse ROM in the forefoot and sagittal ROM in the hallux of the injured side could also be a sign of residual joints stiffness following surgery and immobilization.

The observed reduction of less hindfoot and forefoot plantarflexion and hallux dorsiflexion during preswing could be a compensation strategy for the restricted motion of the injured ankle joint, which indicates that patients tended to lift rather than push off the foot, prolonging the double-support phase.

Although no direction comparison can be made between our study and the study by Becker et al. (1995), our observations of less adducted forefoot in the injured side indicated that the forefoot may be the compensation area of the injured ankle. We also found that compared to the controls, the hallux of the non-injured foot was in more varus during the stance phase. Further investigation is needed to identify whether it was also an influence of the injured ankle.

In our study, the Olerud/Molander ankle score was found to fair-moderately correlate with Hindfoot/Tibia peak dorsiflexion and sagittal ROM in the swing phase, which contradicted the study by Losch *et al.* (2002), who did not find significant correlations between gait and clinical parameters examined by a different functional score. However, temporal-spatial parameters indicated weak correlations with the clinical score both in our and their study.

DYNAMIC JOIONT STIFFNESS AND ITS SUB-COMPONENTS (STUDY II)

The main contribution of this study was to propose and investigate the feasibility of decomposing DJS analytically into sub-components. We succeeded in identifying biomechanical contributions to the ankle DJS by determining pathology-induced changes in subjects with JIA and ITW. As far as we know, it is the first attempt to decompose DJS analytically and to evaluate whether individual contributors to DJS help to explain differences that can be observed in patient groups. These two very different patient groups were specifically chosen to provide a wide spectrum of gait pathologies for this study.

In the control subjects, ankle moment-angle loops showed a counter-clockwise traversed path, which agreed with a recent study from Crenna and Frigo (2011). According to our results, the ankle DJS varied distinctively in the ERP and LRP, and supports the 'ankle-rocker' and 'forefoot-rocker' definitions by Perry and Burnfield (2010). Similar to a previous study, the ERP and the DP of the moment-angle loop at the ankle joint have a relatively similar slope in able-bodied subjects, just shifted along the horizontal axis (Frigo et al., 1996). Although there were some differences found in the JIA group, the shape of the moment-angle loop was similar to that of controls (see Fig 1 in Paper II). The ankle moment-angle loop of the subjects with ITW showed a more complex path due to the double bump moment pattern (see Fig 2 in paper II); there was a unique short descending phase between the ERP and LRP.

Using decomposition, ankle DJS can be isolated into three components. Component 1, the term representing the ratio of changes of GRF moment to the changes in ankle angle, was the dominant contributor, and Components 2 and 3, the terms due to foot accelerations and gravity were negligible (see Fig 4 in Paper II).

Our findings suggest that sub-components 1A and 1B were the primary indicators to identify distinctive, intuitive and interpretable DJS patterns in the control and patient groups (Table 5 and Figs 5A-B in Paper II). Even though the overall DJS can be similar between groups, e.g., in the DP, this could be due to a combination of different biomechanical phenomena, which can only be observed through analytical decomposition.

Walking speed was significantly lower in subjects with JIA and ITW, but, no significant associations with ankle DJS were found. Nevertheless, some associations were observed between walking speed and components 2 and 3.

late rising phase (LRP) and descending phase (DP). The numerator was further decomposed into component 1A and Component 1B (Nm/kg/s). Table 5: The Component 1 was decomposed into numerator and denominator (°/s) in early rising phase (ERP), short descending phase (SDP), Significant group differences were illustrated in bold (Comp1A: Component 1A; Comp1B: Component 1B; JI A: juvenile idiopathic arthritis; ITW: idiopathic toe walking).

		66			9						5	
,		CKF			SUL			LKF			7	
Mean	Nume	Numerator	Deno-	Numerato	rator	Deno-	Nume	Numerator	Deno-	Nume	Numerator	Deno-
(S.D)	Comp 1A	Comp 1B	minator	Comp 1A	Comp 1B	minator	Comp 1A	Comp 1B	minator	Comp 1A	Comp1B	minator
Control	2.67	-0.38	69.54		NA		2.65	3.15	29.56	-3.31	-11.98	-238.2
	(1.25)	(0.47)	(16.92)				(0.69)	(1.07)	(12.62)	(1.46)	(1.89)	(39.55)
All	1.66	-0.41	71.62		NA		2.89	2.22	41.08	-1.96	-11.31	-209.14
	(1.18)	(0.33)	(29.93)				(1.57)	(1.08)	(10.09)	(1.04)	(1.99)	(50.38)
MI	0.89	8.12	158.12	-1.01	-2.31	-47.42	-0.72	3.88	39.57	-2.88	-8.32	-193.28
	(1.22)	(4.87)	(40.02)	(0.65)	(1.89)	(24.74)	(0.54)	(3.18)	(15.79)	(1.69)	(5.11)	(47.08)

INDUCED JOINT ANGULAR ACCELERATIONS AND BODY CENTER OF MASS ACCELERATIONS (STUDY III-V)

Study III

The main contribution of this study was to identify how gait deviations in one plane (i.e. excessive subtalar inversion or eversion) can affect the dynamic function of the TA, GAS and SOL to accelerate joints in other planes (e.g. sagittal plane) and body COM (see Figs 1-4 in Paper III). The findings of the current study attempted to shed some light on the relationship between pathological gait and individual muscle function by simulating a common ankle malalignment.

In accordance with a previous study (Kimmel and Schwartz, 2006), in unaltered gait, the muscles generally acted as expected, i.e. TA dorsiflexed the ankle, and SOL and GAS plantarflexed the ankle. We also found that the GAS can extend knee in the 1st and 3rd rockers, contrary to its anatomical description as a knee flexor, which corresponded to a previous report of the bi-articular muscle's counterintuitive function (Neptune et al., 2004).

Our findings suggest that less effective ankle dorsi/plantarflexors may result from excessive subtalar eversion. This can diminish the GAS' ability to plantarflex the ankle, and the SOL' ability to extend the knee, and increase the TA's ability to flex the hip during the 1st rocker, which may lead to a less plantarflexed ankle, less extended knee and more flexed hip after initial contact.

It is worth noting that in normal gait, we found the SOL and GAS to have potentials to evert the subtalar joint, which was in contrast with their anatomical function as invertors (Perry, 1992; Neptune et al., 2004). This can be interpreted using inertial coupling, where the large plantarflexion acceleration generated by the SOL and GAS at the ankle also caused eversion acceleration at the subtalar joint. It could overwhelm the inversion accelerations caused by the muscles' and ground foot joint reaction force's smaller inversion leverage.

Our findings of vertical support and forward progression accelerations generated by plantarflexors during the late-stance in normal gait corresponded to previously reported findings (Kepple et al., 1997; Gottschall and Kram, 2003). The findings of the TA's ability to support the body and decelerate forward progression after initial contact was consistent with its established action to resist foot fall in the 1st rocker. In our study, the SOL was also found to have greater decelerating potential in the 2nd rocker. Furthermore, excessive subtalar inversion had a negative effect on the ankle dorsiflexor's supporting function, but generated larger support in excessive subtalar eversion.

Study IV

The main contribution of this study was to illustrate the sensitivity of computed (potential) ankle muscle functions to the foot-ground contact models, whose joints had varying locations (comparison 1) and DOFs (comparison 2). The influences of medial and lateral COP shift (comparison 3) on the potential muscle function were also evaluated. The potential muscle function was determined by quantifying the contributions of the GAS, SOL and TA to the angular accelerations of hip, knee, ankle and subtalar joints.

Our findings indicate that both joint locations (i.e., the location of applying constraint force) and prescribed DOFs affect the predicted potential muscle function, while the joint locations were more influential. Qualitative trends in lower joints' sagittal plane muscle induced acceleration (MIA) were similar; but more pronounced differences were found in the hip frontal and transverse plane accelerations (see Figs 2-3 and Table 1 in Paper IV). This was as expected because the location of

application in the horizontal plane (ground) would influence the constraint forces in the frontal and transverse planes.

The influence of COP path are complicated to predict, as MIAs are dependent on the location and direction of the joint axis, muscle moment arm, constraint reaction forces and their moment arms. Our findings suggest that locations of the COP have considerable effects on the potential muscle functions in the non-sagittal plane, though differently for different muscles, joint and sub-phases (see Fig 5-6 and Table 3 in Paper IV).

Among all three muscles, only TA's induced accelerations were affected by all three variations in FGC models, while GAS's and SOL's induced accelerations were negligibly influenced by the constraint joint of DOFs.

Study V

The main contribution of this study was to identify muscles' compensation strategies to overcome increased co-contraction from two antagonistic pairs (GAS-TA and SOL-TA) and retain a normal walking pattern. The findings of the study can provide insights into how synergistic muscles and proximal muscles adapt to the co-contraction of ankle muscles, which would be helpful in clinical interpretation of motion analysis.

In this study, comparable co-contraction index (CI) as in Falconer and Winter's study (1985) can be found in normal gait. The highest CI was found during the mid-stance and the lower in the pre-swing, which reflected the large demand for ankle stability in body weight support and control of shank advancement while stability requirement declined in pre-swing.

Our findings indicate that with high levels of dorsiflexor/plantarflexor co-contraction, one can still perform normal walking through other means; the dynamic equations of motions can be fully satisfied under relatively high levels of muscle co-contraction.

When increased co-contraction in the GAS-TA pair was simulated, the nearby synergistic muscles (e.g. SOL for plantarflexion acceleration, and VAS and RF for knee extension acceleration) contributed most to compensation and least alterations were noticed in remote joint muscles (see Fig 3-4 in paper V). In contrast, with SOL-TA co-contraction, SART and HAMS can provide important compensatory roles in knee accelerations (see Fig 5 in paper V).

We also found that the ankle and knee muscles alone can provide sufficient compensations at the ankle joint, but hip muscles must be involved to generate sufficient knee moment.

GENERAL DISCUSSIONS

Induced Joint Accelerations (Studies III-V)

A muscle can simultaneously accelerate all joints in the body, even those not spanned by the muscles, though a muscle can generate a torque about a joint only if it crosses that joint. From a mathematical point of view, this is due to the fact that the inverse of the system mass matrix is non-diagonal; any one muscle force contributes instantaneously to any acceleration (Eq.7). This phenomenon is referred as dynamic coupling, whereby the force applied by a muscle is transmitted through the bones to all the joints in the body (Zajac and Gordon, 1989). In **Studies III** + IV, ankle muscles were found to have potentials to accelerate all lower limb joints and in all three planes. In **Study V**, ankle muscles could also accelerate the knee joint and vice versa. Moreover, the knee joint muscles may also be involved in the compensation strategy for ankle antagonistic muscle co-contraction. For instance, HAMS and VAS

can alter their contributions at the ankle when if tibialis anterior increases its excitation in the 2^{nd} subphase in SOL-TA pair (see Fig 5 in Paper V).

Dynamic simulation has become an integral part of analyzing human movement, e.g. to understand fundamental muscle functions using IAA, but it is still very challenging. The foundation for generating simulation relies on musculoskeletal models based on many assumptions, e.g physiological properties and paths of muscles and tendons, inertial properties of body segments, the interaction of foot to the ground, etc. (Zajac et al., 2002). In this thesis, we have evaluated the induced joint accelerations with three FGC models – 'fixed joint' (**Studies III+IV**), 'point joint' (**Study IV**), and 'RollingOnSurface' (**Study V**) - and opposing contributions from the GAS, SOL and TA were found in the hip and knee joints (Table 6), but identical at the ankle and subtalar joints. It is worthy to note that a different musculoskeletal model was used in **Study V** than in **Studies III+IV**.

Superposition — which refers to that the sum of the contributions of all forces (e.g. muscles, gravity and centrifugal forces to the GRF must be equal to the overall GRF measured in an experimental motion analysis — has been suggested as a validation method for FGC models and predicted muscle forces. We have evaluated that the sum of all contributions due to e.g. muscles, gravity etc. in two models ('fixed joint' and 'point' in **Study IV** and 'RollingOnSurface' in **Study V**) to the GRF were in relatively good agreement with the measured GRF, which may indicate that superposition is not sufficient to validate the predicted muscle function. A recent study also suggested that superposition error can only quantify the accuracy with which all forces sum to the total GRF; it does not verify the calculations of the contributions of the individual action forces themselves (Dorn et al., 2011). Until today, muscle forces cannot be measured non-invasively in vivo, which has limited the ability to validate the accuracy of muscle force prediction through computational simulations. Previous studies mostly have evaluated using EMG data (Steele et al., 2010; Liu et al., 2006; Jansen et al., 2012), but, the magnitude of the EMG is difficult to validate and the relationship between muscle force magnitude and EMG magnitude is non-linear (Jonkers et al., 2002; Buchanan et al., 2004). In this dissertation, EMG was used only to evaluate the timing of muscle excitation in **Study V**.

Table 6: The summary of the contributions of gastrocnemius (GAS), soleus (SOL), and tibialis anterior (TA) to the hip and knee joints. The shaded region represented that the data was available for comparison in all three foot-ground contact models (FGC). The definition of the sub-phase was according the definition in Paper III (FLEX: flexion; EXT: extension; ABD: abduction; ADD: adduction; EXTR: external rotation; INTR: internal rotation).

		Hip							knee	
	FGC models	Sagittal	Frontal		Transverse			Sagittal		
		2nd	1st	toe-off	1st	2nd	3rd	1st	2nd	
GAS	Fixed	FLEX	ABD	ADD				EXT		
	Point	EXT	ADD	ABD				FLEX		
	RollingOnSurface									
SOL	Fixed		ABD	ADD	EXTR				EXT	
	Point		ADD	ABD	INTR				EXT	
	RollingOnSurface								FLEX	
TA	Fixed		ADD	ABD		INTR	INTR			
	Point		ABD	ADD		EXTR	EXTR			
	RollingOnSurface									

In **Study III**, we have evaluated the effect of excessive subtalar inversion/eversion on potential muscle contributions at lower limb joints, which in fact was the consequences of two factors; one is the excessive subtalar joint angle and another is the corresponding location alteration of the foot-ground contact joint. Although we have used a different FGC model in **Study IV**, interestingly, we found that the medial and lateral COP shift had opposing influences as the combined factors in **Study III**. For instance, the FGC joint location was moved medially in subtalar eversion in **Study III**, which corresponded to the case of medial COP shift in **Study IV**. We observed that the GAS increased its potential to evert the subtalar and to plantarflex the ankle (see Fig 2 in Paper III), but the GAS decreased its potential to evert the subtalar and to plantarflex the ankle when COP was shifted medially (see Fig 7 in Paper IV).

Co-contraction and dynamic joint stiffness (Studies II+V)

The stiffness of a joint is the result of both passive and active stiffness. Passive stiffness depends on the geometry and the tissues surrounding the joint, e.g. capsules, ligaments, and muscles. The muscle stiffness can be modulated dynamically, independently of variations in length, through changes in the activation level (Latash, 1993). Thus, muscle co-contraction is the mechanism most commonly proposed for the regulation of joint stiffness (Holt et al., 2003). This mechanism was demonstrated by the results of studies that reported increases in the stiffness of joints associated with voluntary increases in the intensity of co-contraction of the muscles acting on them (Gardner-Morse and Stokes, 2001). We may also expect that DJS is positively correlated to muscle co-contraction at a joint, i.e. increased co-contraction can increase the stiffness of the joint. However, a study has reported that the co-contraction varied independently from knee DJS during gait in anterior cruciate ligament-deficient patients (Gardinier, 2009).

In **Study V**, we have simulated ankle plantarflexor/dorsiflexor co-contractions in normal, medium and high levels, wherein the ankle DJS was constant. In such cases, the increasing muscle stiffness from an antagonistic pair must be compensated for by decreasing co-contraction from other muscles, which is an interesting question, but, rather complicated since both local and remote muscles contribute to the joint stiffness.

CONCLUSIONS AND FUTURE WORK

The objective of the thesis has been to evaluate gait changes and muscle roles due to foot and ankle injury, malalignment or pathology-related disorders. Gait analysis, analytical studies and computational simulation are independent but integrated methods, and were used in five individual studies. The findings of the studies elucidated the important biomechanical consequences of gait impairment at the foot and ankle and may be useful in clinical interpretation of motion analyses.

Study I presented new data of gait and foot motions in patients one year after ankle fracture surgery. Although the clinical functional score showed fairly good post-operative results, some kinematic deviations were still observed, even in the non-injured area, e.g. the forefoot. Restricted range of motion at and around the injured ankle was believed to be a sign of residual stiffness due to the surgery and immobilization, which also possibly led to the secondary motion restriction and deviations found in the forefoot and hallux segment. Gait analysis can be considered as an additional dynamic post-treatment evaluation for patients with foot injury. The strategy adopted to compensate for ankle injury can be used as a reference for future patient evaluations.

Suggestions for future studies include a 3D multi-segment foot kinetic model and plantar pressure analysis. They will help to relate foot motion with kinetics and loading patterns which may lead to a better understanding of gait strategy and help in the specific rehabilitation decision-making.

Study II proposed and investigated a new analytical decomposition analysis of ankle dynamic joint stiffness (DJS) in healthy subjects and subjects with juvenile idiopathic arthritis and idiopathic toe walking. By evaluating individual components of DJS, we found that the group differences were due almost entirely to changes in component 1 (the term associated with GRF moment) via different subcomponents. For instance, lower DJS in subjects with juvenile idiopathic arthritis in the early rising phase was due to a smaller sub-component 1A (the changes of GRF moment arm times GRF); Large DJS in subjects with idiopathic toe walking in the early rising phase was due to large sub-component 1B (GRF moment arm times changes in GRF). Moreover, changes in ankle angle also influenced ankle DJS. The proposed analytical decomposition confirmed our hypothesis that stiffness changes in pathological gait could be identified and interpreted using individual components, and was applicable in clinical gait evaluation in joint behavior.

A suggestion for future improvement involves investigation of the correlation between muscles' activities, physiological changes and ankle joint passive stiffness. This will help to address the essential cause of the joint stiffness. In addition, the ankle joint behavior may be completely understood only when studied in relation to the other lower limb joints, which could be an interesting future extension of the analytical method.

Study III identified how joint malalignment (subtalar inversion or eversion) can alter the dynamic functions of individual ankle dorsiflexors and plantarflexors. It was confirmed that, in normal gait, muscles generally act as their anatomical definitions and can also create motion in joints they do not span. We also found that excessive subtalar eversion can enhance ankle plantarflexors and tibialis anterior's function. Induced acceleration analysis demonstrated its ability to isolate the contributions of individual muscles to a given factor and provided a means to analyze how muscles can create motion in joints. Although gait deviations here were manipulated from normal configurations, induced acceleration analysis can shed some light on the interaction between pathological gait and individual muscle functions.

Future improvement considering more accurate foot-ground constraints with underfoot spring elements, and real pathological gait data and muscle excitation pattern input will help to create a more realistic computational model and provide a better solution to quantify muscle roles in pathological gait. In addition, analyses involving kinematics, kinetics and individual muscle function can give a whole picture of the biomechanical consequences arising from certain foot deformities or injuries.

Study IV illustrated the sensitivities of computed potential ankle muscle functions on the parameters of the foot-ground contact (FGC) models by quantifying induced lower limb joints accelerations. Our findings indicated that both joint locations and prescribed degrees-of-freedom of FGC models affected the predicted potential muscle function, with the joint locations more influential. In general, small influences were observed in sagittal plane joint accelerations but pronounced influences can be found in the non-sagittal planes. In addition, the locations of the center of pressure also have considerable effects on the potential muscle functions in the non-sagittal planes, though differently for different muscles, joint and sub-phases. Among all three muscles, the tibialis anterior was the only one whose induced accelerations were affected by all three variations in FGC models, while the gastrocnemius and soleus were influenced trivially by the degrees-of-freedom of the constraint joint.

Future improvement considering validating muscle excitation pattern will help to improve confidence in the superposition error and extend the possibility to study the influence of FGC models on the predicted muscle forces considering both the timing and magnitude of muscle excitation pattern. In addition, a larger cohort would also help to establish statistical confidence in the results.

Study V identified how redundancy in muscle contributions to ankle and knee angular accelerations during walking allows the central nervous system to compensate for ankle antagonistic muscle co-contraction to retain a normal walking pattern. Our findings imply that subjects with even a high level of the co-contraction can still perform normal walking. The compensatory mechanisms at the knee joint can mostly be provided by knee muscles, though plantarflexors play an important role at the ankle. The results of the study can be informative for clinical interpretation of motion analyses in persons with motion disorders, when secondary muscle co-contraction or deficits may occur simultaneously.

A suggestion for future improvement involves the actual muscle co-contraction pattern from pathological populations, which would lend confidence in representing the co-contraction in a neuromuscular impairment. It would also be interesting to investigate the static and dynamic relations between muscle force and imposed stretches, which was indicated as one of the possible ways that the central nervous system modulates the muscle coordination.

SUMMARY OF PAPERS

PAPER I

The study aimed to quantify foot kinematics and tempo-spatial changes in patients one year after surgically treated ankle fractures. A validated multi-segment foot model was used in 3D gait analysis. The gait parameters from 18 subjects were compared to age and gender matched controls. Findings of this study showed that unilateral talocrural fractures can still affect other areas in the foot one year after the surgery.

PAPER II

The study aimed to explore the hypothesis that joint stiffness changes in pathological gait could be identified and interpreted using individual components. The ankle dynamic joint stiffness was analyzed and decomposed into three components in thirty able-bodied children, eight children with juvenile idiopathic arthritis and eight children with idiopathic toe-walking during the stance phase of gait. Findings of the current study indicate that analytical decomposition can help identify the individual contributors to joint stiffness and clarify the sources of differences in patient groups.

PAPER III

The study aimed to determine how malalignment in one plane (subtalar inversion or eversion) can alter the capacity of muscles to generate joint angular and body translational accelerations in other planes (e.g. sagittal plane). Induced acceleration analysis was used to compute the accelerations produced by the gastrocnemius, soleus and tibialis anterior in five subtalar inversion or eversion configurations. Excessive subtalar everison was found to enhance the ankle dorsiflexor's and plantarflexor's function.

PAPER IV

This paper described a parametric study on eight healthy adults to analyze how sensitive the muscle-induced joints' accelerations are to the parameters of the rigid foot-ground contact model. We quantified induced accelerations by the gastrocnemius, soleus and tibialis anterior at the hip, knee, ankle and subtalar joints. We compared two types of models, a 'fixed joint' model with three fixed joints under the foot and a 'moving joint' model with one joint located along the moving center of pressure. Findings of the current study indicate that care should be taken in applying appropriate constraints and locations of the foot-ground contact joints, especially in investigations of frontal and transverse plane joint accelerations.

PAPER V

The purpose of this study was to identify the necessary compensation strategies to overcome excessive antagonistic muscle co-contraction at the ankle joint and retain a normal walking pattern. Muscle-actuated simulation of normal walking and induced acceleration analysis were performed to quantify compensatory mechanisms of primary ankle and knee muscles in the presence of normal, medium and high levels of co-contraction of two antagonistic pairs in single-limb stance and pre-swing phases. The study showed that if the co-contraction level increases, the nearby synergistic muscles can contribute most to compensation.

ACKNOWLEDGEMENT

Here, I would like to express my sincere gratitude to all those who have supported me during my invaluable years in studies, and especially to:

Dr. Lanie Gutierrez-Farewik, my main supervisor, for her unwavering confidence and support in me in anytime, for always being unselfishly sharing her knowledge and experience, and guiding me to growing as a researcher. Also, I have very much appreciated Lanie's talking about other important things in life.

Dr. Eva Broström, my co-supervisor, for supporting me to be able to continue my study, for all the time and effort she put into collecting gait data, sharing her wealth of clinical knowledge and for her constructive criticism and critical discussion with me.

Prof. Anders Eriksson, my co-supervisor, for his interest to adopt me into his research group and for his willingness to help and support me in the doctoral study.

Anna-Clara Esbjörnsson, PT, my co-author, for her effects and time in enrolling patients and collecting data, for her hospitality to invite me to spend the first Swedish midsummer and teach me how to make sill smörgås.

Dr. Charlotte K. Thur, and Dr. Per Wretenberg, my co-authors, for sharing their knowledge in clinical practices and enthusiasm in gait analysis.

Dr. Åsa Bartonek, for her willingness to help me with data collecting, inspirited discussion about gait, orthoses, and telling me everything about Sweden.

My group colleagues in Department of Mechanics and Astrid Lindgrens Motorik Lab, for their willingness and time to participate in my study, and for interesting and inspiring scientific discussions.

My other research colleagues, friends and the administration staff in the Department of Mechanics, especially Antonios Monokrousos, Natalia Kosterina, Zeinab Pouransari, Eva Voronkova.

All people who participated in the gait analysis. Without you, there would have been no thesis.

I would like to thank Peter Loan, Julia Stebbins, Ayman Habib, Carlo Frigo and other colleagues from domestic and abroad in field of biomechanics and gait analysis, for them unselfishly sharing their knowledge, being patient to answer me questions and inspiring discussions.

My parents and parents in law, grandparents and grandparents in law, uncle and aunts, and all family members, for inspiring me at my young age, being always loving and supporting me. (谢谢我的父母们,祖父母们,寄伯一家,舅舅一家,大姑一家以及所有的家庭成员,谢谢他们从小的鼓励和后发,永远的爱和支持).

Finally to Wenkan, best friend and my forever love, for bringing new light, courage and endless joy into my life, for his understanding, supporting and tolerance (文侃,最好的朋友和永远的爱人,谢谢你为我的生命带了新的光芒和勇气,谢谢你的支持,理解和宽容).

Funding for this thesis was generously provided by the Swedish Research Council and the Frimurare Barnhuset Foundation.

REFERENCE LIST

Abboud, R. J., (2002). (i) Relevant foot biomechanics. Curr Orthopaed 16, 165-179.

Anderson, F. C., John, C. T., Guendelman, E., Arnold, A. S., Delp, S. L., (2006). SimTrack: Software for Rapidly Generating Muscle-Actuated Simulations of Long-Duration Movement., Taipei, Taiwan.

Anderson, F. C., Pandy, M. G., (1999). A Dynamic Optimization Solution for Vertical Jumping in Three Dimensions. Comp Methods Biomech Biomed Eng 2, 201-231.

Anderson, F. C., Pandy, M. G., (2001). Dynamic optimization of human walking. J Biomech Eng 123, 381-391.

Anderson, F. C., Pandy, M. G., (2003). Individual muscle contributions to support in normal walking. Gait Posture 17, 159-169.

Armand, S., Watelain, E., Mercier, M., Lensel, G., Lepoutre, F. X., (2006). Identification and classification of toe-walkers based on ankle kinematics, using a data-mining method. Gait Posture 23, 240-248.

Arnold, A. S., Salinas, S., Asakawa, D. J., Delp, S. L., (2000). Accuracy of muscle moment arms estimated from MRI-based musculoskeletal models of the lower extremity. J Comp Aid Surg 5, 108-119.

Arnold, E. M., Ward, S. R., Lieber, R. L., Delp, S. L., (2010). A model of the lower limb for analysis of human movement. Ann Bio Eng 38, 269-279.

Bacon, M. C., White, P. H., Raiten, D. J., Craft, N., Margolis, S., Levander, O. A., Taylor, M. L., Lipnick, R. N., Sami, S., (1990). Nutritional status and growth in juvenile rheumatoid arthritis.

Baker, L. D., (1956). A Rational Approach to the Surgical Needs of the Cerebral Palsy Patient. J Bone Joint Surg Am 38, 313-323.

Baker, R., (2007). The history of gait analysis before the advent of modern computers. Gait & Posture 26, 331-342.

Basmajian, J. V., Licht, S. H., (1978). Therapeutic exercise. Williams & Wilkins, Baltimore.

Becker, H. P., Rosenbaum, D., Kriese, T., Gerngross, H., Claes, L., (1995). Gait asymmetry following successful surgical treatment of ankle fractures in young adults. Clin Orthop Relat Res 311, 262-269.

Bengner, U., Johnell, O., Redlund-Johnell, I., (1986). Epidemiology of ankle fracture 1950 and 1980. Increasing incidence in elderly women. Acta Orthop Scand 57, 35-37.

Benoit, D. L., Ramsey, D. K., Lamontagne, M., Xu, L., Wretenberg, P., Renström, P., (2006). Effect of skin movement artifact on knee kinematics during gait and cutting motions measured in vivo. Gait Posture 24, 152-164.

Berntson, L., Andersson-Gäre, B., Fasth, A., Herlin, T., Kristinsson, J., Lahdenne, P., Marhaug, G., Nielsen, S., Pelkonen, P., Rygg, M., (2003). Incidence of juvenile idiopathic arthritis in the Nordic

countries. A population based study with special reference to the validity of the ILAR and EULAR criteria. J Rheumatol 30, 2275-2282.

Berntson, L., Fasth, A., Andersson-Gäre, B., Kristinsson, J., Lahdenne, P., Marhaug, G., Nielsen, S., Pelkonen, P., Svensson, E., (2001). Construct validity of ILAR and EULAR criteria in juvenile idiopathic arthritis: a population based incidence study from the Nordic countries. International League of Associations for Rheumatology. European League Against Rheumatism. J Rheumatol 28, 2737-2743.

Borelli, G. A., (1989). On the movement of animals. Springer-Verlag, Berlin and New York.

Brand, R. A., Crowninshield, R. D., Wittstock, C. E., Pedersen, D. R., Clark, C. R., van Krieken, F. M., (1982). A model of lower extremity muscular anatomy. J Biomech Eng 104, 304-311.

Braune, W., Fischer, O., (1987). The human gait. Springer-Verlag, Berlin.

Brooks, V. B., (1986). The neural basis of motor control. Oxford University Press, New York.

Broström, E., (2004). Juvenile idiopathic arthritis: Disease consequences and treatment effects on muscle strength, gait and pain. Karolinska Institutet.

Buchanan, T. S., Lloyd, D. G., Manal, K., Besier, T. F., (2004). Neuromusculoskeletal modeling: estimation of muscle forces and joint moments and movements from measurements of neural command. J Appl Biomech 20, 367-395.

Campbell, M. J., Machin, D., Walters, S. J., (2007). Medical statistics: a text book for the health sciences. John Wiley & Sons Ltd., Chichester.

Cassidy, J. T., (2002). Textbook of pediatric rheumatology. Churchill Livingstone Inc, New York.

Cheng, P. L., (2000). A spherical rotation coordinate system for the description of three-dimensional joint rotations. Ann Biomed Eng 28, 1381-1392.

Court-Brown, C., McBirnie, J., Wilson, G., (1998). Adult ankle fracture: an increasing problem? Acta Orthop 69, 43.

Crenna, P., Fedrizzi, E., Andreucci, E., Frigo, C., Bono, R., (2005). The heel-contact gait pattern of habitual toe walkers. Gait Posture 21, 311-317.

Crenna, P., Frigo, C., (2011). Dynamics of the ankle joint analyzed through moment-angle loops during human walking: Gender and age effects. Hum Movement Sci 30, 1185-1198.

Czerniecki, J. M., (1988). Foot and ankle biomechanics in walking and running. A review. Am J Phy Med Rehab 67, 246-252.

Daly, P. J., Fitzgerald Jr, R. H., Melton, L. J., Ilstrup, D. M., (1987). Epidemiology of ankle fractures in Rochester, Minnesota. Acta Orthop Scand 58, 539-544.

Damiano, D. L., (1993). Reviewing Muscle Cocontraction. Phys Occup Ther Pediatr 12, 3-20.

Davis, R. B., DeLuca, P. A., (1996). Gait characterization via dynamic joint stiffness. Gait Posture 4, 224-231.

Delp, S. L., Loan, J. P., Hoy, M. G., Zajac, F. E., Topp, E. L., Rosen, J. M., (1990). An interactive graphics-based model of the lower extremity to study orthopaedic surgical procedures. IEEE Trans BioMed Eng 37, 757-767.

Dierick, F., Domicent, C., Detrembleur, C., (2002). Relationship between antagonistic leg muscles cocontractions and body centre of gravity mechanics in different level gait disorders. J Electromyogr Kines 12, 59-66.

DiStefano, V., (2009). Anatomy and biomechanics of the ankle and foot. J Athl Training 16, 43.

Dorn, T. W., Lin, Y. C., Pandy, M. G., (2011). Estimates of muscle function in human gait depend on how foot-ground contact is modelled. Comp Methods Biomech Biomed Eng 1, 1-12.

Ehara, Y., Fujimoto, H., Miyazaki, S., Mochimaru, M., Tanaka, S., Yamamoto, S., (1997). Comparison of the performance of 3D camera systems II. Gait Posture 5, 251-255.

Engelbert, R., Gorter, J. W., Uiterwaal, C., Van De Putte, E., Helders, P., (2011). Idiopathic toe-walking in children, adolescents and young adults: a matter of local or generalised stiffness? BMC musculoskeletal disorders 12, 61-68.

Engström, P., Gutierrez-Farewik, E. M., Bartonek, Å., Tedroff, K., Orefelt, C., Haglund-Åkerlind, Y., (2010). Does botulinum toxin a improve the walking pattern in children with idiopathic toe-walking? J Child Orthop 301-308.

Falconer, K., Winter, D. A., (1985). Quantitative assessment of co-contraction at the ankle joint in walking. Electromyg & Clin 25, 135-149.

Fan, J. S., Wessel, J., Ellsworth, J., (1998). The relationship between strength and function in females with juvenile rheumatoid arthritis. J Rheumatol 25, 1399-1405.

Fox, M. D., Delp, S., (2010a). Contributions of muscles and passive dynamics to swing initiation over a range of walking speeds. J Biomech 43, 1450-1455.

Fox, M. D., Delp, S., (2010b). Contributions of muscles and passive dynamics to swing initiation over a range of walking speeds. J Biomech 43, 1450-1455.

Frigo, C., Crenna, P., Jensen, L. M., (1996). Moment-angle relationship at lower limb joints during human walking at different velocities. J Electromyography Kinesiol 6, 177-190.

Furrer, F., Deonna, T., (1982). Persistent toe-walking in children. A comprehensive clinical study of 28 cases. Helv Paediatr Acta 37, 301-316.

Gabriel, R. C., Abrantes, J., Granata, K., Bulas-Cruz, J., Melo-Pinto, P., Filipe, V., (2008). Dynamic joint stiffness of the ankle during walking: gender-related differences. Phys Ther in Spor 9, 16-24.

Gardinier, E. S., (2009). The relationship between muscular co-contraction and dynamic knee stiffness in ACL-deficient non-coperrs. University of Delaware.

Gardner-Morse, M. G., Stokes, I. A. F., (2001). Trunk stiffness increases with steady-state effort. J Biomech 34, 457-463.

Gäre, B. A., Fasth, A., Andersson, J., Berglund, G., Ekström, H., Eriksson, M., Hammaren, L., Holmquist, L., Ronge, E., Thilen, A., (1987). Incidence and prevalence of juvenile chronic arthritis: a population survey. Ann Rheum Dis 46, 277-281.

Gatev, V., (1972). Role of inhibition in the development of motor coordination in early childhood. Dev Med Child Neurol 14, 336-341.

Giannini, E. H., Brewer, E. J., Kuzmina, N., Shaikov, A., Maximov, A., Vorontsov, I., Fink, C. W., Newman, A. J., Cassidy, J. T., Zemel, L. S., (1992). Methotrexate in resistant juvenile rheumatoid arthritis. Results of the USA-USSR double-blind, placebo-controlled trial. The Pediatric Rheumatology Collaborative Study Group and The Cooperative Children's Study Group. N Engl J Med 326, 1043-1049.

Giannini, M. J., Protas, E. J., (1991). Aerobic capacity in juvenile rheumatoid arthritis patients and healthy children. Arthritis & Rheumatism 4, 131-135.

Goldberg, S. R., Ounpuu, S., Delp, S. L., (2003). The importance of swing-phase initial conditions in stiff-knee gait. J Biomech 36, 1111-1116.

Gottschall, J. S., Kram, R., (2003). Energy cost and muscular activity required for propulsion during walking. J Appl Physiol 94, 1766-1772.

Hagood, S., Solomonow, M., Baratta, R., Zhou, B. H., D'ambrosia, R., (1990). The effect of joint velocity on the contribution of the antagonist musculature to knee stiffness and laxity. Am J Sport Med 18, 182-187.

Hamill, J., Knutzen, K. M., (2006). Biomechanical basis of human movement. Williams & Wilkins, Philadelphia.

Hamner, S. R., Seth, A., Delp, S. L., (2010). Muscle contributions to propulsion and support during running. J Biomech 43, 2709-2716.

Harris, G. F., Smith, P. A., Marks, R. M., (2006). Foot and ankle motion analysis: clinical treatment and technology. CRC Press, Boca Raton.

Hartmann, M., Kreuzpointner, F., Haefner, R., Michels, H., Schwirtz, A., Haas, J. P., (2010). Effects of juvenile idiopathic arthritis on kinematics and kinetics of the lower extremities call for consequences in physical activities recommendation. Int J Pediatri 2010.

Henderson, C. J., Lovell, D. J., Specker, B. L., Campaigne, B. N., (1995). Physical activity in children with juvenile rheumatoid arthritis: quantification and evaluation. Arthritis Care Res 8, 114-119.

Herzog, W., (1996). Force-sharing among synergistic muscles: theoretical considerations and experimental approaches. Exerc Sport Sci Rev 24, 173-202.

Hicks, J., Arnold, A., Anderson, F., Schwartz, M., Delp, S., (2007). The effect of excessive tibial torsion on the capacity of muscles to extend the hip and knee during single-limb stance. Gait Posture 26, 546-552.

Hicks, R., Durinick, N., Gage, J. R., (1988). Differentiation of idiopathic toe-walking and cerebral palsy. J Pediatr Orthop 8, 160-163.

- Hogan, N., (1984). Adaptive control of mechanical impedance by coactivation of antagonist muscles. IEEE T Automat Contr 29, 681-690.
- Holt, K. G., Wagenaar, R. C., LaFiandra, M. E., Kubo, M., Obusek, J. P., (2003). Increased musculoskeletal stiffness during load carriage at increasing walking speeds maintains constant vertical excursion of the body center of mass. J Biomech 36, 465-471.
- Humphrey, D. R., Reed, D. J., (1983). Separate cortical systems for control of joint movement and joint stiffness: reciprocal activation and coactivation of antagonist muscles. Adv in Neuro 39, 347-372.
- Inman, V. T., Ralston, H. J., Todd, F., Lieberman, J. C., (1981). Human walking. Williams & Wilkins, Baltimore.
- Jansen, K., De Groote, F., Massaad, F., Meynas, P., Duysens, J., Jonkers, I., (2012). Similar muscles contribute to horizontal and vertical accelerations of center of mass in forward and backward walking: implications for neural control. J Neurophysiol In Press.
- Jensen, S. L., Andresen, B. K., Mencke, S., Nielsen, P. T., (1998). Epidemiology of ankle fractures. A prospective population-based study of 212 cases in Aalborg, Denmark. Acta Orthop Scand 69, 48-50.
- Jonkers, I., Spaepen, A., Papaioannou, G., Stewart, C., (2002). An EMG-based, muscle driven forward simulation of single support phase of gait. J Biomech 35, 609-619.
- Jonkers, I., Stewart, C., Spaepen, A., (2003). The study of muscle action during single support and swing phase of gait: clinical relevance of forward simulation techniques. Gait Posture 17, 97-105.
- Kannus, P., Parkkari, J., Niemi, S., Palvanen, M., (1996). Epidemiology of osteoporotic ankle fractures in elderly persons in Finland. Ann Intern Med 125, 975-978.
- Karst, G. M., Hasan, Z., (1987). Antagonist muscle activity during human forearm movements under varying kinematic and loading conditions. Exp Brain Res 67, 391-401.
- Kepple, T. M., Siegel, K. L., Stanhope, S. J., (1997). Relative contributions of the lower extremity joint moments to forward progression and support during gait. Gait Posture 6, 1-8.
- Kepple, T. M., Sommer III, H., Lohmann, S. K., Stanhope, S. J., (1998). A three-dimensional musculoskeletal database for the lower extremities. J Biomech 31, 77-80.
- Khazzam, M., Long, J. T., Marks, R. M., Harris, G. F., (2006). Preoperative gait characterization of patients with ankle arthrosis. Gait Posture 24, 85-93.
- Kidder, S. M., Abuzzahab Jr, F. S., Harris, G. F., Johnson, J. E., (1996). A system for the analysis of foot and ankle kinematics during gait. IEEE Trans Rehabil Eng 4, 25-32.
- Kimmel, S. A., Schwartz, M. H., (2006). A baseline of dynamic muscle function during gait. Gait Posture 23, 211-221.
- Klepper, S. E., (1999). Effects of an eight-week physical conditioning program on disease signs and symptoms in children with chronic arthritis. Arthritis Care Res 12, 52-60.
- Klepper, S. E., Darbee, J., Effgen, S. K., Singsen, B. H., (1992). Physical fitness levels in children with polyarticular juvenile rheumatoid arthritis. Arthritis Care Res 5, 93-100.

Koval, K. J., Lurie, J., Zhou, W., Sparks, M. B., Cantu, R. V., Sporer, S. M., Weinstein, J., (2005). Ankle fractures in the elderly: what you get depends on where you live and who you see. J Orthop Trauma 19, 635-639.

Latash, M. L., (1993). Control of human movement. Human kinetics, Champaign, IL.

Lauge-Hansen, N., (1950). Fractures of the ankle. II. Combined experimental-surgical and experimental-roentgenologic investigations. Arch Surg 60, 957-985.

Leardini, A., Benedetti, M. G., Catani, F., Simoncini, L., Giannini, S., (1999). An anatomically based protocol for the description of foot segment kinematics during gait. Clin Biomech 14, 528-536.

Lindehammar, H., Backman, E., (1995). Muscle function in juvenile chronic arthritis. J Rheumatol 22, 1159-1165.

Lindsjö, U., (1985). Classification of ankle fractures: the Lauge-Hansen or AO system? Clin Orthop Relat Res 199, 12-16.

Liu, M. Q., Anderson, F. C., Pandy, M. G., Delp, S. L., (2006). Muscles that support the body also modulate forward progression during walking. J Biomech 39, 2623-2630.

Losch, A., Meybohm, P., Schmalz, T., Fuchs, M., Vamvukakis, F., Dresing, K., Blumentritt, S., Sturmer, K. M., (2002). Functional results of dynamic gait analysis after 1 year of hobby-athletes with a surgically treated ankle fracture. Sportverletz Sportschaden 16, 101-107.

Marshall, R. N., Wood, G. A., Jennings, L. S., (1989). Performance objectives in human movement: A review and application to the stance phase of normal walking. Hum Movement Sci 8, 571-594.

Moseley, L., Smith, R., Hunt, A., Gant, R., (1996). Three-dimensional kinematics of the rearfoot during the stance phase of walking in normal young adult males. Clin Biomech 11, 39-45.

Müller, M. E., Allgöwer, M., Perren, S. M., (1991). Manual of Internal Fixation: Techniques Recommended by the AO-ASIF Group. Springer-Verlag, Berlin.

MusculoGraphics Inc., (2004). SIMM 4.0 (Software for Interactive Musculoskeletal Modeling) user's manual.

Myers, K. A., Wang, M., Marks, R. M., Harris, G. F., (2004). Validation of a multisegment foot and ankle kinematic model for pediatric gait. IEEE Trans Neural Syst Rehabil Eng 12, 122-130.

Myklebust, B. M., Gottlieb, G. L., Agarwal, G. C., (1986). Stretch reflexes of the normal infant. Dev Med Child Neurol 28, 440-449.

Neptune, R. R., Kautz, S. A., Zajac, F. E., (2001). Contributions of the individual ankle plantar flexors to support, forward progression and swing initiation during walking. J Biomech 34, 1387-1398.

Neptune, R. R., Zajac, F. E., Kautz, S. A., (2004). Muscle force redistributes segmental power for body progression during walking. Gait Posture 19, 194-205.

Nester, C., Jones, R. K., Liu, A., Howard, D., Lundberg, A., Arndt, A., Lundgren, P., Stacoff, A., Wolf, P., (2007). Foot kinematics during walking measured using bone and surface mounted markers. J Biomech 40, 3412-3423.

Nilsson, G., Nyberg, P., Ekdahl, C., Eneroth, M., (2003). Performance after surgical treatment of patients with ankle fractures--14-month follow-up. Physiother Res Int 8, 69-82.

Palastanga, N., Field, D., Soames, R., (2006). Anatomy and human movement: structure and function. Butterworth-Heinemann, Oxford.

Pandy, M. G., (2001). Computer modeling and simulation of human movement. Annu Rev Biomed Eng 3, 245-273.

Pandy, M. G., Lin, Y. C., Kim, H. J., (2010). Muscle coordination of mediolateral balance in normal walking. J Biomech 43, 2055-2064.

Peacock, W. J., Arens, L. J., Berman, B., (1987). Cerebral palsy spasticity: selective dorsal rhizotomy. J Pediatr Neurosci 13, 61-66.

Perry, J., (1992). Gait analysis: normal and pathological function. SLACK Inc., Thorofare.

Perry, J., (1998). The contribution of dynamic electromyography to gait analysis. J Rehabil Res Dev 33.

Perry, J., Burnfield, J. M., (2010). Gait analysis: normal and pathological function. SLACK Inc., Thorofare.

Pettrone, F. A., Gail, M., Pee, D., Fitzpatrick, T., Van Herpe, L. B., (1983). Quantitative criteria for prediction of the results after displaced fracture of the ankle. J Bone Joint Surg Am 65, 667-677.

Petty, R. E., Southwood, T. R., Manners, P., Baum, J., Glass, D. N., Goldenberg, J., He, X., Maldonado-Cocco, J., Orozco-Alcala, J., Prieur, A. M., (2004). International League of Associations for Rheumatology classification of juvenile idiopathic arthritis: second revision, Edmonton, 2001. J Rheumatol 31, 390-392.

Reinschmidt, C., Van den Bogert, A., Nigg, B. M., Lundberg, A., Murphy, N., (1997). Effect of skin movement on the analysis of skeletal knee joint motion during running. J Biomech 30, 729-732.

Richards, J. G., (1999). The measurement of human motion: a comparison of commercially available systems. Hum Movement Sci 18, 589-602.

Riley, P. O., Kerrigan, D. C., (1999). Kinetics of stiff-legged gait: induced acceleration analysis. IEEE Trans Rehabil Eng 7, 420-426.

Root, M. L., Orien, W. P., Weed, J. H., (1977). Normal and abnormal function of the foot. Clinical Biomechanics Corp., Los Angeles.

Sala, D. A., Shulman, L. H., Kennedy, R. F., Grant, A. D., Chu, M. L., (1999). Idiopathic toe-walking: a review. Dev Med Child Neurol 41, 846-848.

Saraswat, P., MacWilliams, B. A., Davis, R. B., (2011). A multi-segment foot model based on anatomically registered technical coordinate systems: Method repeatability in pediatric feet. Gait Posture 35, 547-555.

Schneider, R., Passo, M. H., (2002). Juvenile rheumatoid arthritis. Rheum Dis Clin North Am 28, 503-530.

Schwartz, M., Lakin, G., (2003). The effect of tibial torsion on the dynamic function of the soleus during gait. Gait Posture 17, 113-118.

Schwartz, R., Health, A. L., Morgan, D., Towns, S., (1964). A quantitative analysis of recorded variables in the walking pattern of "normal" adults. J Bone Joint Surg Am 46, 324-334.

Sherrington, C. S., (1940). Reciprocal innervation of antagonistic muscles. Selected writings of Sir Charles Sherrington. PB Hoeber Inc., New York, pp. 237-313.

Simon, J., Doederlein, L., McIntosh, A. S., Metaxiotis, D., Bock, H. G., Wolf, S. I., (2006). The Heidelberg foot measurement method: development, description and assessment. Gait Posture 23, 411-424.

Singsen, B. H., (1995). Physical fitness in children with juvenile rheumatoid arthritis and other chronic pediatric illnesses. Pediatr Clin North Am 42, 1035-1050.

Smith, L. K., (1996). Brunnstrom's clinical kinesiology. Davis F.A., Philadelphia.

Stebbins, J., Harrington, M., Thompson, N., Zavatsky, A., Theologis, T., (2006). Repeatability of a model for measuring multi-segment foot kinematics in children. Gait Posture 23, 401-410.

Steele, K. M., Seth, A., Hicks, J. L., Schwartz, M. S., Delp, S. L., (2010). Muscle contributions to support and progression during single-limb stance in crouch gait. J Biomech 43, 2099-2105.

Tateuchi, H., Tsukagoshi, R., Fukumoto, Y., Oda, S., Ichihashi, N., (2011). Dynamic hip joint stiffness in individuals with total hip arthroplasty: Relationships between hip impairments and dynamics of the other joints. Clin Biomech 26, 598-604.

Thelen, D. G., Anderson, F. C., (2006). Using computed muscle control to generate forward dynamic simulations of human walking from experimental data. J Biomech 39, 1107-1115.

Vostrejs, M., Hollister, J. R., (1988). Muscle atrophy and leg length discrepancies in pauciarticular juvenile rheumatoid arthritis. Am J Dis Child 142, 343-345.

Westblad, P., Hashimoto, T., Winson, I., Lundberg, A., Arndt, A., (2002). Differences in ankle-joint complex motion during the stance phase of walking as measured by superficial and bone-anchored markers. Foot Ankle Int 23, 856-863.

White, S. C., Yack, H. J., Winter, D. A., (1989). A three-dimensional musculoskeletal model for gait analysis. Anatomical variability estimates. J Biomech 22, 885-893.

Winter, D. A., (2009). Biomechanics and motor control of human movement. John Wiley & Sons Inc, New Jersy.

Winter, D. A., Patla, A. E., Frank, J. S., Walt, S. E., (1990). The biomechanics and motor control of human gait: normal elderly and pathalogical. Phys Ther 70, 340-347.

Woodburn, J., Nelson, K. M., Siegel, K. L., Kepple, T. M., Gerber, L. H., (2004). Multisegment foot motion during gait: proof of concept in rheumatoid arthritis. J Rheumatol. 31, 1918-1927.

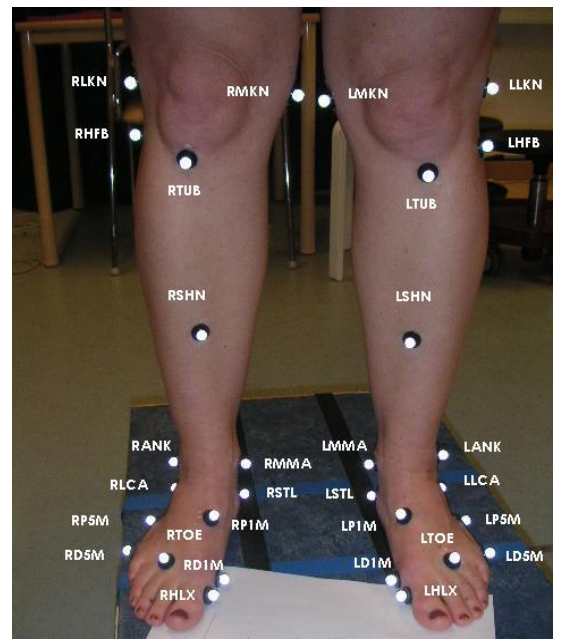
Wright, D. G., Desai, S. M., Henderson, W. H., (1964). Action of the subtalar and ankle-joint complex during the stance. J Bone Joint Surg Am 46, 361-464.

- Zajac, F. E., (1993). Muscle coordination of movement: a perspective. J Biomech 26, 109-124.
- Zajac, F. E., Gordon, M. E., (1989). Determining muscle's force and action in multi-articular movement. Exerc Sport Sci Rev 17, 187-230.
- Zajac, F. E., Neptune, R. R., Kautz, S. A., (2002). Biomechanics and muscle coordination of human walking. Part I: introduction to concepts, power transfer, dynamics and simulations. Gait Posture 16, 215-232.
- Zajac, F. E., Neptune, R. R., Kautz, S. A., (2003). Biomechanics and muscle coordination of human walking: part II: lessons from dynamical simulations and clinical implications. Gait Posture 17, 1-17.
- Zeni Jr, J. A., Higginson, J. S., (2009). Dynamic knee joint stiffness in subjects with a progressive increase in severity of knee osteoarthritis. Clin Biomech 24, 366-371.

APPENDIX

Appendix A: Marker name and placement of modified Oxford foot model.

Fig A1: Marker placement frontal (left) and lateral view (right)



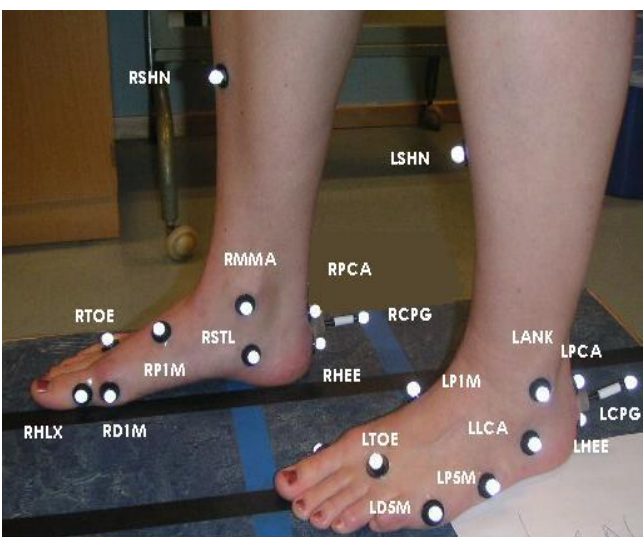
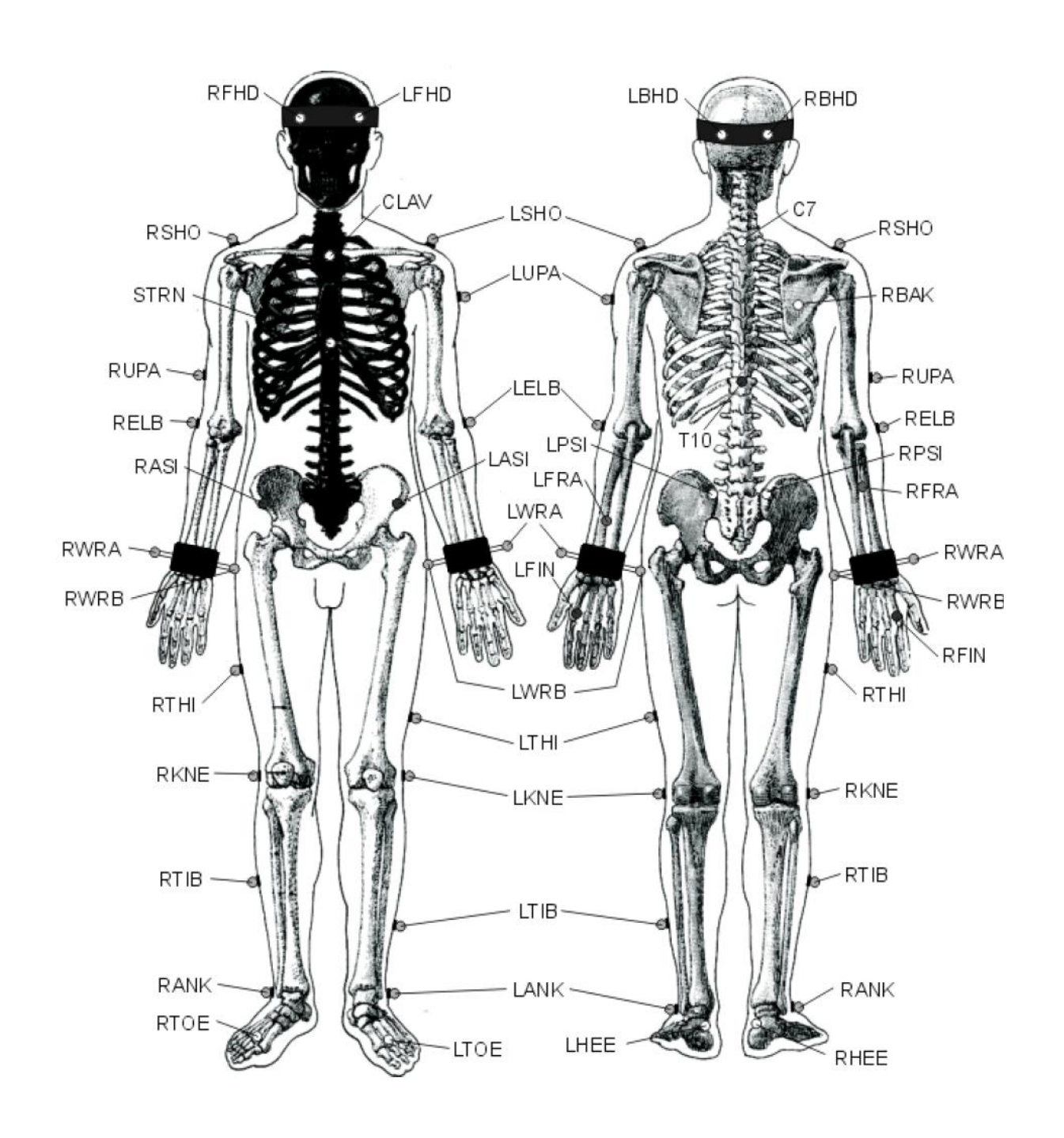


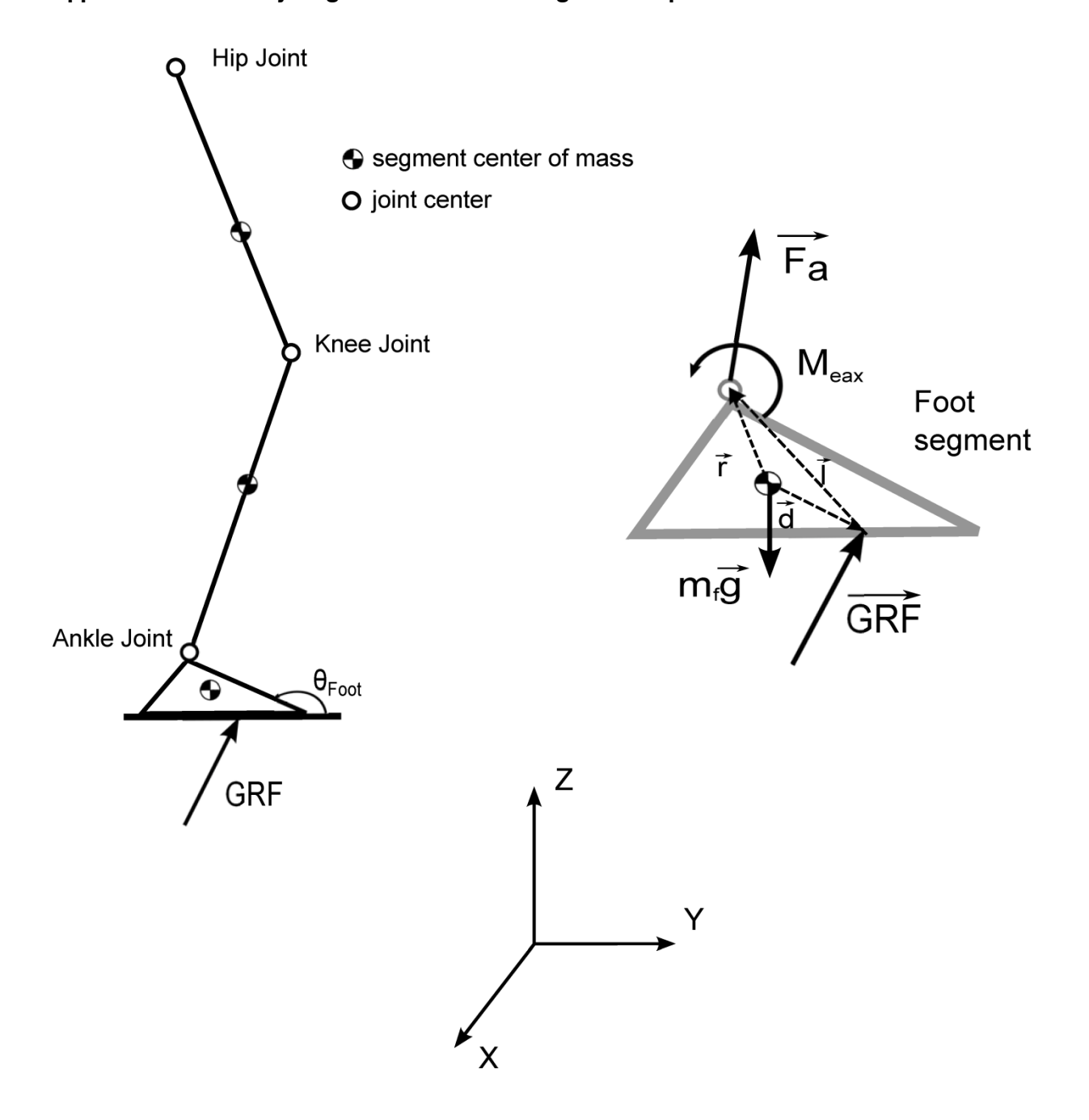
Table A1: Names and positions of markers

Marker Name	Position	Segment
L/RMKN	Left/Right medial femoral condyle	Femur
L/RLKN	Left/Right lateral femoral condyle	Femur
L/RHFB	Left/Right head of fibular	Tibia
L/RTUB	Left/Right tibial tuberosity	Tibia
L/RSHN	Left/Right anterior aspect of shin	Tibia
L/RMMA	Left/Right medial malleolus	Tibia
L/RANK	Left/Right lateral malleolus	Tibia
L/RPCA	Left/Right posterior medial aspect of heel	Hindfoot
L/RCPG	Left/Right wand marker on posterior calcaneus	Hindfoot
L/RHEE	Left/Right posterior distal aspect of heel	Hindfoot
L/RLCA	Left/Right lateral calcaneus	Hindfoot
L/RSTL	Left/Right sustentaculum tali	Hindfoot
L/RP1M	Left/Right base of first metatarsal	Forefoot
L/RP5M	Left/Right base of fifth metatarsal	Forefoot
L/R1DM	Left/Right head of first metatarsal	Forefoot
L/R5DM	Left/Right head of fifth metatarsal	Forefoot
L/RTOE	Left/Right marker between second and third metatarsal heads	Forefoot
L/RHLX	Left/Right base of hallux	Hallux

Appendix B: Marker placement for the whole body model set (Plug In Gait, Vicon, Oxford, UK)



Appendix C: Free body diagram of the foot and leg in stance phase



Appendix D: The equilibrium equations of inverse dynamics (sagittal plane)

With the free body diagram of the foot segment (Appendix B), we have the equations:

$$\sum \vec{F} = m_f \vec{a} \tag{1}$$

$$\sum \vec{M}_f = I_f \vec{\alpha} \tag{2}$$

With the mass of foot m_f , linear acceleration \vec{a} , moment of inertial about the foot's center of mass I_f , we then get

$$\vec{F}_a + \overline{GRF} + m_f \vec{G} = m_f \vec{a} \tag{3}$$

$$M_{eax} + (\vec{r} \times \vec{F}_a)_x + (\vec{d} \times \overline{GRF})_x = I_f \alpha_x \tag{4}$$

Where joint reaction force $\vec{F}_a = \begin{bmatrix} F_{ay} \\ F_{az} \end{bmatrix}$, $\vec{G}\vec{R}\vec{F} = \begin{bmatrix} GRF_y \\ GRF_z \end{bmatrix}$, $\vec{G} = \begin{bmatrix} 0 \\ -g \end{bmatrix}$, $\vec{a} = \begin{bmatrix} a_y \\ a_z \end{bmatrix}$, foot segment angular acceleration α_x , and M_{eax} is the external joint reaction moment in the x-direction (dorsi/plantarflexion moment).

From Eq. (3), we can get:

$$\vec{F}_a = m_f \vec{a} - \overline{GRF} - m_f \vec{G} \tag{5}$$

From Eq. (5) and Eq. (4) with moments summed about the foot's center of mass, we can get:

$$M_{eax} = I_f a_x - m_f(\vec{r} \times \vec{a})_x + \left((\vec{r} - \vec{d}) \times \overline{GRF} \right)_x + m_f (\vec{r} \times \vec{G})_x$$
 (6)

From Appendix C, we know,

$$\vec{l} = \vec{r} - \vec{d} \tag{7}$$

From Eq (6) and Eq (7), we can get:

$$M_{eax} = I_f a_x - m_f (\vec{r} \times \vec{a})_x + (\vec{l} \times \overline{GRF})_x + m_f (\vec{r} \times \vec{G})_x$$
 (8)

We can then define:

$$M_{FAx} = -(I_f \alpha_x - m_f (\vec{r} \times \vec{a})_x) \tag{9}$$

$$M_{GAx} = -m_f(\vec{r} \times \vec{G})_x \tag{10}$$

$$M_{GRFAx} = -(\vec{l} \times \overline{GRF})_x = (\vec{L} \times \overline{GRF})_x \tag{11}$$

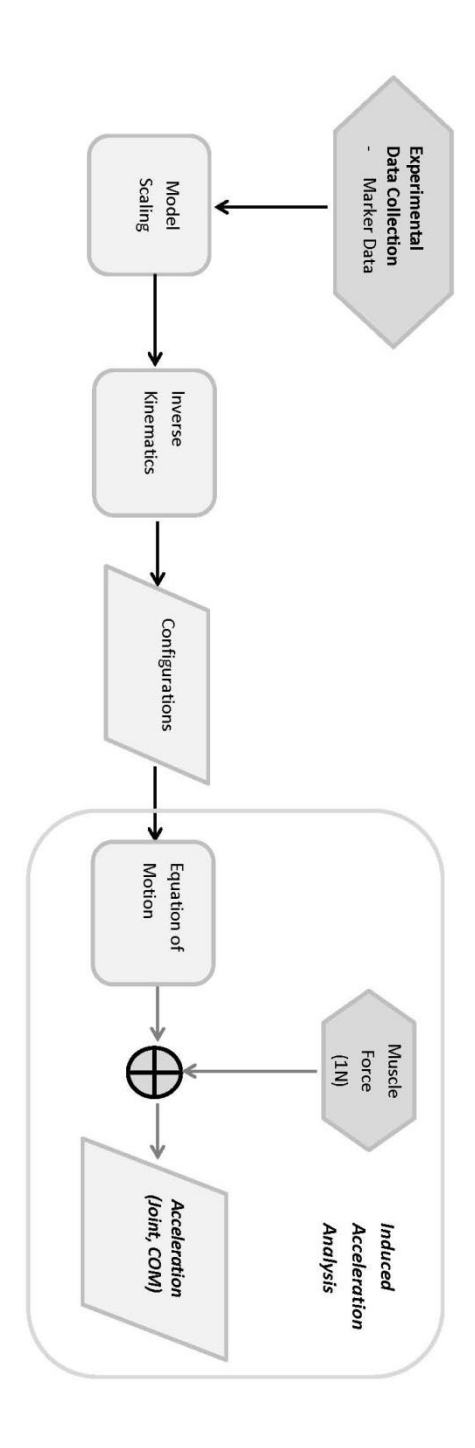
Where M_{FAx} is moment about ankle due to the accelerations (linear and angular), M_{GAx} is moment about ankle due to the segment mass, M_{GRFAx} is moment about ankle due to ground reaction force, and we let $\vec{L} = -\vec{l}$. Eq. (11) can be rewritten as

$$M_{eax} = -M_{GRFAx} - M_{FAx} - M_{GAx} \tag{12}$$

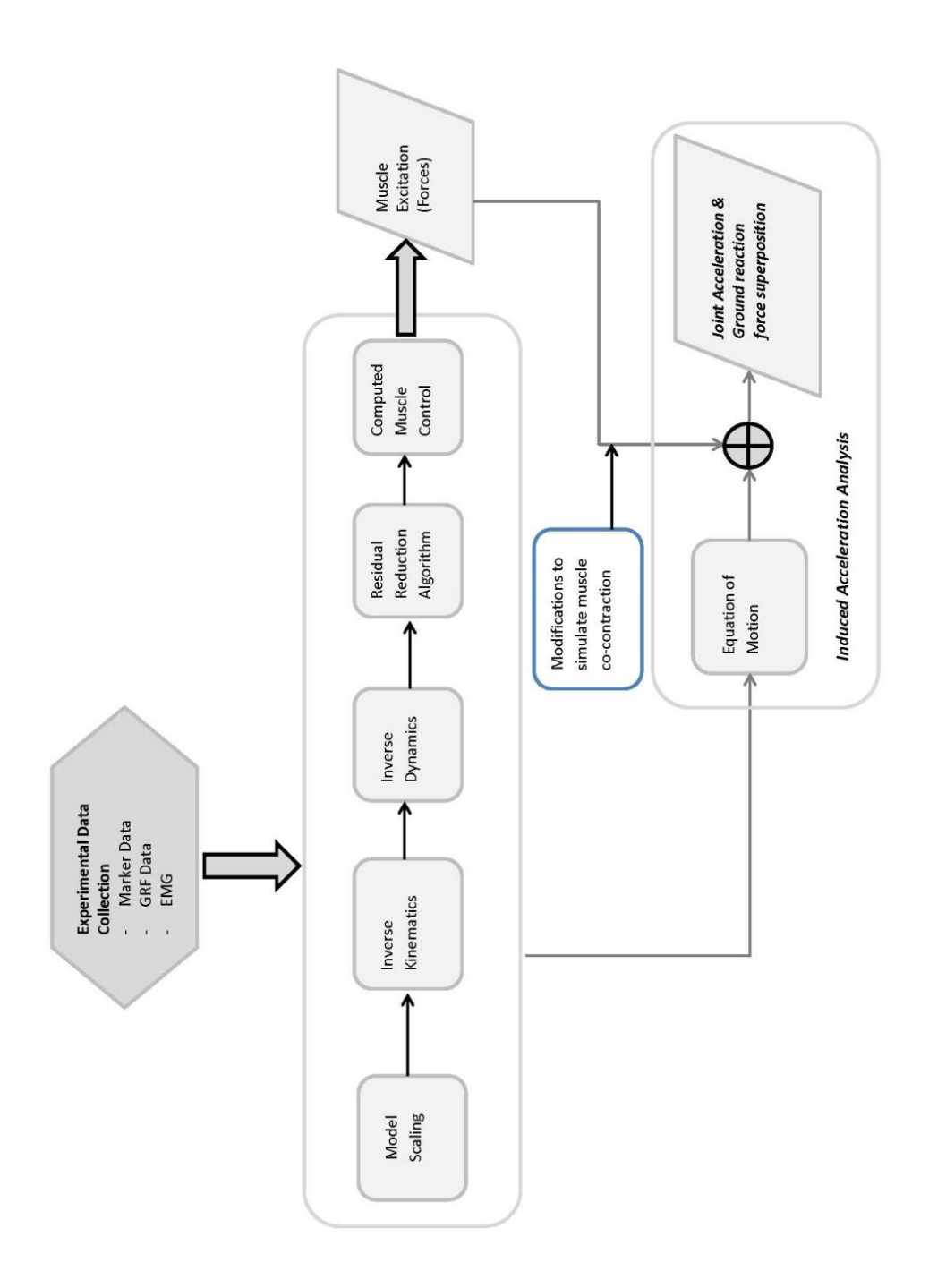
$$M_{ax} = -M_{eax} (13)$$

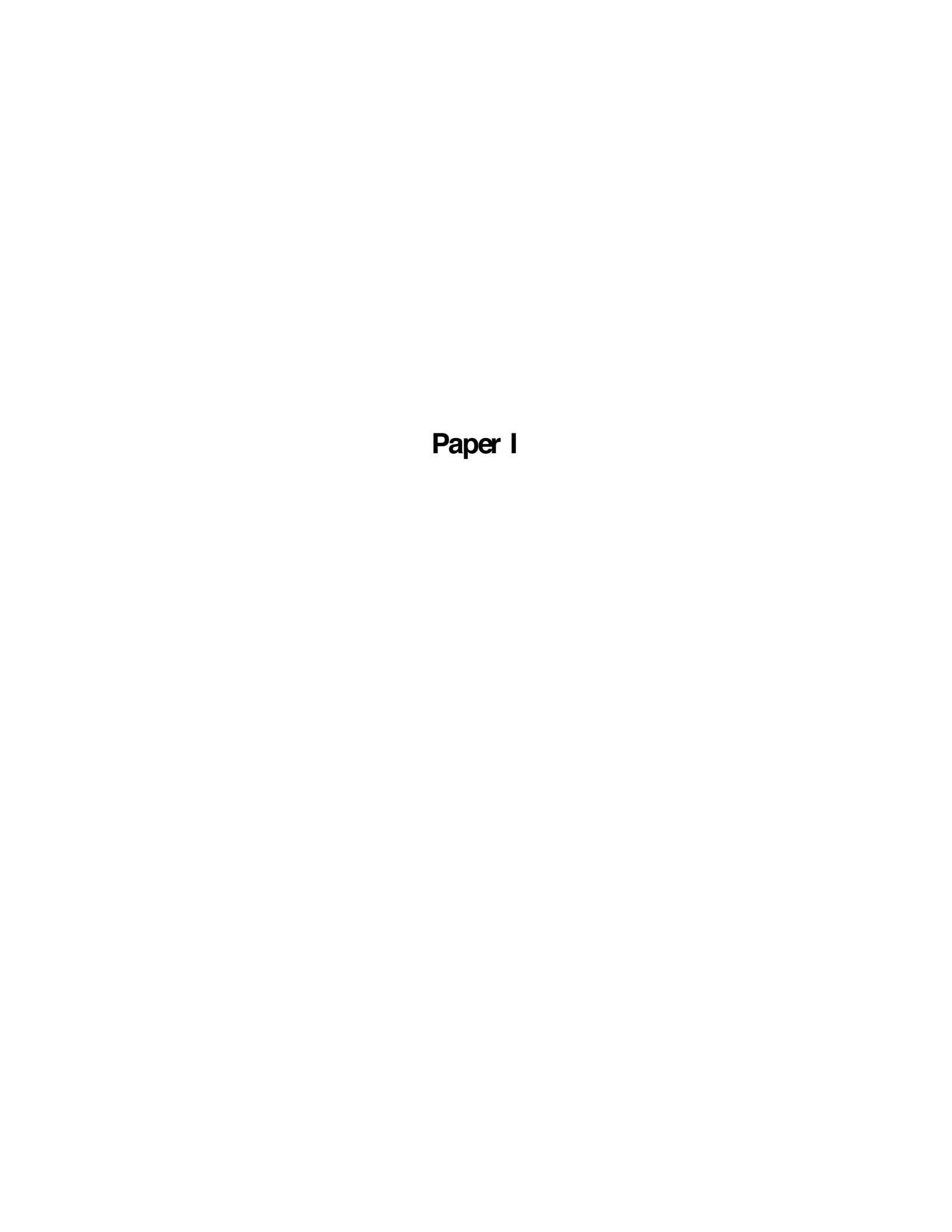
Where M_{ax} is the internal dorsi/plantarflexion moment.

Appendix E: Simulation pipeline of Study III



Appendix F: Simulation pipeline of Study V



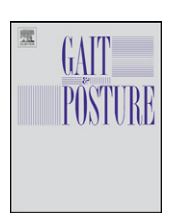


ELSEVIER

Contents lists available at ScienceDirect

Gait & Posture

journal homepage: www.elsevier.com/locate/gaitpost



One year follow-up after operative ankle fractures: A prospective gait analysis study with a multi-segment foot model

Ruoli Wang ^{a,*}, Charlotte K. Thur ^b, Elena M. Gutierrez-Farewik ^{a,c}, Per Wretenberg ^b, Eva Broström ^c

- ^a Department of Mechanics, Royal Institute of Technology, SE-100 44 Stockholm, Sweden
- b Department of Molecular Medicine and Surgery, Section of Orthopaedics and Sports Medicine, Karolinska Institutet, Stockholm, Sweden
- ^c Department of Women's and Children's Health, Karolinska Institutet, Stockholm, Sweden

ARTICLE INFO

Article history: Received 26 February 2009 Received in revised form 9 October 2009 Accepted 25 October 2009

Keywords:
Ankle fractures
Operative treatment
Gait analysis
Multi-segment foot model
Olerud/Molander ankle score (OMAS)

ABSTRACT

Ankle fractures are one of the most common lower limb traumas. Several studies reported short- and long-term post-operative results, mainly determined by radiographic and subjective functional evaluations. Three-dimensional gait analysis with a multi-segment foot model was used in the current study to quantify the inter-segment foot motions in 18 patients 1 year after surgically treated ankle fractures. Data were compared to that from gender- and age-matched healthy controls. The correlations between Olerud/Molander ankle score and kinematics were also evaluated. Patients with ankle fractures showed less plantarflexion and smaller range of motion in the injured talocrural joint, which were believed to be a sign of residual joint stiffness after surgery and immobilization. Moreover, the forefoot segment had smaller sagittal and transverse ranges of motion, less plantarflexion and the hallux segment had less dorsiflexion and smaller sagittal range of motion. The deviations found in the forefoot segment may contribute to the compensation mechanisms of the injured ankle joint. Findings of our study show that gait analysis with a multi-segment foot model provides a quantitative and objective way to perform the dynamic assessment of post-operative ankle fractures, and makes it possible to better understand not only how the injured joint is affected, but also the surrounding joints.

© 2009 Elsevier B.V. All rights reserved.

1. Introduction

Fractures of the ankle joint are one of the most common intraarticular injuries of the lower extremity, probably due to the high forces it withstands and the mass it supports [1]. Several investigators have reported short- and long-term results after surgery. However, radiographic assessment and subjective functional evaluations have been the main instruments to determine the results [2,3,4].

The human foot, the only body segment that acts on an external surface in upright, unsupported positions, supports and balances the body during gait. Ankle injuries, foot pain and dysfunction may affect its ability to cope with uneven ground and maintain dynamic stability [5]. Dynamic foot and ankle motion has been studied using mathematical modeling [6] and cadaveric specimen measurements [7]. Techniques for objective evaluation of gait have been utilized in assessment of patients with cerebral palsy [8], myelomeningocele [9], and rheumatoid arthritis [10], among others. Three-dimensional gait analysis provides objective information about gait changes, which may help document disease

progression or improvement [11]. However, the conventional gait model representing the foot as a single segment with a revolute ankle joint can only document the ankle motion in the sagittal plane, which is not adequate to describe complex three-dimensional foot motion [12]. During the last few years, various multisegment foot models have been developed and applied to describe normal and pathological gait [13,14,15].

Few gait studies have focused on ankle fractures. Lower walking velocity, decreased stride length and reduction of the internal dorsiflexion moment in the injured ankle joint immediately following heel contact were observed in a 1-year surgical treatment follow-up study [16]. Although gait asymmetry was found in a plantar pressure distribution study, no control subjects with perfect symmetry were found either [17]. It was believed that most compensation mechanisms for the hindfoot probably occur in the forefoot [17].

The aim of the present study was to quantify foot motion changes in patients with ankle fractures 1 year after open reduction and internal fixation (ORIF) and compare those findings with a matched control group. The specific aims were to determine whether:

(1) The injury resulted in a decreased range of motion (ROM) at or around the injured area.

^{*} Corresponding author. Tel.: +46 8 790 7159; fax: +46 8 796 9850. E-mail address: ruoli@mech.kth.se (R. Wang).

- (2) Motion between other segments in either limb was affected by the unilateral ankle fractures, i.e. whether secondary restriction or increase of motion exists. Since these secondary effects are unknown, complete kinematics between all segments (tibia, hindfoot, forefoot, and hallux) are presented.
- (3) The ankle functional outcomes measured by Olerud/Molander ankle score (OMAS) were associated with altered kinematics observations [18].

2. Methods

2.1. Subject

Eighteen patients with unilateral ankle fractures who were treated with ORIF at the Department of Orthopaedic Surgery at Karolinska Institutet University Hospital November 2005 to December 2006, were invited to participate in a follow-up study using clinical gait analysis including a multi-segment foot model at least 1 year post-operatively. All patients were selected on the basis of availability and willingness to participate. Twelve patients had a lateral malleolar fracture and six had a trimalleolar fracture. One patient with a lateral malleolar fracture had suffered an infection that required oral antibiotics and revision surgery. The median age (range) of the 18 ankle fracture patients was 39 (17–64) years and 10 were male. The average height and body weight were 173 cm and 76 kg. The mean (S.D.) follow-up time was 13 (3) months post-operatively. An age- (median: 40, range: 19–64 years) and gender-matched control group (average height: 172 cm and body weight: 72 kg) was gathered from a cohort of healthy adults without musculoskeletal disease or history of lower-extremity injury. Ethical approval for this study was obtained. All subjects participated with written informed consent.

2.2. Treatment methods

All patients received the department's standardized treatment. Severely dislocated fractures were adequately reduced on admission and immobilized in a semicircular cast. General indication for surgery was incongruity of the ankle joint and/or displacement of >2 mm in any plane on the X-ray. ORIF according to the AO principle [19] was performed. Transfixation of the syndesmosis was performed in all type C fractures¹ or if pathological movement was found at intraoperative testing. Post-operatively, the ankle was elevated and immobilized in a semicircular cast for 1-2 days, then in a circular cast. Partial or full weight bearing on crutches was allowed and instructed by a physiotherapist. All patients were examined two and six weeks after surgery with regards to wound healing and function. After six weeks the external fixation was terminated and the patients were again instructed by a physiotherapist concerning movement and weight bearing. All patients received a written training program and were offered further training in an ankle fracture group. The patients were evaluated by a physiotherapist 6 and 12 months post-operatively and the OMAS was recorded. The OMAS is a self-reported functional outcome score, designed for evaluating symptoms after ankle fractures. The score includes nine questions regarding pain, stiffness, swelling, stair-climbing, running, jumping, squatting, supports and activities of daily life. It ranges from 0 (totally impaired) to 100 (completely unimpaired)[18].

2.3. Multi-segment foot model

A modified version of the Oxford Foot Model (Stebbins et al. [14]) was used in the study. The model simplified complex anatomical foot structure to three rigid segments (tibia, hindfoot, and forefoot) and one vector (hallux). The midfoot was regarded as a mechanism transmitting motion between the hindfoot and forefoot. All inter-segment motions except hallux motion were three-dimensional. Euler angles were calculated for inter-segment rotation following the sequence of Grood and Suntay (flexion, adduction, and rotation) [21]. The following motions were determined: hindfoot relative to tibia (Hindfoot/Tibia), forefoot relative to hindfoot forefoot/Hindfoot), forefoot relative to tibia (Forefoot/Tibia), and hallux relative to forefoot (Hallux/Forefoot).

Since metatarsophalangeal joints were of interest, a modified method based on a spherical rotation coordinate system [22] was created to obtain frontal hallux joint rotation (varus/valgus) relative to the forefoot. A unit vector was used to represent the long axis of the hallux segment and the rotation was determined in a reference coordinate system which was assumed to be fixed to and aligned with the forefoot segment. Thus Hallux/Forefoot varus/valgus can be measured as an angle between the unit vector of the hallux and its projection on the sagittal plane of the forefoot.

2.4. Gait analysis

All patients walked barefoot along a 10 m walkway at a self-selected speed. 3D gait analysis with an 8-camera motion system (Vicon MX 40, Oxford, UK) was performed. A set of 36 markers (9 mm) was placed bilaterally on bony landmarks to

model the tibia, hindfoot, forefoot and hallux based on the multi-segment foot model (Stebbins et al. [14]). Series of barefoot walking trials were collected to achieve three left and three right trials yielding complete data sets for each subject. Discrete kinematics and temporal-spatial parameters were calculated for each gait cycle, and the averages from the three left and three right gait cycles were used for further analysis.

2.5. Statistics analysis

Data (inter-segment foot kinematics and temporal-spatial parameters) were analyzed initially using a two-way repeated measures ANOVA with side (injured side or non-injured side) as the within-group factor and group (ankle fractures or control group) as the between-group factors. Right and left side data from the control group were randomized and matched to the fracture group's injured and non-injured sides, to eliminate possible bias due to a dominant side. If a significant interaction ($p \le 0.05$) was found between factors, simple main effects tests were performed, i.e. effects of one factor holding the other factor fixed. One procedure, suggested by Kirk [23], to correct the error rate for these tests is to assign the same error rate to the collection of tests as that allotted to the "family". The simple main effects sums of squares represent a partition of families (just as many as the number of effects in the model). Therefore the overall error rate is 0.05 times the number of "families". The Bonferroni procedure can then be used for the simple tests (the overall error rate divided by the number of simple main effects tests). For our analysis, each simple main effects F-statistic was evaluated at the 0.15/4 = 0.0375level of significance [23]. The Spearman's rank correlation coefficient was used to identify associations between OMAS and inter-segment foot kinematics parameters.

3. Results

3.1. Kinematics

3.1.1. Hindfoot/Tibia motion

A group-side interaction was determined in the Hindfoot/Tibia peak plantarflexion in both the stance (p = 0.048) and swing phases (p < 0.001), and sagittal ROM (p < 0.001) in the swing phase (Fig. 1, Table 1). In the fracture group, the injured side was less plantarflexed (p = 0.003) and showed less ROM (p = 0.002) in the swing phase than the non-injured side. No significant differences were found in the frontal or transverse planes.

3.1.2. Forefoot/Hindfoot motion

A group-side interaction was determined in the Forefoot/ Hindfoot transverse ROM in both stance (p = 0.050, Fig. 1, Table 2) and swing phase (p = 0.001), where the injured side showed less ROM than both the non-injured side (stance: p = 0.020, swing: p = 0.007) and control (swing: p = 0.021). No significant differences were found in the sagittal and frontal plane.

3.1.3. Forefoot/Tibia motion

A group-side interaction was determined in the Forefoot/Tibia peak plantarflexion (p < 0.001), sagittal ROM (p < 0.001), peak adduction (p = 0.040), and transverse ROM (p = 0.013) in the swing phase (Fig. 1, Table 3). Compared to the non-injured side and to controls, the injured side showed less plantarflexion (p = 0.001, p = 0.037). Compared to the non-injured side, the injured side showed less adduction (p = 0.030), and smaller ROM in the sagittal (p < 0.001) and transverse planes (p = 0.030). No significant differences were found in the frontal plane.

3.1.4. Hallux/Forefoot motion

A group-side interaction was determined in the Hallux/Forefoot peak dorsiflexion (p = 0.021) and sagittal ROM (p = 0.010) in the swing phase, peak varus (p = 0.020), peak valgus (p = 0.031) and average varus (p = 0.019) in the stance phase (Fig. 1, Table 4). Compared to the non-injured side, in the sagittal plane, the injured side was less dorsiflexed (p = 0.011) and had a lower ROM (p = 0.005) in the swing phase. Compared to the control, the non-injured side showed a higher ROM (p = 0.012) in the sagittal plane in the swing phase, and a higher peak and average varus angle (p = 0.003, p = 0.020) in the stance phase.

¹ Weber type C fractures [20] (fibular fracture above the level of syndesmosis).

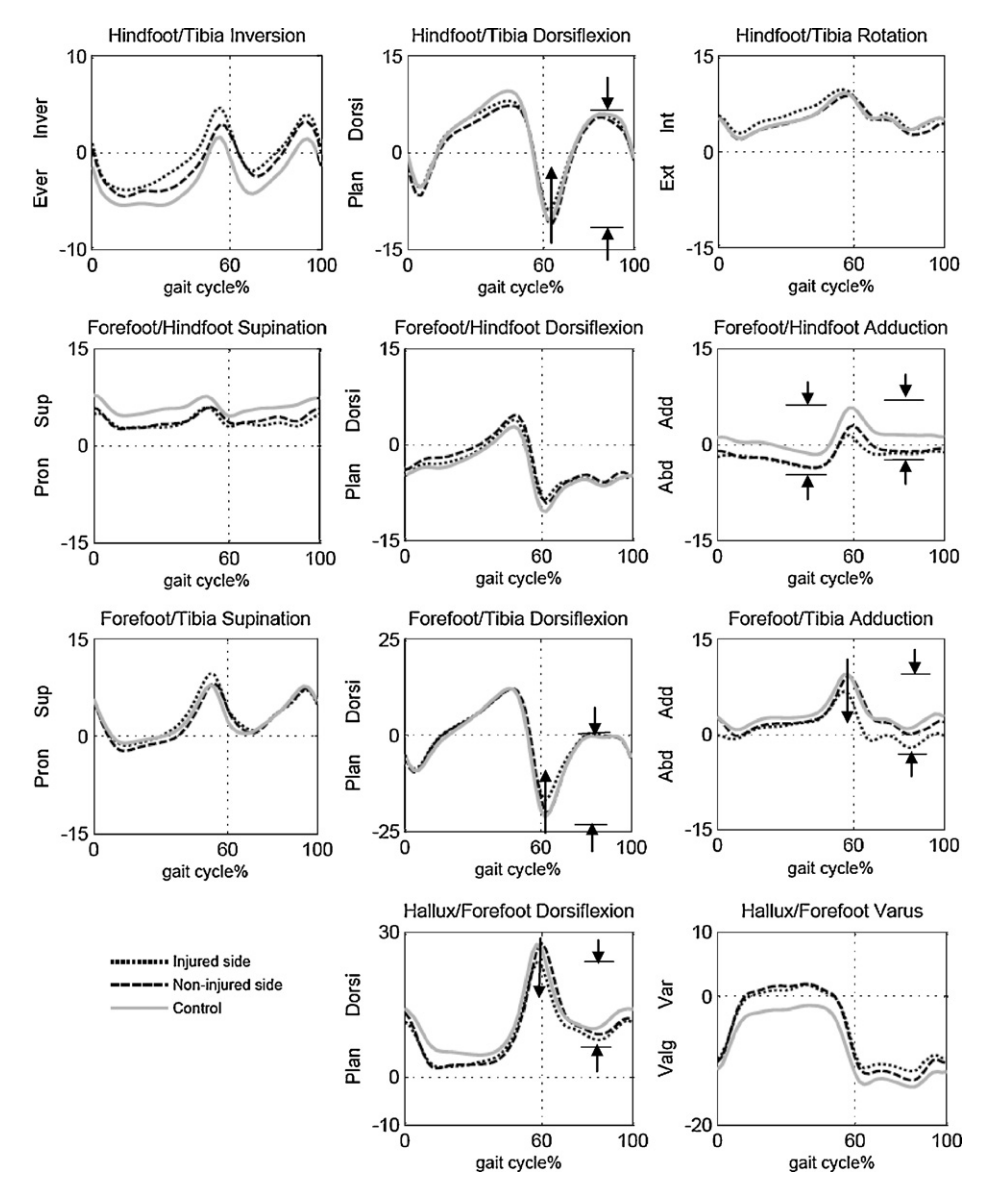


Fig. 1. Multi-segment foot kinematics (°) in sagittal, frontal and transverse planes. Mean traces of ankle fracture patients' injured and non-injured limb, and average trace of left and right limb of controls are shown in the figure (not used for any statistical calculation). Arrows illustrate differences found within the fracture group (i.e. injured vs. non-injured side). Dotted lines at 60% of the gait cycle illustrate the average toe-off time (Dorsi: dorsiflexion, Plan: plantarflexion, Inv: inversion, Ever: eversion, Ext: external rotation, Int: internal rotation, Sup: supination, Pron: pronation, Add: adduction, Abd: abduction, Var: varus, Valg: valgus).

3.1.5. Temporal-spatial parameters

Walking speed, stride length, and step length were normalized by subjects' limb lengths. A group-side interaction was determined in the stride length (p=0.040), single-support time (p=0.020) and foot-off time (p=0.001). Compared to the non-injured side, single support time on the injured side was shorter (p=0.003) and foot-off time was earlier (p=0.003). Compared to the control, stride length (injured: p=0.030, non-injured: p=0.020) was shorter, and foot-off time was delayed in the non-injured side (p=0.002).

3.1.6. OMAS and gait parameters

Median OMAS was 85 points in the present study. A significant but fair-moderate correlation was determined between OMAS and Hindfoot/Tibia peak dorsiflexion (r = 0.60, p = 0.010), sagittal ROM (r = 0.50, p = 0.040) in the swing phase, and frontal ROM (r = 0.50, p = 0.040) in the stance phase. Forefoot/Hindfoot transverse ROM (r = 0.48, p = 0.050), Forefoot/Tibia frontal ROM (r = 0.51, p = 0.040), and peak adduction (r = 0.54, p = 0.030) were found moderately correlated with OMAS. Moreover, Hallux/Forefoot

sagittal (r = 0.49, p = 0.040) and transversal (r = 0.47, p = 0.050) ROM revealed fair correlation with OMAS.

4. Discussion

Very few gait studies have focused on the ankle joint and this is the first study we know of evaluating post-operative ankle fractures with a multi-segment foot model. Despite the apparent symmetry present in the figures, the current study showed that a number of statistical differences between the injured and the non-injured sides; compared to the non-injured side, patients with ankle fractures displayed less plantarflexion and decreased ROM in the injured talocrural joint. The hallux was less dorsiflexed and had a smaller sagittal ROM. Compared to both controls and to the non-injured side, the injured side's forefoot was less plantarflexed and adducted in the swing phase, and had smaller ROM in the sagittal and transverse planes. Significant alterations in temporal-spatial parameters associated with decreased step and stride length were also observed. The findings indicated that even with fairly good

 Table 1

 Hindfoot/Tibia kinematics during gait. Mean (standard deviation) values with respect to side and group are shown in degree (°).

Group	Side	Dorsiflexio	n/plantarflo	exion (sagit	tal plane)			Inversion/	eversion (frontal plane)				Internal/ex	kternal rot	ation (trar	sverse pla	ine)	
		Stance			Swing			Stance			Swing			Stance			Swing		
		Max. Dorsi ¹	Max. Plan ^{2,*}	ROM ³	Max. Dorsi	Max. Plan ^{*,&}	ROM*,&	Max. Inv ⁴	Max. Ever ⁵	Avg. Inv/Ever (-Ever)	Max. Inv	Max. Ever	Avg. Inv/Ever (-Ever)	Max. Int ⁶	Min. Ext ⁷	ROM	Max. Int	Min. Ext	ROM
FG ⁸	IS ⁹ NIS ¹⁰	, ,		, ,	, ,	9.1 (6.3) 12.5 (6.1)	, ,	, ,	, ,	-2.3 (8.9) -3.5 (6.4)	` ,	3.0 (9.7) 3.7 (6.6)	0.0 (10.1) -0.7 (6.7)	11.2 (4.3) 10.8 (6.4)		, ,	. ,	, ,	, ,
CG ¹¹	IS-cont ¹² NIS-cont ¹³					12.0 (5.0) 9.2 (5.5)			, ,	-4.9 (4.9) -4.5 (5.0)		, ,	-2.7 (5.4) -1.9 (5.0)	10.7 (5.2) 11.0 (5.4)		, ,	, ,	, ,	, ,

¹Dorsiflexion; ²Plantarflexion; ³Range of motion; ⁴Inversion; ⁵Eversion; ⁶Internal rotation; ⁷External rotation; ⁸Fracture group; ⁹Injured side; ¹⁰Non-injured side; ¹¹Control group; ¹²Control injured side; ¹³Control non-injured side; ⁵Significant side and group interactions using repeated ANOVA test; ⁸Significant side differences within fracture group using Bonferroni adjustments; [#]Group differences respect to injured side using Bonferroni adjustments.

Table 2Forefoot/Hindfoot kinematics during gait. Mean (standard deviation) values with respect to side and group are shown in degree (°).

Group	Side	Dosiflexio	n plantarfle	xion (sagitta	al plane)			Supinatio	n/pronatio	n (frontal p	lane)			Adduction	n/abduction	n (transver	se plane)		
		Stance			Swing			Stance			Swing			Stance			Swing		
		Max. Dorsi ¹	Max. Plan ²	ROM ³	Max. Plan	Min. Plan	ROM	Max. Sup ⁴	Min. Sup ⁵	Avg. Sup/Pron	Max. Sup	Min. Sup	Avg. Sup/Pron	Max. Add ⁶	Max. Abd ⁷	ROM ^{*,&,#}	Max. Add	Min. Add (-Abd)	ROM*,&,#
FG ⁸	IS ⁹ NIS ¹⁰	4.7 (5.7) 5.4 (4.1)	` ,	14.5 (3.6) 15.8 (3.9)	` ,	3.5 (5.8) 3.2 (5.2)	, ,	` ,	0.9 (9.2) 1.0 (7.2)	` '	` ,	, ,	` '	, ,	, ,	` ,	, ,	-2.8 (6.2) -2.5 (5.3)	3.3 (0.9) 4.6 (1.9)
CG ¹¹	IS-cont ¹² NIS-cont ¹³	, ,		14.9 (3.4) 15.4 (3.6)	, ,	, ,	, ,		, ,		, ,	, ,	, ,	, ,	, ,	8.7 (2.8) 8.5 (2.6)	3.8 (5.9) 5.2 (5.8)	-0.8 (5.2) 1.4 (5.4)	4.6 (2.1) 3.8 (1.7)

¹Dorsiflexion; ²Plantarflexion; ³Range of motion; ⁴Supination; ⁵Pronation; ⁶Adduction; ⁸Fracture group; ⁹Injured side; ¹⁰Non-injured side; ¹¹Control group; ¹²Control injured side; ¹³Control non-injured side; ⁵Significant side and group interactions using repeated ANOVA test; ⁸Significant side differences within fracture group using Bonferroni adjustments; [#]Group differences respect to injured side using Bonferroni adjustments.

Table 3Forefoot/Tibia kinematics during gait. Mean (standard deviation) values with respect to side and group are shown in degree (°).

Group	Side	Dorsiflexio	n/plantarfle	xion (sagitt	al plane)			Supination	/pronatior	(frontal p	lane)			Adduction	/abduction (t	ransverse p	lane)		
		Stance			Swing			Stance			Swing			Stance			Swing		
		Max. Dorsi ¹	Max. Plan	ROM ³	Max. Plan ^{*,&,#}	Min. Plan	ROM*,&,#	Max. Sup ⁴	Max. Pron ⁵	Avg. Sup/Pron	Max. Sup	Max. Pron	Avg. Sup/Pron	Max. Add ⁶	Min. Add ⁷ (–Abd)	ROM	Max. Add ^{*,&,#}	Max. Abd	ROM ^{*,&}
FG ⁸	IS ⁹ NIS ¹⁰				16.7 (8.6) 22.2 (6.1)									, ,	-0.2 (5.1) -0.9 (5.5)	13.4 (4.0) 15.0 (3.6)	, ,	. ,	6.7 (2.2) 9.4 (3.8)
CG ¹¹	IS-cont ¹² NIS-cont ¹³	13.1 (3.0) 14.7 (4.0)			22.5 (7.6) 19.5 (5.2)									15.8 (7.2) 18.0 (4.9)	0.5 (5.0) 2.7 (4.8)	15.4 (4.4) 15.3 (4.6)	, ,	, ,	, ,

¹Dorsiflexion; ²Plantarflexion; ³Range of motion; ⁴Supination; ⁵Pronation; ⁶Adduction; ⁸Fracture group; ⁹Injured side; ¹⁰Non-injured side; ¹¹Control group; ¹²Control injured side; ¹³Control non-injured side, ⁸Significant side and group interactions using repeated ANOVA test; ⁸Significant side differences within fracture group using Bonferroni adjustments; [#]Group differences respect to injured side using Bonferroni adjustments.

Table 4
Hallux/Forefoot kinematics during gait. Mean (standard deviation) values with respect to side and group are shown in degree (°).

Group	Side	Dorsiflexion/p	lantarflexion (s	agittal plane)				Varus/valgus	(transverse plane)				
		Stance			Swing			Stance			Swing		_
		Max. Dorsi ¹	Min. Dorsi	ROM ^{2,*,&}	Max. Dorsi*,&	Min. Dorsi	ROM ^{*,&,‡}	Max. Var ³ (-Valg)*,&,‡	Max. Valg ^{4,*,&,‡}	Avg. Var/Valg (-Valg)*,&,‡	Max. Valg*	Min. Valg	Avg. Var/Valg (-Valg)
FG ⁵	IS ⁶ NIS ⁷	27.1 (10.0) 31.1 (9.9)	1.2 (3.8) 0.6 (5.3)	25.9 (10.2) 30.6 (8.6)	19.9 (8.8) 25.0 (9.8)	5.9 (5.4) 7.2 (5.4)	14.0 (5.7) 17.9 (6.1)	0.8 (7.2) 5.6 (7.1)	18.4 (8.4) 14.9 (7.0)	-2.0 (7.4) 2.3 (6.8)	19.1 (8.4) 16.8 (6.5)	12.9 (7.7) 10.3 (7.0)	-16.5 (7.8) -14.4 (6.4)
CG ⁸	IS-cont ⁹ NIS-cont ¹⁰	31.1 (8.5) 31.3 (6.7)	4.9 (4.1) 3.4 (4.3)	27.1 (6.5) 27.9 (5.0)	23.1 (7.5) 21.8 (5.2)	8.9 (5.1) 8.8 (4.8)	14.2 (5.7) 13.0 (5.1)	0.3 (6.6) -1.4 (6.1)	18.9 (6.8) 20.6 (7.1)	-2.6 (6.4) -4.5 (5.7)	19.4 (6.8) 21.1 (7.6)	14.0 (7.1) 15.2 (7.3)	-17.3 (7.0) -18.9 (7.5)

¹Dorsiflexion; ²Range of motion; ³Varus; ⁴Valgus; ⁵Fracture group; ⁶Injured side; ⁷Non-injured side; ⁸Control group; ⁹Control injured side; ¹⁰Control non-injured side; ⁵Significant side and group interactions using repeated ANOVA test; ⁸Significant side differences within fracture group using Bonferroni adjustments; ¹Group differences respect to non-injured side using Bonferroni adjustments.

OMAS, the injured ankle joint was not fully recovered and tended to affect other joints in the foot.

Losch et al. [16] examined gait in 20 patients 1 year after surgically treated ankle fractures. The authors found walking speed and step length to be decreased. The current study demonstrated a similar decrease in step length, but unlike Losch et al., the slightly lower walking speed found in the patients with ankle fractures was not significant. Additional slight alterations, i.e. shorter single-support time (injured 0.40 s, non-injured 0.41 s) and earlier foot-off time (injured 59.63% gait cycle, non-injured 60.77% gait cycle) in the injured side were noticed in the current study, but the small magnitude of the differences can be considered clinically irrelevant.

In the current study, limited motion was observed not only in the injured ankle joint, but also in other joints in the foot. Compared to the non-injured side, decreased sagittal and transversal ROM were found in the forefoot, and reduced sagittal ROM was observed in the hindfoot and hallux segments. Restricted movement in the ankle was noted by some authors and was attributed to pain and joint stiffness, depending on the severity of the injury. Lindsjö et al. [24] reported that the capacity for dorsiflexion and plantarflexion was restricted up to 10° in 31% and 17% respectively of 162 follow-up ankle fracture patients. More than half of patients experienced pain, stiffness and swelling in a 14-month follow-up study after surgical treatment of ankle fractures [25]. However, it is noteworthy that decreased ankle ROM was also found in a gait analysis with 20 patients indicating good clinical results and no deficit complaints. Authors suggested that it could be due to an adapted and internalized strategy for unloading the injured joint [16].

In this study, the injured side was found to have a less plantarflexed hindfoot, forefoot, and a less dorsiflexed hallux during pre-swing than the non-injured side. In normal gait, the ankle and foot rapidly move to be largely plantarflexed in pre-swing, preparing for initial-swing. At the same time, the toe extensor muscle helps to dorsiflex the toes to clear the foot. It remains unclear whether the gait deviations observed here were adapted strategies for restricted motion of the ankle joint. One interpretation could be that patients with ankle fractures tended to lift rather than push off the foot, and prolong the double-support phase. Further observations of knee and hip kinematics may be useful to confirm our findings.

Becker et al. [17] examined whether surgical treatment of ankle fractures led to gait symmetry by measuring plantar pressure distribution. They found different pressure distributions in some locations between the injured and non-injured limbs, both in patients with good and with poor clinical results. Increased loading in the lateral forefoot of the injured limb in patients with good results and decreased pressure under the metatarsal heads of patients with poor results were reported. Authors suggested that the forefoot is probably the area of compensation mechanism for fractures of the hindfoot. In our study, a less adducted forefoot was observed in swing, which may indicate that the loading was slightly increased in the medial forefoot of the injured side, contradicting Becker's study. We also found that compared to the controls, the non-injured side's hallux was more varus during stance. Further investigation is needed to identify whether it was also an influence of the injured ankle.

The OMAS is a self-administrated patient questionnaire, which has been frequently used to evaluate subjectively scored function after ankle fractures [26] and has been found to correlate well with static ROM in loaded dorsiflexion [18]. An earlier study showed a similar mean OMAS score 1 year post-operatively as in the present study [25]. As a crude rule of thumb, correlations between 0.25–0.5 indicates a fair relationship and 0.5–0.7 indicates a moderate relationship [27]. In our study, OMAS was also found fair-

moderately correlated with kinematic parameters in the sagittal plane, for instance, Hindfoot/Tibia peak dorsiflexion and sagittal ROM in the swing phase. This finding contradicted the study by Losch et al. [16], who did not find significant correlations between gait and clinical parameters, though they employed a different functional score. However, temporal-spatial parameters indicated weak correlations with the clinical score both in our and their studies.

The reason for using an ANOVA and simple main effects tests with Bonferroni adjustments in the study was to detect group and side interactions. It was believed that a bilateral change of gait could also occur, caused by the unilateral joint status after ankle fractures [17,16]. In our study, some kinematic deviations were found between limbs within the fracture group, as well as between groups. It was necessary to analyze the complete inter-segment kinematics, since they were presented in the manner of one segment with respect to another in the Oxford foot model. This was a simple way to identify the region where the deviation truly occurred.

It should be noted that our study did not include force data, because to our knowledge, only one validated multi-segmental 3D kinetic model of the foot was developed [28] and it has not been intensively applied. Authors were also aware of the variability in the measurement of inter-segment foot motion. A previous repeatability study of a multi-segment foot model reported that the overall variability was acceptable and its good consistency implied repeatable and systematic artifacts from skin movements [29]. Sagittal plane motion was found to be the most repeatable, and transverse plane, the most variable on a group of healthy children [14]. Nevertheless, our study cohort was relatively small, which made it difficult to do subgroup analyses based on fracture classification, gender or age.

In conclusion, patients following surgically treated ankle fractures experienced a decrease of ROM in the injured talocrural joint and restricted transverse ROM in the forefoot segment which are believed to be a sign of residual joint stiffness. Moreover, the forefoot is likely a primary area for compensation due to ankle injury. Findings of the study showed that unilateral ankle fractures affected not only the injured joint but also the surrounding joints in the foot. In addition, gait analysis with a multi-segment foot model provide a subjective and quantitative assessment of post-operative ankle fractures, while only passive ankle ROM is usually examined during clinical evaluations, which often can make it difficult to detect small differences due to the limited measurement accuracy.

Acknowledgements

This work was funded by the Stiftelsen Frimurare Barnhuset i Stockholm and Stiftelsen Promobilia.

Conflict of interest

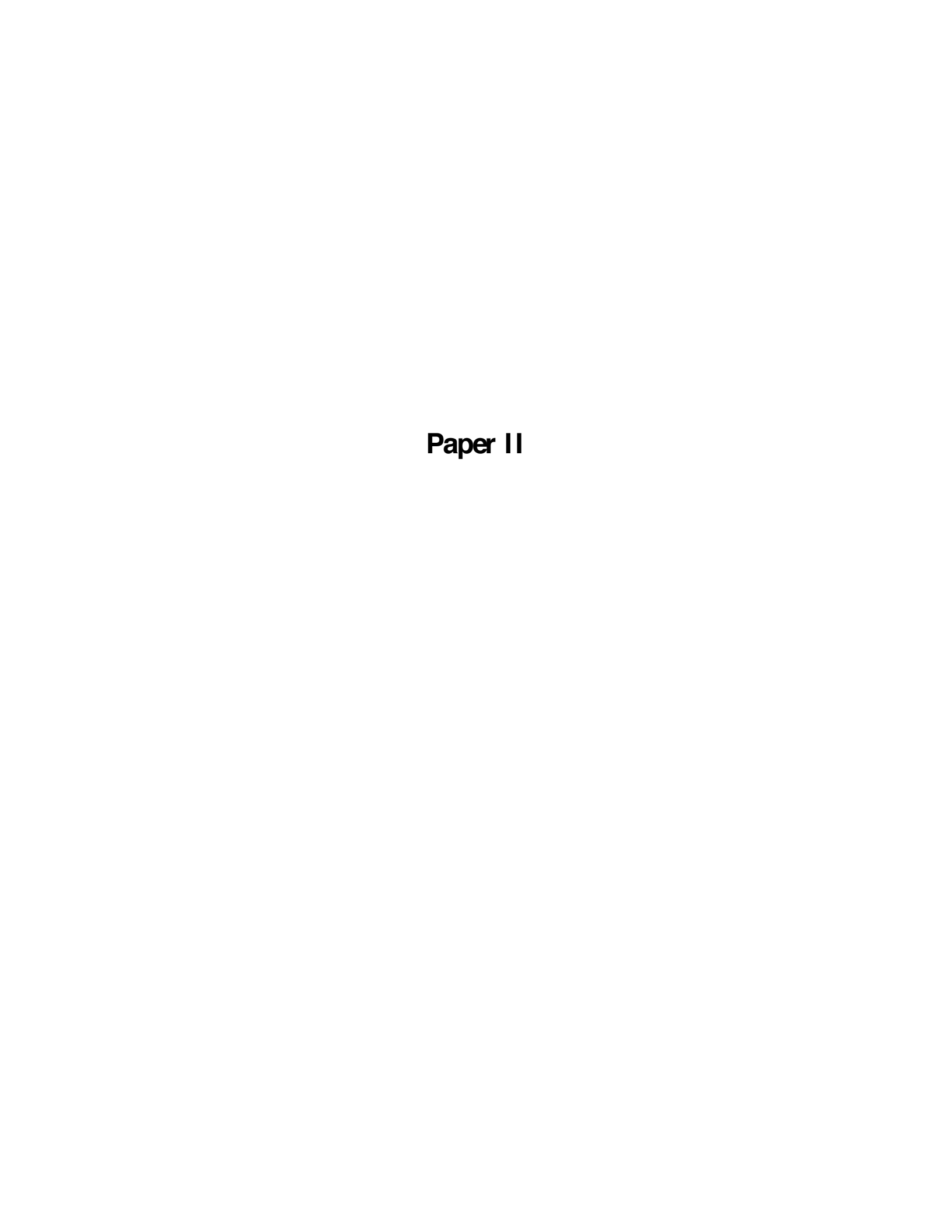
No authors had any conflict of interest that may have biased this work

References

- [1] Michelson JD. Fractures about the ankle. J Bone Joint Surg Am 1995;77:142–52.
- [2] Bauer M, Jonsson K, Nilsson B. Thirty-year follow-up of ankle fractures. Acta Orthop Scand 1985;56:103–6.
- [3] Day GA, Swanson CE, Hulcombe BG. Operative treatment of ankle fractures: a minimum ten-year follow-up. Foot Ankle Int 2001;22:102–6.
- [4] Belcher GL, Radomisli TE, Abate JA, Stabile LA, Trafton PG. Functional outcome analysis of operatively treated malleolar fractures. J Orthop Trauma 1997:11:106–9.
- [5] Smith LK, Weiss EL, Don L. Brunnstrom's clinical kinesiology. Philadelphia: F.A. Davis Co.; 1996.
- [6] Stauffer RN, Chao EY, Brostrom E. Force and motion analysis of the normal, diseased, and prosthetic ankle joint. Clin Orthop Relat Res 1977;127:189–96.

- [7] Arndt A, Westblad P, Winson I, Hashimoto T, Lundberg A. Ankle and subtalar kinematics measured with intracortical pins during the stance phase of walking. Foot Ankle Int 2004;25:357–64.
- [8] Gage JR. Gait analysis in cerebral palsy. Oxford: Mac Keith; 1991.
- [9] Gutierrez EM, Bartonek A, Haglund-Åkerlind Y, Saraste H. Characteristic gait kinematics in persons with lumbosacral myelomeningocele. Gait Posture 2003; 18:170–7.
- [10] Weiss RJ, Wretenberg P, Stark A, Palmblad K, Larsson L, Gröndal L, et al. Gait pattern in rheumatoid arthritis. Gait Posture 2008;28:229–34.
- [11] Weiss RJ, Broström E, Stark A, Wick MC, Wretenberg P. Ankle/hindfoot arthrodesis in rheumatoid arthritis improves kinematics and kinetics of the knee and hip: a prospective gait analysis study. Rheumatology (Oxford) 2007;46:1024–8.
- [12] Wang RL, Broström E, Gutierrez-Farewik EM. Analysis of foot kinematics during gait in adults with rheumatoid arthritis. Gait Posture 2007;26:S20-1.
- [13] Khazzam M, Long JT, Marks RM, Harris GF. Preoperative gait characterization of patients with ankle arthrosis. Gait Posture 2006;24:85–93.
- [14] Stebbins J, Harrington M, Thompson N, Zavatsky A, Theologis T. Repeatability of a model for measuring multi-segment foot kinematics in children. Gait Posture 2006;23:399–400.
- [15] Woodburn J, Nelson KM, Siegel KL, Kepple TM, Gerber LH. Multisegment foot motion during gait: proof of concept in rheumatoid arthritis. J Rheumatol 2004;31:1918–27.
- [16] Losch A, Meybohm P, Schmalz T, Fuchs M, Vamvukakis F, Dresing K, et al. Functional results of dynamic gait analysis after 1 year of hobby-athletes with a surgically treated ankle fracture. Sportverletz Sportschaden 2002;16:101-7.
- [17] Becker HP, Rosenbaum D, Kriese T, Gerngross H, Claes L. Gait asymmetry following successful surgical treatment of ankle fractures in young adults. Clin Orthop Relat Res 1995;311:262–9.

- [18] Olerud C, Molander H. A scoring scale for symptom evaluation after ankle fracture. Arch Orthop Trauma Surg 1984;103:190-4.
- [19] Ruedi TP, Murphy W, Colton C, Fernandez Dell'Oca A, Holz U, Kellam J, et al. AO principles of fracture management. Stuttgart: Thieme Verlag; 2000.
- [20] Müller ME, Allgöwer M, Perren SM. Manual of internal fixation: techniques recommended by the AO-ASIF group. Berlin: Springer-Verlag; 1991.
- [21] Grood ES, Suntay WJ. A joint coordinate system for the clinical description of three-dimensional motions: application to the knee. J Biomech Eng 1983; 105:136.
- [22] Cheng PL. A spherical rotation coordinate system for the description of threedimensional joint rotations. Ann Biomed Eng 2000;28:1381–92.
- [23] Kirk RE. Experimental design: procedures for the behavioral sciences. Pacific Grove: Brooks-Cole; 1995.
- [24] Lindsjö U. Operative treatment of ankle fractures. Acta Orthop Scand Suppl 1981;189:1–131.
- [25] Nilsson G, Nyberg P, Ekdahl C, Eneroth M. Performance after surgical treatment of patients with ankle fractures—14-month follow-up. Physiother Res Int 2003:8:69–82.
- [26] Shah NH, Sundaram RO, Velusamy A, Braithwaite IJ. Five-year functional outcome analysis of ankle fracture fixation. Injury 2007;38:1308–12.
- [27] Colton T. Regression and correlation. Statistics in medicine, vol. 189. New York: McGraw-Hill; 1974. p. 218.
- [28] MacWilliams BA, Cowley M, Nicholson DE. Foot kinematics and kinetics during adolescent gait. Gait Posture 2003;17:214–24.
- [29] Carson MC, Harrington ME, Thompson N, O'Connor JJ, Theologis TN. Kinematic analysis of a multi-segment foot model for research and clinical applications: a repeatability analysis. J Biomech 2001;34:1299.



Analytical decomposition can help to interpret ankle joint moment-angle relationship

Ruoli Wang¹, Eva W Broström², Anna-Clara Esbjörnsson², Elena M. Gutierrez-Farewik^{1,2}

¹ Department of Mechanics, Royal Institute of Technology, Stockholm, Sweden ² Department of Women's and Children's Health, Karolinska Institutet, Stockholm, Sweden

Accepted in Journal of Electromyography and Kinesiology

Abstract

Moment-angle relationship (dynamic joint stiffness) - the relationship between changes in joint moment and changes in joint angle - is useful for demonstrating interaction of kinematics and kinetics during gait. However, the individual contributors of dynamic joint stiffness are not well studied and understood, which has thus far limited its clinical application. In this study, ankle dynamic joint stiffness was analyzed and decomposed into three components in thirty able-bodied children during the stance phase of the gait. To verify the accuracy of the decomposition, the sum of decomposed components was compared to stiffness computed from experimental data, and good to very good agreement was found. Component 1, the term associated with changes in ground reaction force moment, was the dominant contribution to ankle dynamic joint stiffness. Retrospective data from eight children with juvenile idiopathic arthritis and idiopathic toe-walking was examined to explore the potential utility of analytical decomposition in pathological gait. Compared to controls, component 1 was the source of highest deviation in both pathological groups. Specifically, ankle dynamic joint stiffness differences can be further identified via two sub-components of component 1 which are based on magnitudes and rates of change of the ground reaction force and of its moment arm, and differences between the two patient groups and controls were most evident and interpretable here. Findings of the current study indicate that analytical decomposition can help identify the individual contributors to joint stiffness and clarify the sources of differences in patient groups.

Keywords gait analysis, stiffness, inverse dynamics, juvenile idiopathic arthritis, idiopathic toe walking

1. Introduction

Human walking patterns are typically characterized by plotting single kinematics and kinetics curves as a function of time or percentage of gait cycle. During the stance phase, the progression of gait is assisted by four foot rockers: heel-rocker, ankle-rocker, forefootrocker and toe-rocker (Perry and Burnfield, 2010). The foot rockers are often used to describe pathological gait, e.g. toe walking has been identified as absent of heel rocker (Armand et al., 2006); In post-stroke hemiplegic gait, weight transfer impairments have been observed in the heel and forefoot rockers (Nolan and Yarossi, 2011). A number of relevant dynamic effects, however, can be identified when pairs of kinematics and kinetic variables are examined together and correlations among them are concurrently assessed (Crenna and Frigo, 2011). Davis et al. introduced the concept of dynamic joint stiffness (DJS) as the slope of the joint moment plotted as a function of the joint angle, and showed that ankle DJS was a repeatable and approximately constant parameter in the 2nd rocker (Davis and DeLuca, 1996), which corresponds to Perry and Burnfield's ankle- and forefoot-rockers (Perry and Burnfield, 2010). Moment-angle relationships at the hip, knee and ankle joints have been investigated at different walking velocities, and the ankle moment-angle relationship computed during steady-state walking revealed a relatively simple, loopshaped contour (Frigo et al., 1996). In a clinical study, knee DJS was evaluated in subjects with moderate and severe knee osteoarthritis at different walking velocities, and higher joint stiffness was associated with advanced stages of knee osteoarthritis irrespective of walking speed (Zeni Jr and Higginson, 2009). In general, increased DJS is often thought to result from decreased joint angle and increased joint moment. However, a recent study showed that DJS was not necessarily positively related to joint angle and joint moment (Tateuchi et al., 2011).

The DJS has also been identified as 'quasistiffness' of a joint, and can be interpreted as the resistance that muscles and other joint structures provide during intersegmental displacement and as a reaction to an external moment of force (Latash and Zatsiorsky, 1993). Therefore, the DJS is expected to be influenced by a number of factors involving functional and/or structural changes, e.g. walking speed, muscle activity, bone and soft tissue injury, joint mobilityaffecting diseases etc. However, although the concept of the DJS has been well-documented, the biomechanical contributors to the DJS have not been clear, particularly as influential factors are often coupled. These have limited the intuitiveness and clinical applicability of the DJS.

In practice, gait characterization, particular kinetics, is often interpreted through the changes of moment associated with ground reaction force, body gravity etc. Analytically, DJS is the derivative of the joint moment with respect to the joint angle during a motor task (dM/dΘ) (Gabriel et al., 2008). Since resultant joint moment is the sum of several dynamic factors, the DJS can be decomposed into several major mechanical contributors which may help to interpret differences in DJS in some patient populations or after interventions. Decomposition usually refers to a generic term for solutions of problems and algorithms in which the basic concept is to decompose the problem/variable into sub-problems/variables, and has also been applied in movement science. instance, researchers have used decomposition method to resolve a composite quantitative electromyography (EMG) signal into its constituent motor unit potentials (MUP) trains, which can represent the morphology of the MUP and was capable of detecting the severity of muscle dystrophy (Doherty and Stashuk, 2003; Derry et al., 2012). However, to the authors' knowledge, the current study is the first attempting to analytically decompose DJS to its sub-components.

Computing DJS is simple, understanding it is not. Why it increases or decreases after treatment or why it is higher in some

pathological populations is not well understood. The objective of this study, therefore, is to determine whether individual contributors to DJS help to explain differences that can be observed in two different patient groups, in this case juvenile idiopathic arthritis (JIA) and idiopathic toe walking (ITW).

2. Methods

2.1. Subjects

Thirty healthy children (mean \pm standard deviation, age: 12 ± 4 yrs, body weight: 38 ± 11 kg, height: 144 ± 14 cm) without history of neurological or orthopedic disease were examined in this retrospective study. To investigate the potential clinical application of the concept, eight children with JIA and active disease involvement bilaterally in at least the ankle (age: 13 ± 5 yrs, body weight: 40 ± 20 kg, height: 150 ± 24 cm) and eight children with ITW (age: 9 ± 2 yrs, body weight: 35 ± 14 kg, height: 136 ± 14.5 cm) were selected from the database at Gait Analysis Laboratory at Karolinska University Hospital. Children with JIA were classified according to ILAR classification (Petty et al., 1998) and exclusion criteria were 1) history of lower limb surgery and 2) having undergone treatment within 4 weeks prior data collection. All children with ITW underwent a neurological examination by a pediatric neurologist confirming no underlying neurological or muscular pathology. Their exclusion criteria were previous treatments such as Achilles tendon surgery, casting, orthotics, and botulium toxin injection before the data collection. Ethic approval for data collection was obtained. All subjects participated with informed consent.

2.2. Motion capture

All participants walked barefoot along a 10 m walkway at a self-selected speed. During all of the walking trials, three-dimensional kinematics data was recorded at 100Hz from 34 markers (9mm) using an 8-camera motion system (Vicon MX 40, Oxford, UK). Ground reaction forces (GRF) and center of pressure (COP) data were obtained from two force plates (Kistler, Winterthur, Switzerland) at 1000Hz.

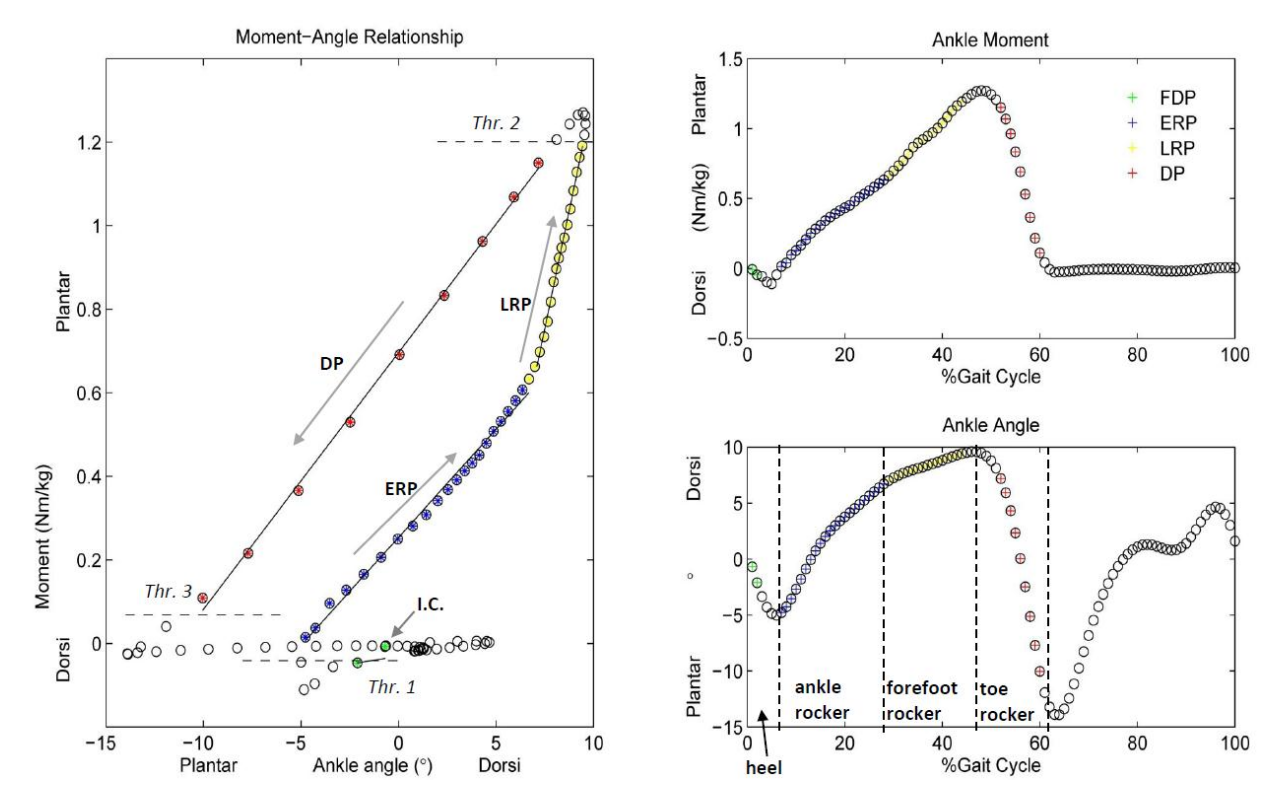


Figure 1. An example moment-angle loop in one healthy subject. Dynamic ankle joint stiffness was calculated as the slope of the linear regression line of ankle joint moment plotted as a function of ankle joint angle. After initial contact (I.C.), the stance phase was divided into four sub-phases by three thresholds (in dash lines): the first descending phase (FDP), early rising phase (ERP), late rising phase (LRP) and descending phase (DP). The ERP, LRP and DP correspond approximately to ankle-rocker, forefoot-rocker and toe-rocker (Perry and Burnfield, 2010). Arrows indicated the direction of the path. Due to the small number of data points, FDP was excluded in this study.

2.3. Data processing

Gait data was analyzed with a conventional model (Vicon Plug-In-Gait). The ankle joint kinematics, moments and gait events as well as relevant markers' trajectories, GRF and COP data were imported into Matlab (MathWorks, Inc., Natick, USA) for further analysis. Linear interpolation was applied to the original data points to obtain data points for joint angles and moments at every 2% of stride duration. Ankle joint moment was computed by inverse dynamics, using subjects' measurements and anthropometric properties (Robertson, 2004) and normalized to body weight. The ankle moment for each trial was plotted as a function of the corresponding ankle angle (moment-angle loop).

2.4. Sub-phases determination

Three sequential phases were determined within each moment-angle loop according to

Crenna *et al.* (Fig. 1): early rising phase (ERP), late rising phase (LRP), and descending phase (DP) with a threshold value to avoid the nonlinearity of the turning points (Crenna and Frigo, 2011). The threshold value (ThrV) was defined as 5% of maximum ankle moment. The ERP was the period between threshold 1 (Thr. 1 = minimum ankle moment + ThrV) and the point at which the local slope was 1.7 times that of the average slope of the previous points. The LRP was the period between the end of ERP and a second threshold (Thr. 2 = maximum ankle moment - ThrV). The DP was the period between Thr. 2's second instance to threshold 3 (Thr. 3 = Thr V). The period from foot-contact to Thr. 1 (first descending phase, FDP) was excluded in the analysis, due to the small number of data points. The ERP, LRP and DP correspond to Perry's definition (Perry and Burnfield, 2010) of 'ankle-rocker',' forefootrocker' and 'toe-rocker'. For subjects with ITW, sub-phase definitions and thresholds were

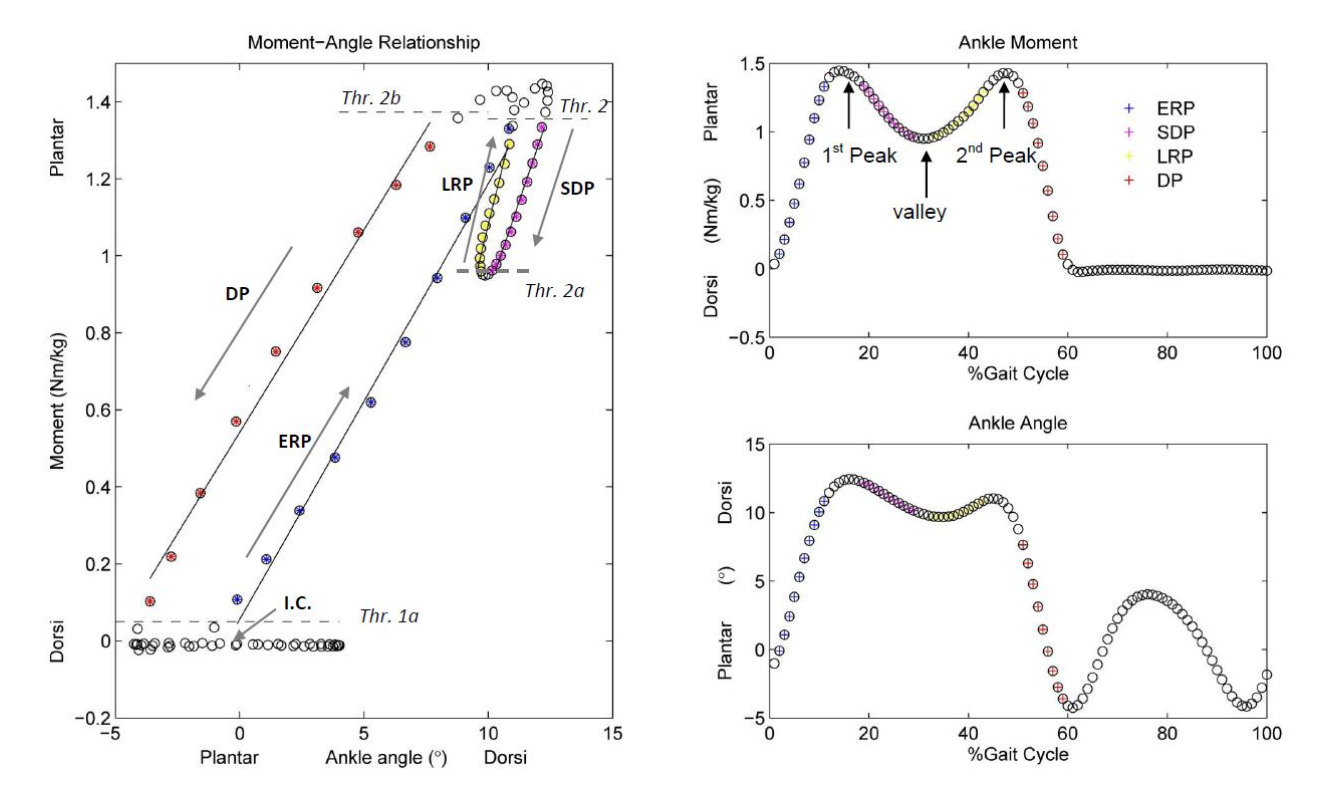


Figure 2. An example moment-angle loop in one subject with idiopathic toe walking. Dynamic ankle joint stiffness was calculated as the slope of the linear regression line of ankle joint moment plotted as a function of ankle joint angle. Different to healthy subjects, after initial contact (I.C.), first descending phase ('heel-rocker') did not exist, but a unique short descending phase (SDP) was found between the early rising phase (ERP) and the late rising phase (LRP). Four thresholds were illustrated as dash lines. Arrows indicated the direction of the path.

modified to include a short descending phase (SDP) due to the double bump ankle joint moment pattern (Fig. 2), and include a modified Thr. 1a and new thresholds 2a and 2b (Thr. 2a, Thr. 2b):

$$Thr. 1a = ThrV$$
 (1)

$$Thr. 2 = 1^{st} peak moment - ThrV$$
 (2)

$$Thr. 2a = valley moment + ThrV$$
 (3)

$$Thr. 2b = 2^{nd} peak moment - ThrV$$
 (4)

The ERP was identified between Thr. 1a and Thr. 2. The SDP was identified between Thr. 2 and Thr. 2a when appropriate. The LRP was reidentified as the interval between Thr. 2a and Thr. 2b. The DP was identified as the interval between Thr. 2b and Thr. 1a.

2.5. Analytical decomposition

In the analytical decomposition, ankle DJS and each component were derived based on the

equilibrium equations of 2D inverse dynamics. With the 2D free body diagram of the foot segment (Fig. 3), we have the equations:

$$\sum \vec{F} = m_f \vec{a} \tag{5}$$

$$\sum \vec{M}_f = I_f \vec{\alpha} \tag{6}$$

with the mass of foot m_f , linear acceleration \vec{a} , moment of inertial about the foot's center of mass I_f . We then get:

$$\vec{F}_a + \overline{GRF} + m_f \vec{G} = m_f \vec{a} \tag{7}$$

$$M_{eax} + (\vec{r} \times \vec{F}_a)_x + (\vec{d} \times \overline{GRF})_x = I_f \alpha_x(8)$$

Where joint reaction force $\vec{F}_a = \begin{bmatrix} F_{ay} \\ F_{az} \end{bmatrix}$, $\overrightarrow{GRF} = \begin{bmatrix} F_{ay} \\ F_{az} \end{bmatrix}$

$$\begin{bmatrix} GRF_y \\ GRF_z \end{bmatrix}$$
, $\vec{G} = \begin{bmatrix} 0 \\ -g \end{bmatrix}$, $\vec{a} = \begin{bmatrix} a_y \\ a_z \end{bmatrix}$, foot segment angular acceleration is α_x , and M_{eax} is the external joint reaction moment in the x-direction

external joint reaction moment in the x-direction (dorsi/plantarflexion moment).

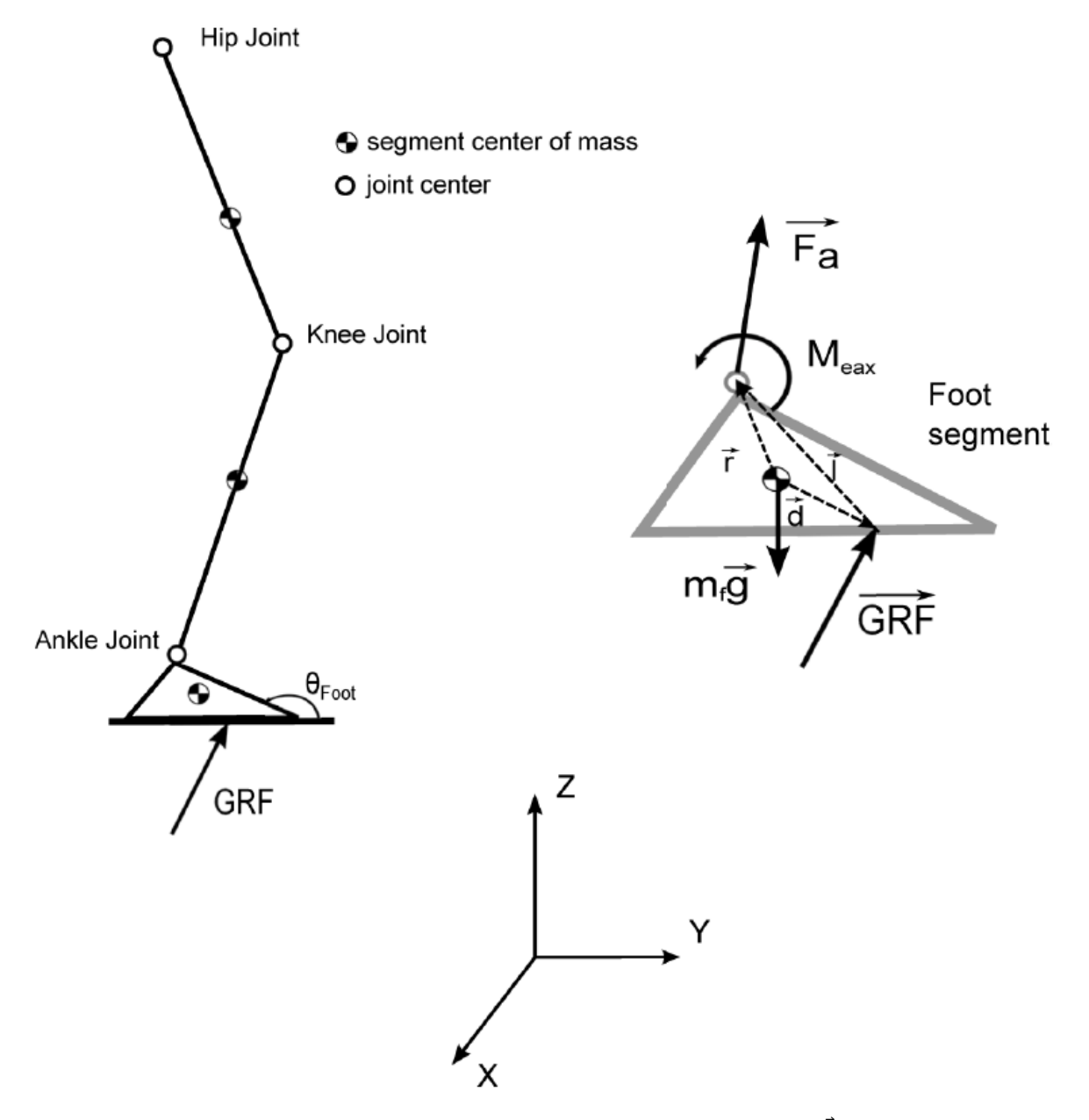


Figure 3. 2D lower limb diagram with free body diagram of the foot segment (\vec{F}_a : joint reaction force, \overline{GRF} : ground reaction force, M_{eax} : external joint moment, $m_f \vec{g}$: gravitational force of foot segment, θ_{Foot} : the segment angle of foot segment).

From Eq. (7) and Eq. (8), with moments summed about the foot's center of mass, we can get:

$$\begin{split} M_{eax} &= I_f \alpha_x - m_f (\vec{r} \times \vec{a})_x \\ &+ \left(\left(\vec{r} - \vec{d} \right) \times \overline{GRF} \right)_x \\ &+ m_f \left(\vec{r} \times \vec{G} \right)_x \end{split}$$

From Eq. (9) and Eq. (10), we can get:

$$M_{eax} = I_f \alpha_x - m_f (\vec{r} \times \vec{a})_x + (\vec{l} \times \overline{GRF})_x + m_f (\vec{r} \times \vec{G})_x$$
(11)

We can then define:

$$M_{FAx} = -(I_f \alpha_x - m_f(\vec{r} \times \vec{a})_x)$$
 (12)

From Fig. 3, we know that

$$\vec{l} = \vec{r} - \vec{d} \qquad (10) \qquad M_{GAx} = -m_f(\vec{r} \times \vec{G})_x \qquad (13)$$

(9)

$$M_{GRFAx} = -(\vec{l} \times \overline{GRF})_x = (\vec{L} \times \overline{GRF})_x$$
(14)

Where M_{FAx} is moment about ankle due to the accelerations (linear and angular), M_{GAx} , is moment about ankle due to the segment mass, M_{GRFAx} is moment about ankle due to ground reaction force, and we let $\vec{L} = -\vec{l}$. Eq. (11) can be rewritten as:

$$M_{egx} = -M_{GRFAx} - M_{FAx} - M_{GAx} \tag{15}$$

$$M_{ax} = -M_{eax} \tag{16}$$

where M_{ax} is the internal dorsi/plantarflexion

The Ankle DJS
$$q$$
 is defined as:

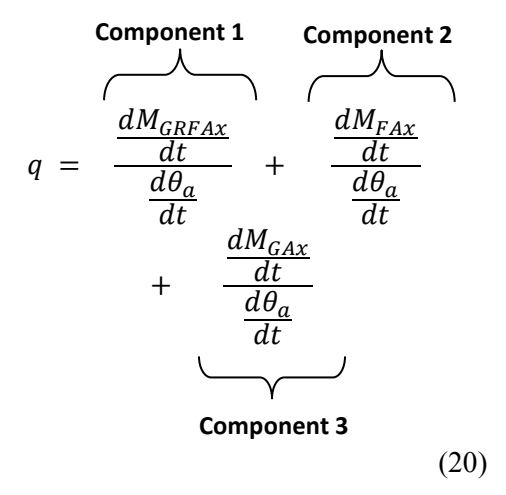
$$q = \frac{dM_{ax}}{d\theta_a}$$
(17)

where θ_{a} is the sagittal plane ankle angle and, due to the chain rule, Eq. (17) can be represented as:

$$q = \frac{dM_{ax}}{d\theta_a} = \frac{\frac{dM_{ax}}{dt}}{\frac{d\theta_a}{dt}}$$
 (18)

$$\alpha_{\chi} = \frac{d^2 \theta_{Foot}}{dt^2} \tag{19}$$

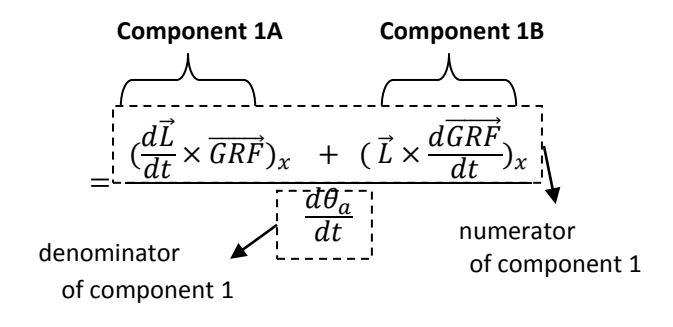
where θ_{Foot} is the foot segment angle. From Eq. (15-19), ankle DJS q can be decomposed into three components:



Component 1 represents the ratio of changes in GRF moment to changes in ankle angle; Component 2 represents the ratio of changes in moment due to foot accelerations to changes in ankle angle; Component 3 represents the ratio of changes in moment due to foot mass to changes in ankle angle.

Component was subsequently decomposed further into Eq. (21):

$$\frac{\frac{dM_{GRFAx}}{dt}}{\frac{d\theta_a}{dt}} = \frac{\frac{d}{dt}(\vec{L} \times \overrightarrow{GRF})_x}{\frac{d\theta_a}{dt}}$$



(21)

Sub-component 1A represents the changes of GRF moment arm $(d\vec{L}/dt)$ times the GRF (\overrightarrow{GRF}) , and sub-component 1B represents the GRF's moment arm (\vec{L} , the vector from COP to ankle joint center) times the change in GRF $(d\overline{GRF}/dt)$. As such, component 1A will be large when the GRF magnitude is large and/or the COP advances towards the toe. Component 1A will be negative when the COP moves proximally towards the ankle or the ankle advances towards a loaded forefoot. Component 1B will be large if the COP is located far distally under the toes, or if the GRF increases rapidly. Component 1B can likewise be negative if either the GRF decreases or if the COP is posterior to the ankle. Numerical time derivatives were estimated using central difference and solved using Matlab.

2.6. Linear regression

In order to confirm that the analytical decomposition was accurate, DJS q from Eq. (20) was compared to the slope of the momentangle loop derived from linear regression of experimental data. For each of the sub-phases, a linear regression line, minimizing the least square distance between the data points and the line, was computed to quantify the slope of the curve (DJS, Nm(kg·deg)⁻¹) over the interval within the moment-angle loop (Frigo et al., 1996).

Table 1. Ankle dynamic joint stiffness (DJS) was calculated using linear regression and analytical decomposition prospectively in the four sub-phases: early rising phase (ERP), short descending phase (SDP), late rising phase (LRP) and descending phase (DP). Significant difference from controls in ankle DJS are indicated in bold. The intraclass correlation coefficient (ICC 2) was determined to show the agreement in computed ankle DJS between the two methods.

			ERP	SDP	LRP	DP
		Linear regression	4.06		20.30	6.31
		(mean± S.D.)	(1.56)		(1.79)	(1.29)
	Control	Analytical				
		decomposition	3.84		19.77	6.68
		(mean± S.D.)	(1.54)		(1.18)	(1.44)
		ICC 2	0.85	N/A	0.90	0.98
		Linear				
		regression	3.27		12.24	5.78
Dynamic joint stiffness		(mean± S.D.)	(1.27)		(2.75)	(1.30)
100Nm(kg·deg) ⁻¹	JIA	Analytical				
, 5		decomposition	3.15		12.42	6.07
		(mean± S.D.)	(1.27)		(3.74)	(1.43)
		ICC 2	0.87		0.72	0.96
		Linear				
		regression	8.10	9.52	6.76	6.34
		(mean± S.D.)	(3.80)	(3.75)	(3.33)	(2.37)
	ITW	Analytical				
		decomposition	7.75	9.27	7.10	6.96
		(mean± S.D.)	(3.81)	(3.00)	(3.64)	(2.66)
		ICC 2	0.99	0.98	0.94	0.96

2.7. Statistical analysis

The analytical decomposition and linear regression were applied to three individual trials per subject (left and right sides separately) and a mean value for each side was calculated for each subject in each sub-phase. All values were multiplied by 100 for more convenient numerical representation. The intraclass correlation coefficient (ICC 2) was determined to test the assumption of agreement in computed ankle DJS computation from linear regression and from analytical decomposition. Data (ankle DJS and each component) were analyzed using a two-way repeated measures ANOVA with side as the within-group factor and group (control group or JIAs, and control group or ITWs) as between-group factor. The differences in ankle DJS and its components were also analyzed with individual one-way ANCOVA with walking speed as a covariance to determine whether the walking speed influenced the differences between groups. All statistical tests were performed using SPSS v14 software (Chicago, IL, USA). The significance was determined at the p < 0.05 level.

3. Results

There were no significant group-side interactions or side differences in any group. As such, data from right side is presented.

3.1. Group differences in ankle DJS from analytical decomposition

In the control group, ankle DJS was lowest during the ERP ($q = 3.84 \ 100 \text{Nm}(\text{kg} \cdot \text{deg})^{-1}$), highest during the LRP ($q = 19.77 \ 100 \text{Nm}(\text{kg} \cdot \text{deg})^{-1}$), and moderate during DP ($q = 6.68 \ 100 \text{Nm}(\text{kg} \cdot \text{deg})^{-1}$). Compared to controls, subjects with JIA had significantly lower joint stiffness ($q = 3.15 \ 100 \text{Nm}(\text{kg} \cdot \text{deg})^{-1}$, p = 0.034)

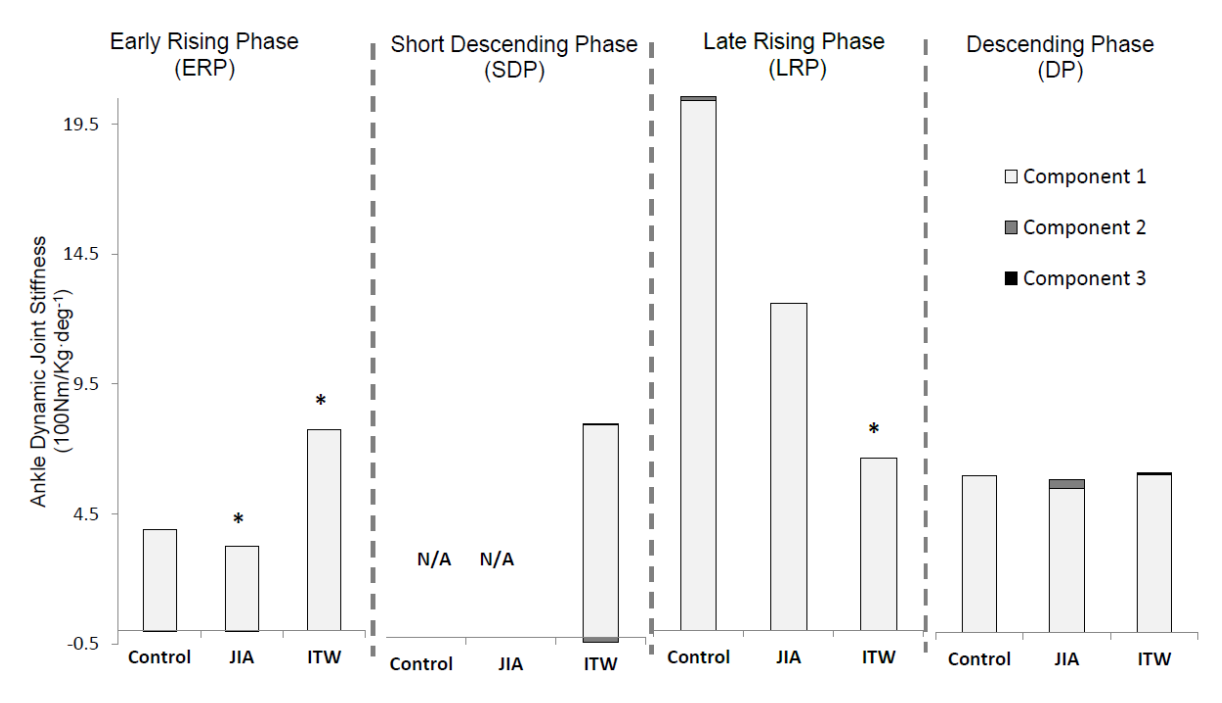


Figure 4. Ankle dynamic joint stiffness was analytically decomposed into three components in the control, JIA and ITW groups. Significant group differences were indicated with asterisks.

in the ERP, but no differences were found in the LRP and DP (Table 1). Subjects with ITW had significantly higher joint stiffness (q = 7.75 100Nm(kg·deg)⁻¹, p < 0.01) in the ERP and lower stiffness (q = 7.10 100Nm(kg·deg)⁻¹, p = 0.02) in the LRP phase, but no differences were seen in the DP. Only the ITW group had a SDP between the ERP and LRP (q = 9.27 100Nm (kg·deg)⁻¹). Agreements (ICC2) of ankle DJS between analytical decomposition and linear regression in control, JIA and ITW groups were summarized in Table 1.

3.2. Group differences in ankle DJS Components

Component 1 was by far the largest positive contributor to ankle DJS in all sub-phases (Table 2, Fig 4). Compared to controls, in the JIA group, component 1 was significantly lower (p = 0.01) in the ERP, but no significant differences were found in the LRP and DP. In the ITW group, component 1 was significantly larger in the ERP (p = 0.02) and smaller in the LRP (p = 0.03). Component 2 and 3 had very small contributions to the ankle DJS, although there were some differences found between group.

3.2.1 Subcomponents of component 1 (Eq. 21)

The numerator (changes in the GRF moment) and denominator (changes in ankle angle) of component 1 are expressed as percents of the control group's mean in each sub-phase. The numerator was further decomposed into component 1A, the changes of the GRF's moment arm times the GRF and component 1B. the GRF's moment arm times changes in the GRF (Fig. 5A). In the ERP, the numerator was smaller in JIA group (p = 0.04, component 1A: 62% p = 0.04, component 1B: 111%), but the denominator was similar as controls (103%). The ITW group had a larger numerator (p <0.01, component 1A: 33% p < 0.01, component 1B: 2137% p < 0.01) and denominator (227%, p < 0.01) than controls. In the LRP, the numerator in the JIA group was similar to that in the control group (component 1A: component 1B: 71%) but was significantly smaller than control in ITW, with contributions from a negative component 1A and a larger component 1B (p < 0.01, component 1A: -27% p < 0.01, component 1B: 159% p < 0.01), and the denominator was larger in both JIA and ITW groups (JIA: 141% p = 0.03; ITW: 133% p =0.04) than controls.

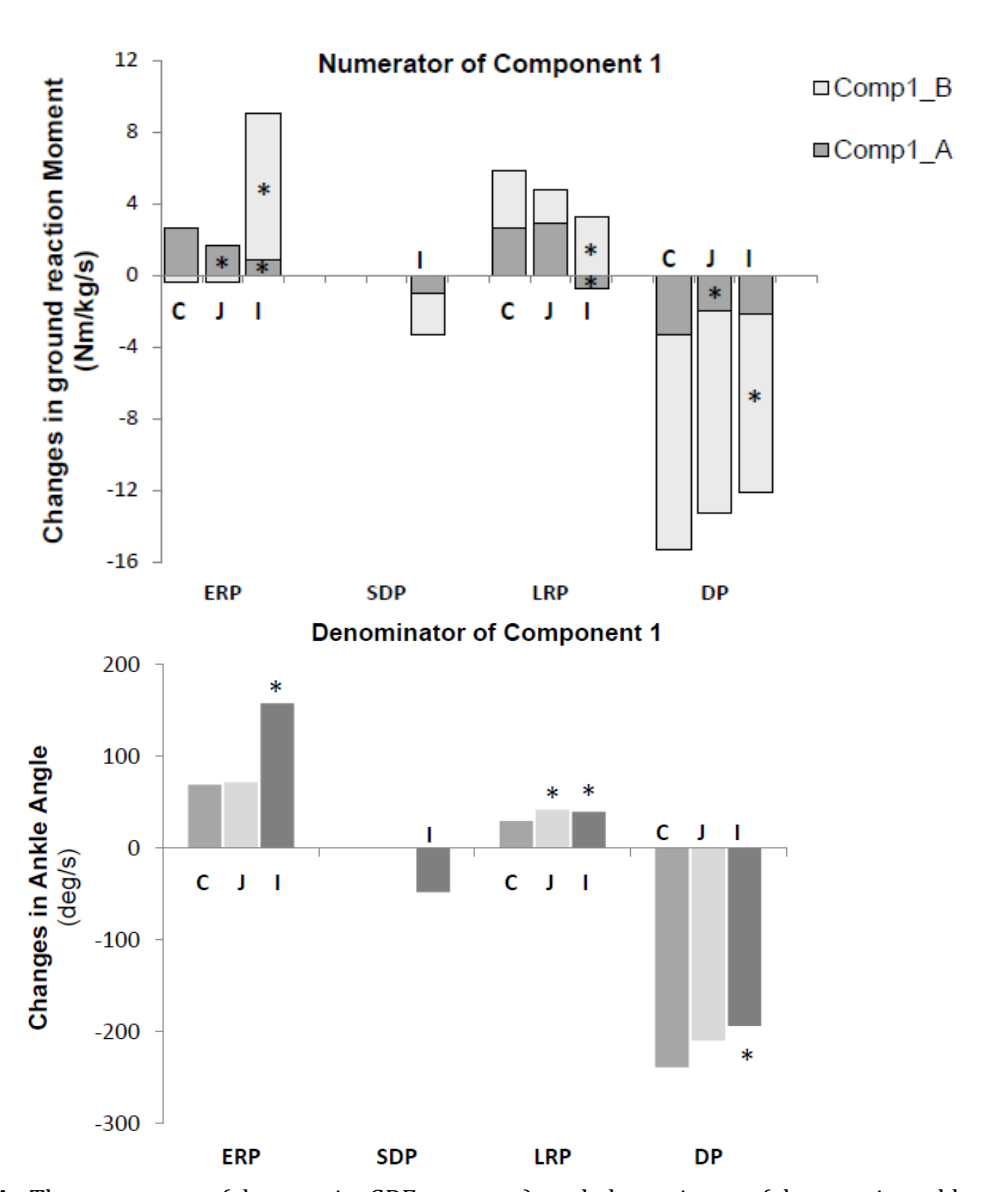


Figure 5A. The numerator (changes in GRF moment) and denominator (changes in ankle angle) of component 1 were averaged during each phase in control (C), JIA (J) and ITW (I) groups. The numerator of component 1 was further decomposed into component 1A (the changes of GRF moment arm times the GRF, comp1_A), and component 1B (the GRF moment arm times changes in GRF, comp1_B). Significant differences compared to the control group in the numerator components and in the denominator were indicated with asterisks.

In the DP, the JIA group had a somewhat smaller numerator due to a smaller Component 1A, as well as a somewhat smaller denominator (component 1A: 59% p = 0.01, component 1B: 94%, denominator 87%). The ITW group likewise had a somewhat smaller numerator due to a lower component 1B (component 1A: 87%, component 1B: 69% p < 0.02), while the denominator (81%, p < 0.01) was smaller than that of controls.

3.3. The influence of walking speed

Walking speed was significantly slower in subjects with JIA (1.15 ± 0.12 m/s, p < 0.01) and subjects with ITW (1.03 ± 0.11 m/s, p < 0.01) than in controls (1.33 ± 0.13 m/s). Using the speed as a covariance, no significant differences in ankle DJS were found between control and JIA group or control and ITW group, i.e. the observed differences in DJS between groups were not speed dependent. Speed was, however, a factor in components 2 and 3; significantly larger component 2 (p = 0.02) was found in JIA group in the DP.

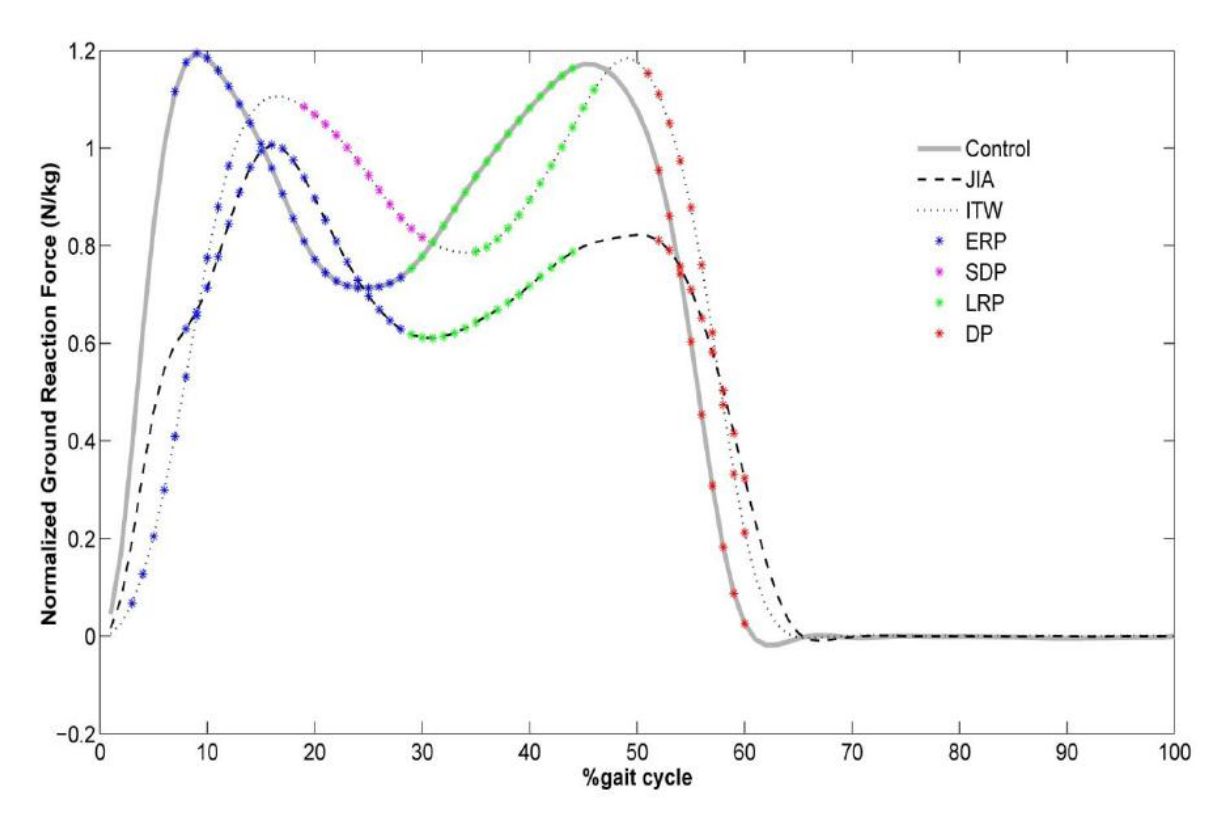


Figure 5B. Representative vertical ground reaction force was normalized by the body weight in control, JIA and ITW groups (ERP: early rising phase, SDP: short descending phase, LRP: late rising phase, DP: descending phase).

A positive and significantly different component 3 (p = 0.02) was found in the ERP and larger component 3 (p < 0.01) in the DP the ITW group.

4. Discussion

In the current study, the ankle DJS was decomposed analytically into individual components. Our findings showed that the decomposition succeeded in quantitatively identifying biomechanical contributors to the ankle DJS in determining pathology-induced changes in subjects with JIA and ITW.

The foundation of this study was that ankle DJS computed with regression could be accurately reproduced with analytical decomposition. According to rule of thumb by Landis and Koch (Landis and Koch, 1977), ICC between 0.61 - 0.80 indicates good agreement and 0.81 - 1 indicates very good agreement. We found good to very good agreement between the sum of decomposed parts and the direct linear regression of experimental data (Table 1), primarily due to the quasi-linear relationship

between ankle moment and angle. It also indicated that the analytical decomposition was accurate and that DJS components can therefore examined individually.

In the control subjects, ankle moment-angle loops showed a counter-clockwise traversed path, comprising three quasi-linear phases ERP, LRP and DP, which agreed with a recent study from Crenna & Frigo (Crenna and Frigo, 2011). No quantitative comparison can be made, however, because of the different angle and moment conventions. Earlier studies have attempted to define the period of the ERP and LRP as one sub-phase (Davis and DeLuca, 1996; Gabriel et al., 2008) between the first local maximum plantarflexion in early stance and maximum dorsiflexion in mid-stance. According to our results, the ankle DJS varied distinctively in the ERP and LRP (Table. 1), and supports the 'ankle-rocker' and 'forefootrocker' definitions by Perry and Burnfield (Perry and Burnfield, 2010). In the ERP, the ankle passively dorsiflexes through the shank's rotation over the stationary foot. The steep LRP was initiated by heel rise and completed when the ankle reached its maximum dorsiflexion. Similar to a previous study, the ERP and the DP of the moment-angle loop at the ankle joint have a relatively similar slope in able-bodied subjects, just shifted along the horizontal axis (Frigo et al., 1996). Although there were some differences found in the JIA group, the shape of the moment-angle loop was similar to that of controls. The ankle moment-angle loop of the subjects with ITW showed a more complex path due to the double bump moment pattern (Fig. 2); there was a unique short descending phase between the ERP and LRP. Compared to controls, the ITW group showed more similar slopes in all the sub-phases.

Using analytical decomposition, ankle DJS can be isolated into components, and component 1 was the dominant contributor. Components 2 and 3, the terms due to foot accelerations and gravity, were negligible due to the trivial mass of the foot. Although the nature of ankle DJS is the coupling of the kinetics and kinematics, the decomposition enabled us to separate the ankle DJS into better understood parameters. In the quasi-linear phase, component 1 represents the ratio of the changes in GRF moment to the changes in ankle angle. The changes in GRF moment can be further decomposed into components 1A and 1B (Fig. 5A). A higher component 1A implies a higher GRF and/or a more rapidly changing GRF moment arm. A higher component 1B is due to a larger GRF moment arm and/or a more rapidly changing GRF. It was primarily in these sub-components that we were able to identify distinctive, more intuitive and interpretable patterns. In normal gait, GRF moment increased during the ERP, due to the increased GRF moment arm $(d\vec{L}/dt >$ 0, component 1A > 0) when the COP advanced. However, GRF decreased after the first peak, which led to a negative component 1B $(d\overline{GRF})$ dt < 0, Fig 5B). During the LRP, both the GRF and its moment arm increased, leading to positive sub-components 1A and 1B. In the DP, GRF moment decreased since both the GRF and its moment arm decreased $(d\overline{GRF}/dt < 0)$ and $d\vec{L}/dt < 0$) when the ankle plantarflexed rapidly and the COP had a very limited distance to advance forward.

The potential clinical utility of momentangle diagram and the analytical decomposition can be illustrated through the examination of the subjects with JIA and ITW (Fig. 5A, 5B).

However, for clarification, the comparison between patient groups and controls aimed to identify biomechanical contributors to ankle DJS differences, not to provide a basis for clinical conclusions, for which larger sample sizes would be required. These two very different patient groups were specifically chosen to provide a wider spectrum of gait pathology for this study. JIA is the most common rheumatic disease in childhood and foot involvement is frequently reported in clinical manifestation (Truckenbrodt et al., 1994). Compared to controls, the JIA group had smaller ankle DJS in the ERP, mainly because of the smaller changes in GRF moment via subcomponent 1A, i.e. due to the smaller GRF and/or more slowly advancing COP. In the LRP, the JIA group had slightly smaller changes in GRF moment but dorsiflexed the ankle more rapidly. Hence, ankle DJS was not significantly different. Our findings are partially supported by the observations of Broström et al. and Hartmann et al. (Broström et al., 2002; Hartmann et al., 2010), who reported that compared to controls, children with JIA had either smaller peak GRF or larger valley vertical GRF, which indicated smaller vertical GRF changes during that period. In the DP, although significant differences found in DJS, significantly smaller changes in GRF moment via sub-component 1A were reported. This may also be explained by the smaller 2nd peak GRF in JIA group reported by a previous study (Hartmann et al., 2010).

ITW is diagnosed by excluding other causes of toe-walking such cerebral palsy, myopathy etc., and can be described in terms of decreased ankle range of motion and inability to heel strike at the initial-contact of gait (Sala et al., 1999). In this study, subjects with ITW had larger ankle DJS in the ERP due to the greater changes in GRF moment via sub-component 1B even though sub-component 1A was smaller than controls (Fig 5A); the midfoot/forefoot initial contact led to a larger GRF moment arm than in controls, which led to a larger sub-component 1B. This agrees with previous reports that the more anterior initial position of COP in toe walking can lead to a ground reaction force moment that is about 2.5 times greater than that in normal heel-toe walking (Casey Kerrigan et al., 2000; Couillandre et al., 2002). In the unique SDP, the ankle had a short period of plantarflexing, while GRF moment decreased

along with the decreasing GRF. In the LRP, lower ankle DJS than control was mainly attributable to the smaller changes in GRF moment via a negative component 1A and larger changes in ankle angle. The negative component 1A was caused by the decreasing GRF moment arm. In the DP, subjects with ITW plantarflexed slowly than controls more (smaller denominator), but the changes in GRF moment were also slightly smaller (smaller numerator), which together resulted in the similar ankle DJS as controls. More generally, while overall DP stiffness was nearly identical in all three groups, this was due to a combination of different biomechanical phenomena, which can only be observed through analytical decomposition.

Differences in walking speed may also influence joint excursions, joint moments and subsequently joint stiffness. In this study, walking speed was found lower in subjects with JIA and ITW. However, no significant associations with ankle DJS were found, which contrasted with previous reports (Frigo et al., 1996; Hansen et al., 2004), possibly because of the small group cohort in our study. Nevertheless, some associations were found between walking speed and components 2 and 3

In the present study, ankle DJS and components were determined based on inverse dynamics, but did not address the relationship between muscles' activities, physiological changes and ankle joint passive stiffness, which worthy further investigations, areas particularly in pathological subjects when muscle activity disorder and pain are present. In addition, although differences were found between groups, the sample sizes of especially the patient groups were small. Thus future work, using groups with larger sample sizes, are needed to apply the findings clinically and more generally. Moreover, during human gait, the ankle joint behavior may be completely understood only when studied in relation to the other lower limb joints, which could be an interesting future extension of the analytical method.

5. Conclusion

This study decomposed ankle DJS into individual components analytically, and explored the hypothesis that stiffness changes in pathological gait could be identified and

interpreted using individual components. To investigate this concept, the ankle DJS and components were calculated in able-bodied children in each phase during stance. Data from subjects with JIA and ITW were examined to explore the potential clinical utility of the decomposition through a wider spectrum of gait pathology. We found that the group differences found in ankle DJS were due almost entirely to changes in component 1, the term associated with GRF moment. More specifically, lower DJS in subjects with JIA in the early rising phase was due to a smaller sub-component 1A (the changes of GRF moment arm times GRF); Larger DJS in subjects with ITW in the early rising phase was due to larger sub-component 1B (GRF moment arm times changes in GRF) and lower DJS in the late rising phase was due to negative sub-component 1A (decreasing GRF moment arm). Moreover, changes in ankle angle also influenced ankle DJS, however, smaller changes in ankle angle did not necessarily indicate higher DJS, e.g. ITW group in early The proposed rising phase. analytical decomposition confirmed our hypothesis and can help interpret the concept of 'joint stiffness', and was applicable in clinical gait evaluation of joint behavior.

Acknowledgements

Funding for this project was generously provided by the Swedish Research Council and Stiftelsen Promobilia. The authors would like to thank Åsa Bartonek and Mikael Reimeringer for their help in data collection.

Table 2. The ankle dynamic joint stiffness was decomposed into four components. Mean (standard deviation) values with respect to sub-phases and groups were shown in 100Nm/(kg⁰)⁻¹. Significant group differences were illustrated in bold. Significant group differences using walking speed as a covariance were illustrated in bold Italic.

Component		ERP			SDP			LRP			OP.	
(mean ± S.D.)	Control	All	MLI	Control	JIA	ITW	Control	JIA	ITW	Control	All	MI
Component 1	3.88	3.25	7.73			9.45	19.64	12.43	6.99	99.9	5.69	6.87
Tallolloding	(1.60)	(1.15)	(3.79)			(3.38)	(3.10)	(2.74)	(2.49)	(1.29)	(1.28)	(1.31)
Component 2	-0.04	-0.10	0.02	V/N	X	-0.19	0.14	0.01	0.03	0.01	0.37	0.07
Components	(0.01)	(0.03)	(2E-3)		C	(2E-3)	(0.02)	(0.05)	(7E-3)	(0.05)	(0.05)	(0.04)
Component 3	-2E-3	-5E-3	4E-4			0.01	-6E-3	-5E-3	-0.01	0.01	0.01	0.02
Callibolication	(6E-4)	(2E-3)	(1E-4)			(1E-3)	(1E-3)	(2E-3)	(5E-3)	(2E-3)	(3E-3)	(4E-3)

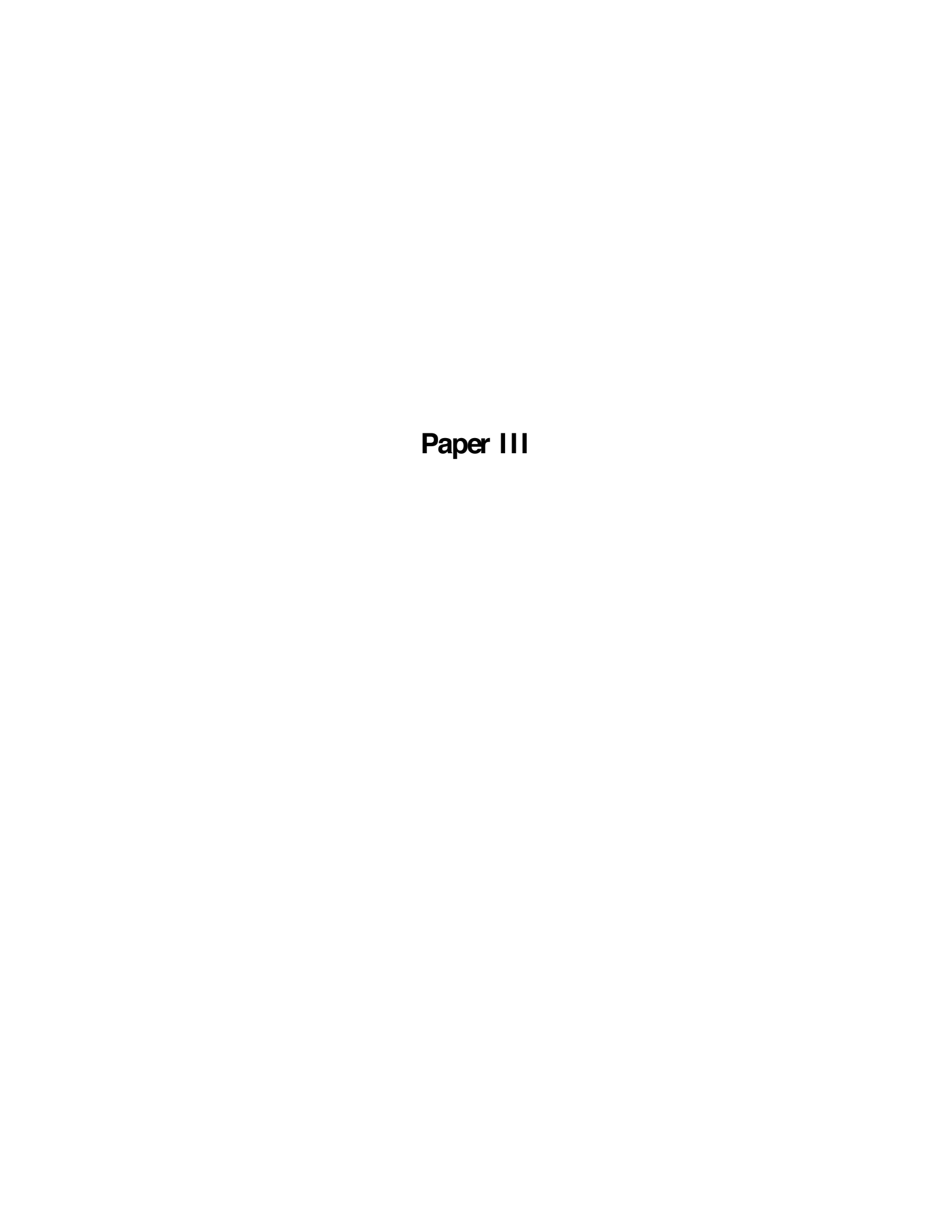
ERP = early rising phase; SDP = short descending phase; LRP = late rising phase; DP = descending phase; JIA = juvenile idiopathic arthritis; ITW = idiopathic toe walking;

Reference List

- Armand, S., Watelain, E., Mercier, M., Lensel, G., Lepoutre, F. X., (2006). Identification and classification of toe-walkers based on ankle kinematics, using a data-mining method. Gait & Posture 23, 240-248.
- Broström, E., Haglund-Akerlind, Y., Hagelberg, S., Cresswell, A. G., (2002). Gait in children with juvenile chronic arthritis. Timing and force parameters. Scandinavian journal of rheumatology 31, 317-23.
- Casey Kerrigan, D., Riley, P. O., Rogan, S., Burke, D. T., (2000). Compensatory advantages of toe walking. Arch Phys Med Rehabil 81, 38-44.
- Couillandre, A., Maton, B., Breniere, Y., (2002). Voluntary toe-walking gait initiation: electromyographical and biomechanical aspects. Exp Brain Res 147, 313-321.
- Crenna, P., Frigo, C., (2011). Dynamics of the ankle joint analyzed through momentangle loops during human walking: Gender and age effects. Human movement science In press.
- Davis, R. B., DeLuca, P. A., (1996). Gait characterization via dynamic joint stiffness. Gait & Posture 4, 224-231.
- Derry, K. L., Venance, S. L., Doherty, T. J., (2012). Decomposition-based quantitative EMG in the evaluation of muscular dystrophy severity. Muscle & nerve 45, 507-513.
- Doherty, T. J., Stashuk, D. W., (2003). Decomposition-based quantitative electromyography: Methods and initial normative data in five muscles. Muscle & nerve 28, 204-211.
- Frigo, C., Crenna, P., Jensen, L. M., (1996). Moment-angle relationship at lower limb joints during human walking at different velocities. Journal of electromyography and kinesiology 6, 177-190.
- Gabriel, R. C., Abrantes, J., Granata, K., Bulas-Cruz, J., Melo-Pinto, P., Filipe, V., (2008). Dynamic joint stiffness of the ankle during walking: gender-related differences. Physical therapy in sport 9, 16-24.
- Hansen, A. H., Childress, D. S., Miff, S. C., Gard, S. A., Mesplay, K. P., (2004). The human ankle during walking: implications

- for design of biomimetic ankle prostheses. Journal of biomechanics 37, 1467-1474.
- Hartmann, M., Kreuzpointner, F., Haefner, R., Michels, H., Schwirtz, A., Haas, J. P., (2010). Effects of Juvenile Idiopathic Arthritis on Kinematics and Kinetics of the Lower Extremities Call for Consequences in Physical Activities Recommendations. Int J Pediatr 2010.
- Landis, J. R., Koch, G. G., (1977). The measurement of observer agreement for categorical data. Biometrics 33, 159-174.
- Latash, M. L., Zatsiorsky, V. M., (1993). Joint stiffness: Myth or reality? Human movement science 12, 653-692.
- Nolan, K. J., Yarossi, M., (2011). Preservation of the first rocker is related to increases in gait speed in individuals with hemiplegia and AFO. Clinical Biomechanics 26, 655-660.
- Perry, J., Burnfield, J. M., (2010). Gait analysis: normal and pathological function. SLACK Inc., Thorofare.
- Petty, R. E., Southwood, T. R., Baum, J., Bhettay, E., Glass, D. N., Manners, P., Maldonado-Cocco, J., Suarez-Almazor, M., Orozco-Alcala, J., Prieur, A. M., (1998). Revision of the proposed classification criteria for juvenile idiopathic arthritis: Durban, 1997. The Journal of rheumatology 25, 1991-1994.
- Robertson, D. G. E., (2004). Research methods in biomechanics. Human Kinetics, Champaign.
- Sala, D. A., Shulman, L. H., Kennedy, R. F., Grant, A. D., Chu, M. L., (1999). Idiopathic toe-walking: a review. Developmental medicine and child neurology 41, 846-848.
- Tateuchi, H., Tsukagoshi, R., Fukumoto, Y., Oda, S., Ichihashi, N., (2011). Dynamic hip joint stiffness in individuals with total hip arthroplasty: Relationships between hip impirments and dynamics of the other joints. Clinical Biomechanics 26, 598-604.
- Truckenbrodt, H., Häfner, R., von Altenbockum, C., (1994). Functional joint analysis of the foot in juvenile chronic arthritis. Clinical and experimental rheumatology 12, S91-96.
- Zeni Jr, J. A., Higginson, J. S., (2009). Dynamic knee joint stiffness in subjects

with a progressive increase in severity of knee osteoarthritis. Clinical biomechanics (Bristol, Avon) 24, 366-371.



ELSEVIER

Contents lists available at ScienceDirect

Gait & Posture

journal homepage: www.elsevier.com/locate/gaitpost



The effect of subtalar inversion/eversion on the dynamic function of the tibialis anterior, soleus, and gastrocnemius during the stance phase of gait

Ruoli Wang a, Elena M. Gutierrez-Farewik a,b,*

ARTICLE INFO

Article history: Received 21 August 2009 Received in revised form 29 December 2010 Accepted 7 March 2011

Keywords: Induced acceleration analysis Subtalar joint Excessive inversion/eversion Gastrocnemius Soleus Tibialis anterior

ABSTRACT

The purpose of this study was to determine how gait deviation in one plane (i.e. excessive subtalar inversion/eversion) can affect the dynamic function of the tibialis anterior, gastrocnemius, and soleus to accelerate the subtalar, ankle, knee and hip joints, as well as the body center of mass. Induced acceleration analysis was performed based on a subject-specific three-dimensional linkage model configured by stance phase gait data and driven by one unit of muscle force. Eight healthy adult subjects were examined in gait analysis. The subtalar inversion/eversion was modeled by offsetting up to 20° from the normal subtalar angle while other configurations remained unaltered. This study showed that the gastrocnemius, soleus and tibialis anterior generally functioned as their anatomical definition in normal gait, but counterintuitive function was occasionally found in the bi-articular gastrocnemius. The plantarflexors play important roles in the body support and forward progression. Excessive subtalar eversion was found to enlarge the plantarflexors and tibialis anterior's function. Induced acceleration analysis demonstrated its ability to isolate the contributions of individual muscle to a given factor, and as a means of studying effect of pathological gait on the dynamic muscle functions.

© 2011 Elsevier B.V. All rights reserved.

1. Introduction

The subtalar joint, situated between the talus and calcaneus, is a major ankle functional unit. The joint axis' oblique orientation, which can vary in able-bodied persons [1], allows complex motion of the foot relative to the tibia [2]. If normal subtalar motion is lost, the ankle has no relief from super-imposed rotational forces from talar torsion, which may lead to secondary degenerative arthritis [3]. Excessive subtalar inversion or eversion or joint axis misalignment can be caused by static deformity or inappropriate muscle function during development [4]. Subtalar inversion is commonly found in children with cerebral palsy and spasticity of the tibialis posterior, pes equinovarus adductus and cavus foot deformities, and subtalar eversion in persons with pes planus, rheumatoid arthritis and myelomeningocele [5]. Foot function may alter significantly with any variation in lower extremity alignment [6]. The dynamic functions of a joint's surrounding muscles can also vary as a result of abnormal joint motion.

The tibialis anterior has a powerful dorsiflexion mechanical advantage [6], but can also create subtalar inversion moment by

E-mail address: lanie@mech.kth.se (E.M. Gutierrez-Farewik).

adducting the calcaneus. The gastrocnemius and soleus act via the Achilles tendon as ankle plantarflexors. However, in a neutral position, the Achilles tendon passes slightly medial to the subtalar joint and therefore produces an inversion moment [2]. When both cross-sectional area and distance from the subtalar joint axis were considered, the gastrocnemius and soleus were reported as major dynamic stabilizers preventing excessive pronation [7]. Although the tibialis anterior, gastrocnemius and soleus all have considerable inversion leverage, the extent to which they function in gait remains unclear. In addition, how a planar gait deviation (i.e. excessive subtalar inversion/eversion), can alter the capacities of muscles to generate joint accelerations in other planes (e.g. the sagittal plane) remains unexplored.

Determining individual contributions of muscles during movement is complex because a muscle can accelerate joints and segments it does not span [8]. Biarticular muscles may have counterintuitive functions which oppose their anatomical classifications [9]. Induced acceleration analysis (IAA) is an analytical method for computing accelerations produced by an application force to a body or system of bodies [10]. Zajac and Gordon first introduced IAA to demonstrate that the gastrocnemius, anatomically a knee flexor and ankle plantarflexor, can in certain circumstances act to extend the knee [8]. Clinical research using IAA has demonstrated that external tibial rotation can reduce the soleus' knee extension capacity during single-limb stance [11], but the effects of malalignment in the subtalar joint have not previously been investigated.

^a Department of Mechanics, Royal Institute of Technology, Stockholm, Sweden

^b Department of Women's and Children's Health, Karolinska Institutet, Stockholm, Sweden

^{*} Corresponding author at: Department of Mechanics, Royal Institute of Technology, SE-100 44, Stockholm, Sweden. Tel.: +46 8 790 7159; fax: +46 8 796 9850.

The current study aims to determine the effect of subtalar inversion/eversion on the dynamic function of the tibialis anterior, gastrocnemius, and soleus to accelerate the subtalar, ankle, knee and hip joints. The forward and vertical accelerations of the body center of mass (COM) were also computed. A baseline of induced accelerations was presented and muscles' capacities to accelerate joints in the presence of varying degrees of subtalar inversion/eversion were evaluated.

2. Methods

2.1. Musculoskeletal model

A generic 3D linkage model was scaled to fit each subject, configured by gait data and driven by muscle force. The model consisted of 28 rigid segments (torso, head + neck, arms, pelvis, thighs, shanks, patellas, taluses, feet and toes) and 88 muscles. The pelvis could rotate and translate in 3D with respect to the ground. Hips were modeled as ball-and-socket joints, and knees as planar joints [12]. The talocrural, subtalar, and metatarsophalangeal joints were modeled as hinge joints. The subtalar axis was defined from Inman [1]. Muscle paths, bone geometry, and segment inertial parameters were based on previous studies [12,13]. The generic model was scaled based on tracked marker data using SIMM Motion Module [14]. The dynamic equations of model were outlined by Zajac and Gordon [8] and detailed in a previous study [15]. Analyses were performed using SIMM Dynamic Pipeline [16] and SD/FAST (Symbolic Dynamics, Inc., CA).

2.2. Configuration data

Eight healthy adults, five females and three males (age: 32 ± 10 yrs, weight: 62 ± 14 kg), were examined while walking at a self-selected speed, using an 8-camera motion capture system (Vicon MX40, Oxford, UK). Each subject's motion was obtained by fitting the musculoskeletal model to tracked marker data from one representative trial [14]. Sixty-four reflective markers (9 mm) were placed bilaterally on bony

Inversion

landmarks based on a conventional full-body marker set (Vicon Plug-in-Gait), plus a multi-segment foot model marker set [17]. Subtalar inversion/eversion was modeled by offsetting $\pm 10^\circ$ and $\pm 20^\circ$ from the observed subtalar angle. Four sub-phases were identified for both limbs: initial-contact to foot-flat ('1st rocker'), foot-flat ('2nd rocker'), heel-lift to toe-flat ('3rd rocker'), and toe-flat to foot-off ('toe-off'). Ethical approval for this study was obtained. Subjects participated with informed consent.

2.3. Ground-foot contact

Three ground-foot joints were added bilaterally in the linkage model – at the posterior inferior point of the heel ('GFH'), the distal end of the third metatarsal ('GFM'), and the distal end of the hallux ('GFT') – which served as constraints for the estimated center of pressure (COP) in gait (Fig. 1A). In 2nd rocker, the foot was completely fixed to the ground. During the rest of stance phase, 3-DOFs were allowed at the GFH, GFM and GFT joints. Because these explicit joints, instead of measured ground reaction forces, were used to constrain the foot, the joint reaction forces as calculated by the dynamic simulation acted to constrain these joints. After the muscle force was applied, the calculated joint reaction force (from SD/FAST) was equal to the ground reaction force induced by this muscle. The magnitude and direction of the joint reaction force was recalculated when the subtalar angle was manipulated, and the locations of ground-foot joints relative to the foot were modified accordingly.

Since a previous study indicated that the COP path tends to move medially in foot pronation and laterally in supination [18], the following modifications to ground-foot contact were made: heel ground contact was modeled as rolling of a rigid sphere with a local coordinate system over a rigid plate (according to Hagman [19]). The new contact point in the configuration of subtalar inversion or eversion was estimated as the most inferior point of the sphere after rotating 10° or 20° along the subtalar joint axis (Fig. 1B). The same method was used to calculate the new locations of GFT and GFM joints. The spheres' radiuses were estimated by tracked markers' trajectories individually.

IAA was used to calculate the effects of excessive subtalar inversion/eversion on the potential dynamic function of the tibialis anterior, gastrocnemius (medial head), and soleus during stance phase. The potential dynamic function was

(A) Ground-foot joints description (B) Ground-foot contact alternation in configuration of subtalar eversion Sub-phase 2nd rocker 1st rocker 3rd rocker Toe-off Ground-foot GEH GEH GEM GET GEM GET joint Rotationa ٥ DOF Locations relative the marker (D) Subtalar joint inversion/eversion in 5 configurations (C) Moment arm lengths of gastrocnemius, soleus and tibialis anterior Right foot Gastrocnemius medial 20 -- Soleus Tibialis anterior nversion ost inferior point of the subtalar moment arm length(m) 10 COP positio calcaneus, COP position in everted position observed gait 0 -0.01 -20 92 100 30

Fig. 1. (A) Three ground-foot joints were added under the foot- at the posterior inferior point of the heel ('GFH'), the distal end of the third metatarsal ('GFM') and the lifting point of the foot ('GFF'). During 2nd rocker, the foot was fixed to the ground, and in the rest of the sub-phases, only one joint was activated and three-rotational DOFs were allowed. (B) The ground-foot contact alterations in the configuration of subtalar eversion20°. The point was estimated as the most inferior point of the sphere after rotating 20° along the subtalar joint axis. (C) Moment arm versus subtalar joint rotation angle for the gastrocnemius, soleus and tibialis anterior, average of the eight subjects in the study. A negative value indicates an eversion moment arm, a positive one an inversion moment arm. (D) Subtalar joint rotation (inversion/eversion) in five configurations, average of the eight subjects in the study. Excessive inversion or eversion was manipulated by offsetting $\pm 10^\circ$ and $\pm 20^\circ$ from the observed configuration.

%stance phase

represented by the amount of joint and body COM accelerations produced by one unit muscle contractile force (joint acceleration: $^\circ/s^2$ N, COM acceleration: $^\circ/s^2$ N). Each subject's acceleration data was averaged over both limbs and normalized to percent of stance phase. A baseline was calculated by averaging all subjects' normalized IAA data from the observed configuration.

3. Results

Six plots illustrate the IAA profile: angular acceleration of hip flexion/extension, knee flexion/extension, ankle dorsiflexion/plantarflexion and subtalar inversion/eversion, and linear acceleration of the COM in the global anterior and vertical directions. Local effects refer to accelerations at joints spanned by the muscle, while remote effects refer to accelerations of joints not spanned by the muscle. Support refers to the potential to accelerate the COM vertically, and propulsion/deceleration refers to the potential to accelerate the COM anteriorly/posteriorly.

3.1. Observed gait

The gastrocnemius had potentials to plantarflex the ankle throughout the stance phase and to flex the knee in most of the stance phase, but to extend the knee in 1st and some of 3rd rocker (Fig. 2). Subtalar eversion potential was found in 1st rocker. As for remote effects, the gastrocnemius had potentials to extend the hip in 1st rocker, but to flex in the reminder of stance. Meanwhile, its potential to accelerate the COM decreased after initial contact, and remained decelerating until the 3rd rocker, increasing to propulsion afterwards. Support potential can be observed after the 2nd rocker.

Other than to plantarflex the ankle, the soleus had a considerable potential to evert the subtalar joint in the 1st rocker (Fig. 3). As for remote effects, the soleus could cause knee and hip extension, but hip flexion at the end of the 3rd rocker. The soleus

had a longer COM-decelerating potential period than the gastrocnemius, and larger support potential during the 2nd rocker.

The tibialis anterior had dorsiflexion potential throughout the stance phase (Fig. 4). In contrast to the gastrocnemius and soleus, the tibialis anterior had large potential to invert the subtalar joint in 1st rocker. As for remote effects, the tibialis anterior had potentials to flex the hip and knee during most of stance. The tibialis anterior decreased its COM-decelerating effects after initial contact and could propel the COM in the 2nd and most of the 3rd rocker. Support potentials were found in the 1st rocker only.

3.2. Excessive subtalar inversion/eversion

Potentials are expressed as percents of the observed condition at the midpoint of each sub-phase. Excessive subtalar eversion increased the gastrocnemius' knee extension potential (Eversion10°: 112%, Eversion20°: 127%) in 1st and 3rd rockers (Eversion10°: 102%, Eversion20°: 180%). Subtalar inversion reduced its ankle plantarflexion potential in 1st rocker (Inversion10°: 77%, Inversion20°: 73%) and plantarflexion potential increased in subtalar eversion (1st rocker: Eversion10°: 150%, Eversion20°: 240%; 3rd rocker: Eversion10°: 101%, Eversion20°: 126%; toe-off: Eversion10°: 102%, Eversion20°: 115%). As for remote effects, subtalar eversion reduced the gastrocnemius' hip flexion potential in 3rd rocker (Eversion10°: 92%, Eversion20°: 46%). The gastrocnemius had a higher subtalar eversion potential in eversion (Eversion10°: 158%, Eversion20°: 208%) but had opposite effects in inversion (Inversion10°: 54%. Inversion20°: 24%). The gastrocnemius's potential to propel the COM increased in eversion (Eversion10°: 101%, Eversion20°: 130%).

Excessive subtalar eversion increased the soleus' plantarflexion potential (Eversion10°: 142%, Eversion20°: 222%) and knee

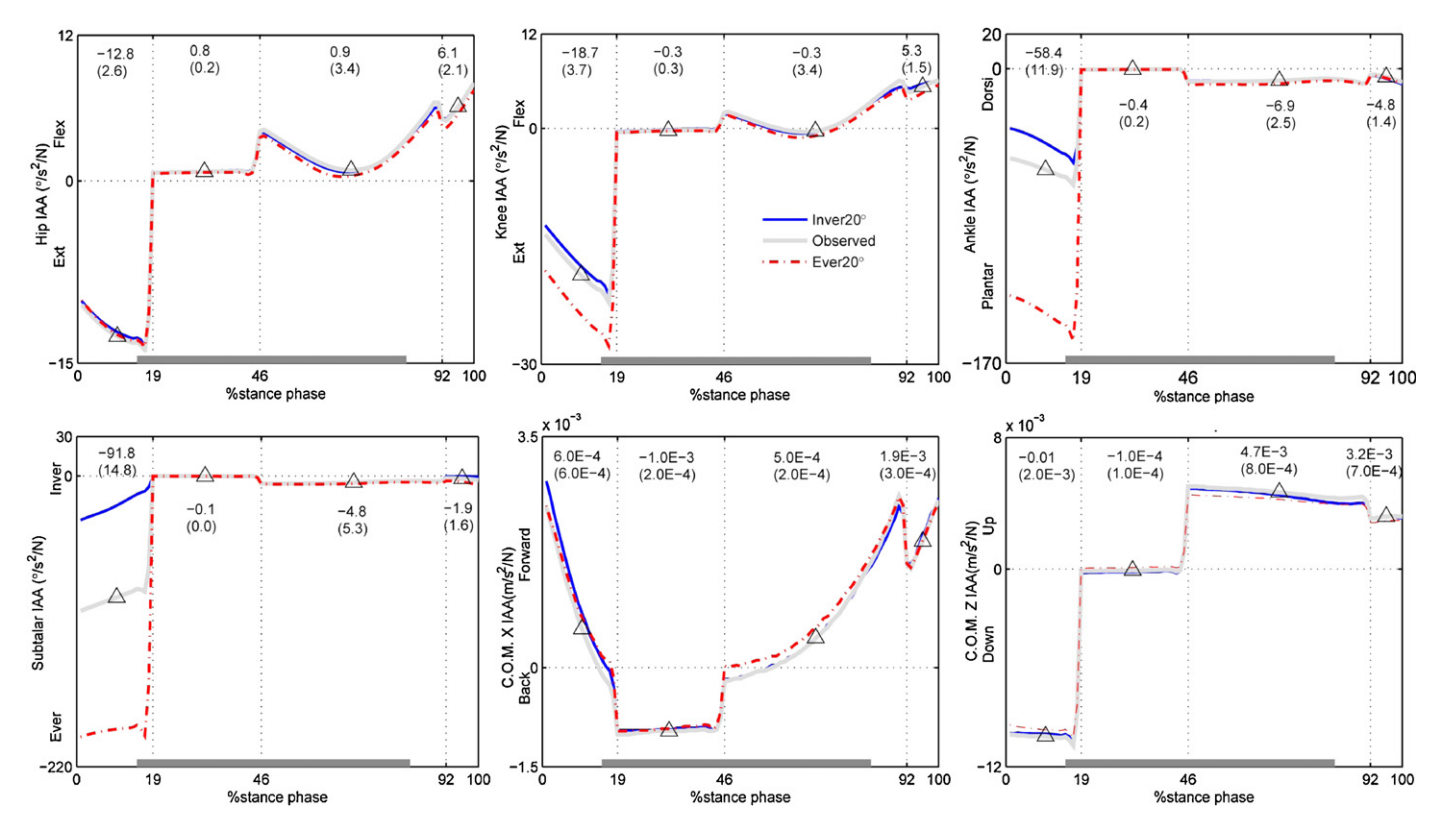


Fig. 2. Normalized gastrocnemius (medial head) IAA profile in the stance phase. Separate solid lines demonstrated the data in the configuration of Inversion20°, Observed and Eversion20°. Dash lines divided the stance phase into four sub-phases: 1st rocker, 2nd rocker, 3rd rocker and toe-off. Gastrocnemius' expected activation duration was shown above the *x*-axis. Mean and standard deviations of the midpoints (indicated with triangles) of each sub-phase were noted only for the normal configuration (Flex: flexion, Ext: extension, Dorsi: dorsiflexion, Plan: plantarflexion, Inver: inversion, Ever: eversion).

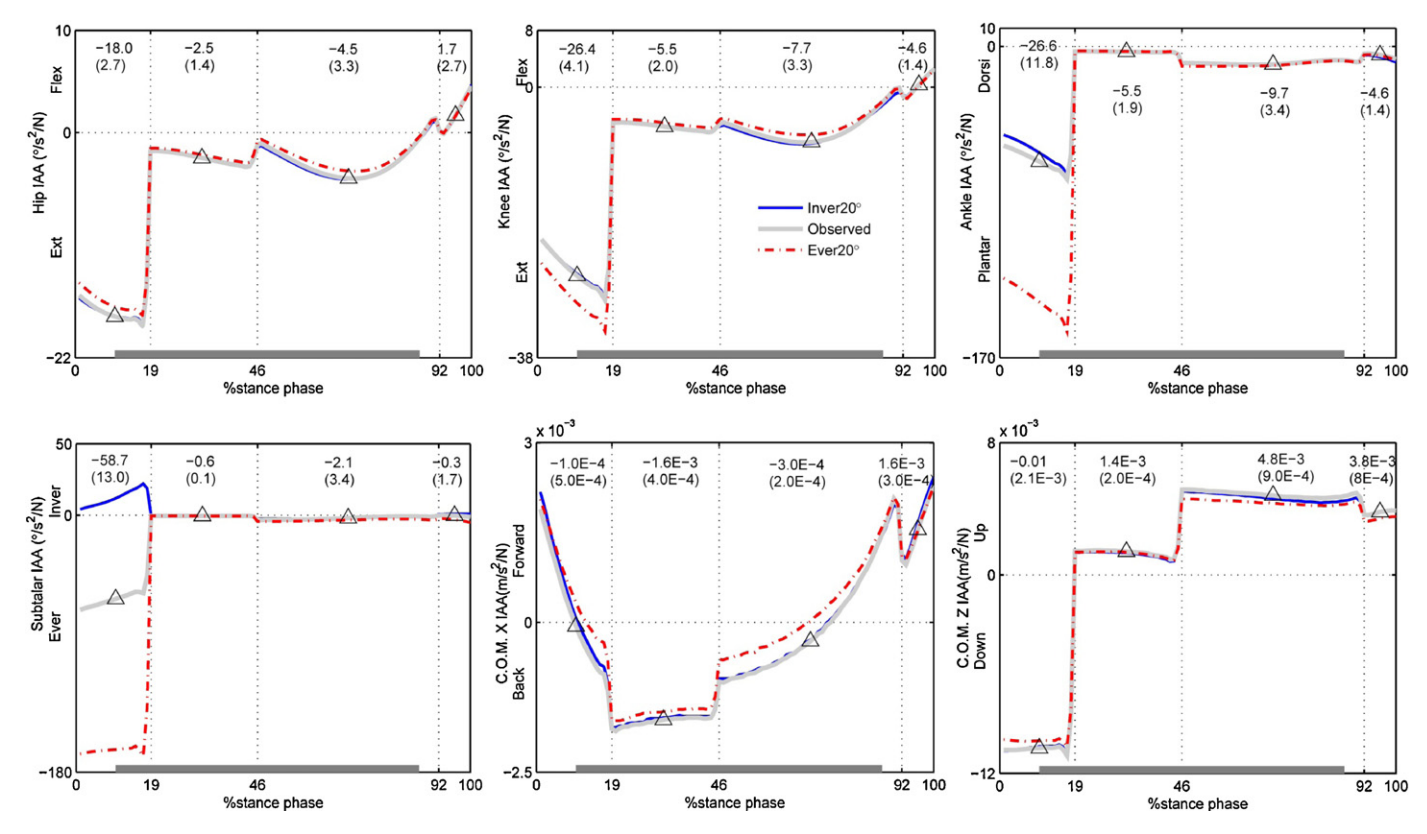


Fig. 3. Normalized soleus IAA profile in the stance phase. Separate solid lines demonstrated the data in the configuration of Inversion20°, Observed and Eversion20°. Dash lines divided the stance phase into four sub-phases: 1st rocker, 2nd rocker and toe-off. Soleus' expected activation duration was shown above the *x*-axis. Mean and standard deviations of the midpoints (indicated with triangles) of each sub-phase were noted only for the normal configuration (Flex: flexion, Ext: extension, Dorsi: dorsiflexion, Plan: plantarflexion, Inver: inversion, Ever: eversion).

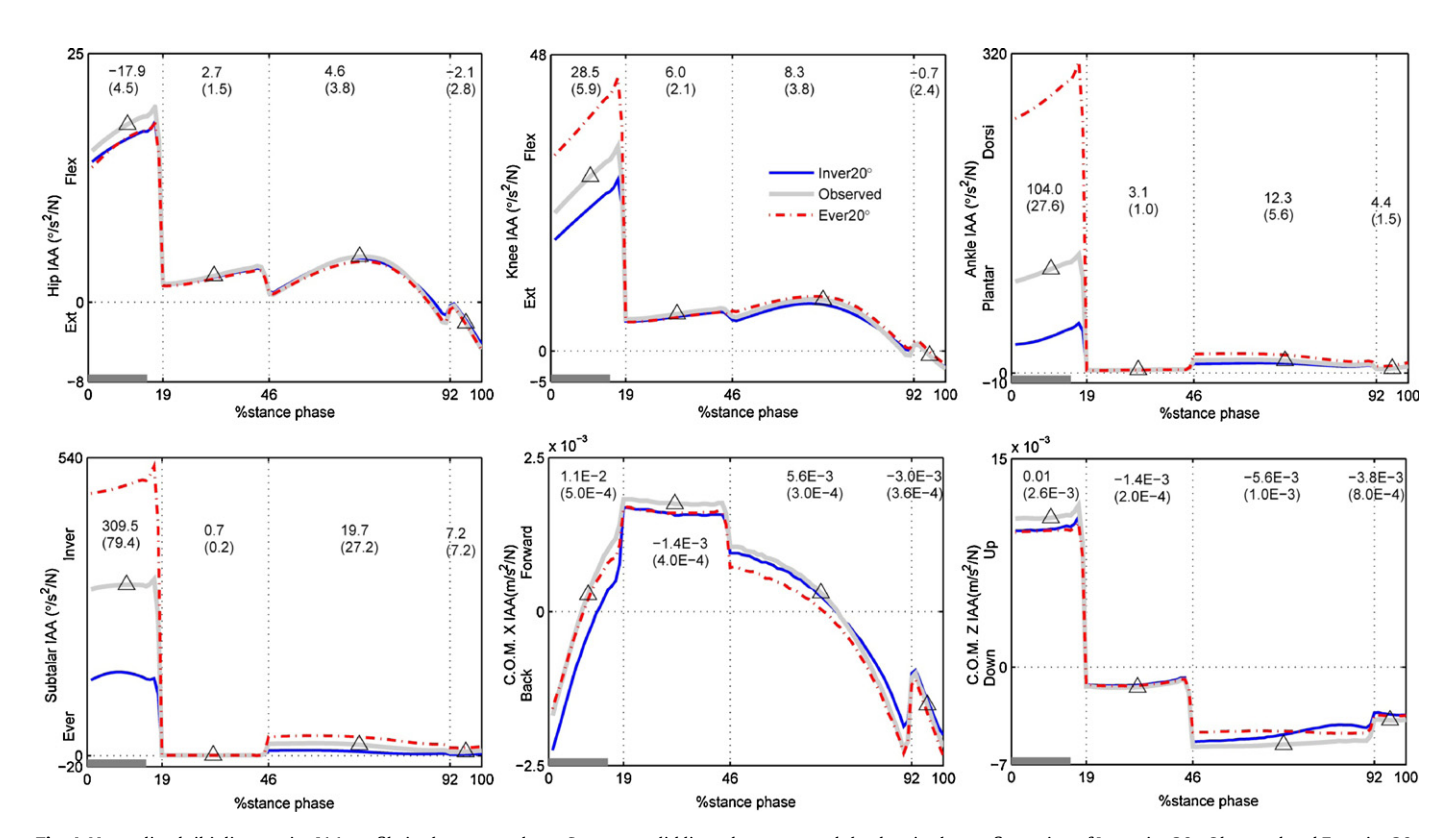


Fig. 4. Normalized tibialis anterior IAA profile in the stance phase. Separate solid lines demonstrated the data in the configuration of Inversion20°, Observed and Eversion20°. Dash lines divided the stance phase into four sub-phases: 1st rocker, 2nd rocker, 3rd rocker and toe-off. Tibialis anterior's expected activation duration was shown above the *x*-axis. Mean and standard deviations of the midpoints (indicated with triangle) of each sub-phase were noted only for the normal configuration (Flex: flexion, Ext: extension, Dorsi: dorsiflexion, Plan: plantarflexion, Inver: inversion, Ever: eversion).

extension potential (Eversion10°: 108%, Eversion20°: 114%). Similar to the gastrocnemius, subtalar eversion increased the soleus' subtalar eversion potential (Eversion10°: 191%, Eversion20°: 279%) but had opposite effects when slightly inverted (Inversion10°: 29%) and generated inversion potential when the subtalar joint was greatly inverted (Inversion20°: –20%). The soleus also tended to increased COM propulsion potential in subtalar eversion before toe-off.

Subtalar inversion reduced the tibialis anterior's dorsiflexion potential (Inversion10°: 56%, Inversion20°: 35%) and knee flexion potential (Inversion10°: 90%, Inversion20°: 82%) in 1st rocker. Subtalar eversion increased knee flexion potentials (Eversion10°: 117%, Eversion20°: 134%) and ankle dorsiflexion potentials (Eversion10°: 174, Eversion20°: 267%) in 1st rocker. Inversion reduced the tibialis anterior's potential to further invert the subtalar joint (Inversion10°: 71%, Inversion20°: 48%), to decelerate the COM (Inversion10°: -22%, Inversion20°: -131%), but eversion increased its potential to invert the subtalar joint (Eversion10°: 135%, Eversion20°: 158%).

4. Discussion

Excessive subtalar inversion/eversion was found to alter potentials of the gastrocnemius, soleus and tibialis anterior to accelerate joints and the COM. Based on the hypothesis that sophisticated dynamic muscle functions result from the interaction of muscle force, ground reaction force and the multi-body system [15], only stance phase was analyzed.

Analysis of individual muscles' roles in accelerating segments is important for understanding coordinations of a multi-body movement. In observed gait, the muscles generally acted as expected. Ankle dorsiflexion acceleration potentials caused by the tibialis anterior agreed with its anatomical definition, which help to restrain the rate of plantarflexion in 1st rocker. It was stated that tibialis anterior's local effect can provide a heel rocker to initiate knee flexion for shock absorption during weight acceptance [20]. which corresponds to the present study, in which knee flexion potential was observed during 1st rocker. The soleus caused ankle plantarflexion potentials, which can restrain the rate of tibial advancement in 3rd rocker. The soleus' remote effects to extend the hip and knee agreed with its previous definition as a knee and hip extensor [10,11]. It was reported that the gastrocnemius acted similarly to the soleus, with the additional function as a knee flexor. However in our analysis, knee extension potential was found in 1st and part of 3rd rocker. Some studies have shown that biarticular muscles can act in a counterintuitive manner which opposes their anatomical classification, since the anatomical definition does not consider how a moment applied at one joint can act remotely on other segments [9].

The link between a pathological posture and muscle function is believed to have important clinical implications [21]. Our findings showed that excessive subtalar eversion can actually increase muscle potentials. Eversion increased the gastrocnemius and soleus' ability to extend the knee and plantarflex the ankle, and increased the tibialis anterior's ability to flex the knee and dorsiflex the ankle during 1st rocker. Since opposing influences were found

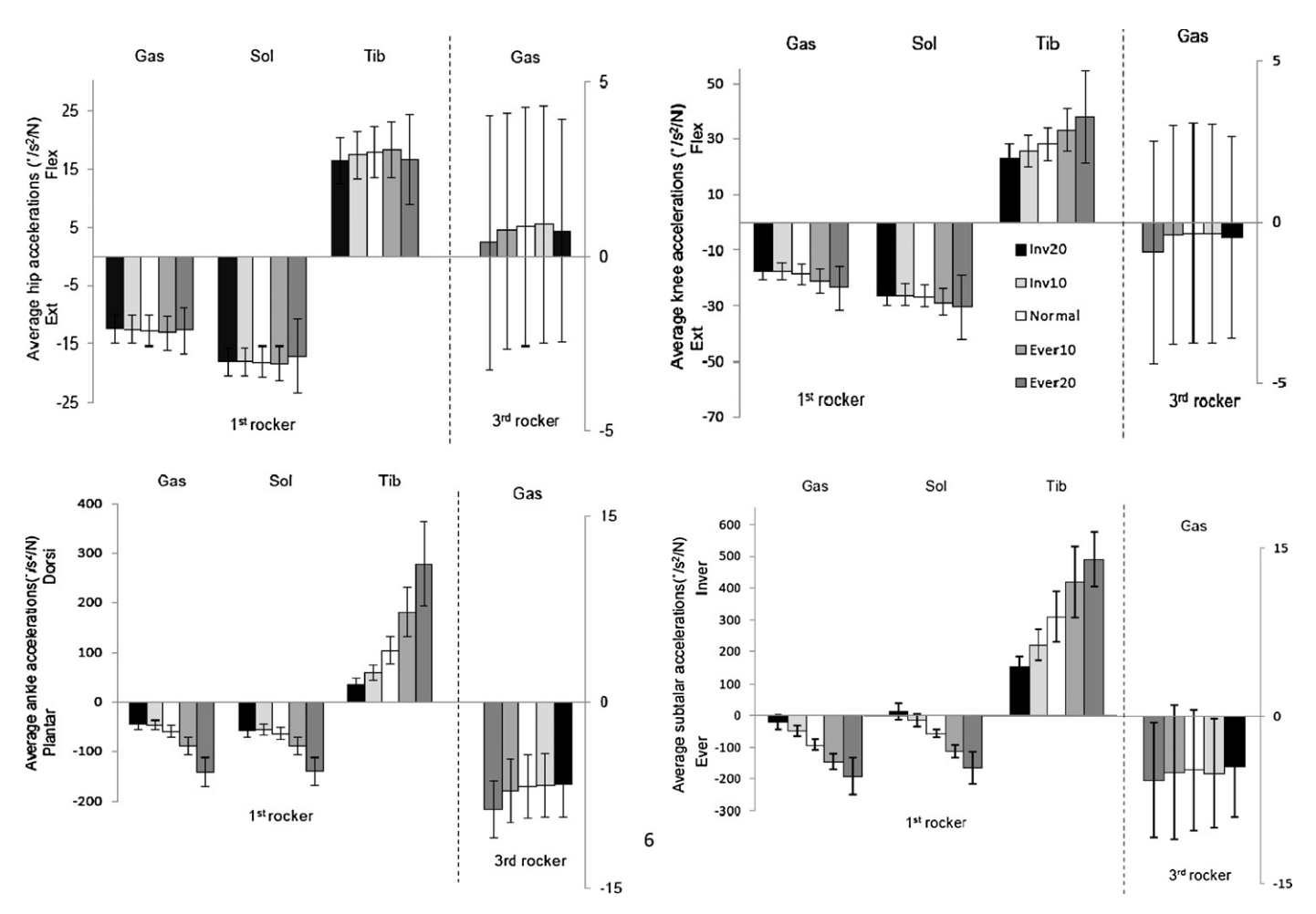


Fig. 5. Angular accelerations of the hip, knee, ankle and subtalar joints induced by gastrocnemius, soleus and tibialis anterior during 1st rocker (left axis) and by the gastrocnemius during the 3rd rocker (right axis). Each bar represents the mean \pm 1 S.D. of the eight subjects in this study.

from ankle plantarflexors and dorsiflexor, the dominant tendency should be further explored by considering muscle activation and induced acceleration magnitude at each joint. Subtalar inversion reduced tibialis anterior's potential to flex the knee and dorsiflex the ankle, which could lead to slower forward progression by diminishing its function to control foot drop and advance the tibia. Also, both eversion and inversion were found to have trivial effects on the most proximal joint; the hip.

In the current study, the observed subtalar joint motion corresponds well with reported motion [17] (Fig. 1C). Similar to Klein et al. [22], the soleus and gastrocnemius were found to have inversion moment arms in a subtalar everted position and an eversion moment arm in a subtalar inverted position, while the tibialis anterior had a consistent inversion moment arm (Fig. 1C), which indicates that gastrocnemius and soleus can switch moment directions according to the position of the subtalar joint. However, this observation cannot fully explain our findings that considerable eversion potential was observed when gastrocnemius and soleus had inversion moment arms, e.g. Eversion 10° (Figs. 1C and 5). The talocrural and subtalar joint axes are not perpendicular and the dominant muscle functions are related to ankle control [23], which can be interpreted using inertial couplings representing the inertial effect of angular acceleration of one joint on another [24]. The large plantarflexion acceleration generated by the soleus and gastrocnemius at the ankle also caused eversion acceleration at the subtalar joint due to the effect of inertial coupling, and it was larger than the inversion accelerations caused by the muscles' and reaction force's smaller inversion leverage. When subtalar joint was more everted, though the gastrocnemius and soleus had larger inversion moment arm (Fig. 1C), eversion potentials were found to increase (Figs. 2, 3 and 5). This suggested that the eversion potential due to inertial couplings may be able to overwhelm the inversion potential from the increased inversion moment arm.

Muscles enable walking by providing vertical support and maintaining forward progression [25]. It was reported that plantarflexors are mainly responsible for generating both support and progression during late stance [26,27]. Neptune et al. found that in early single-stance, both soleus and especially gastrocnemius slowed forward progression [9]. Similar trends were found in the present study, but soleus was found with greater decelerating potential in 2nd rocker. The tibialis anterior had potential to support the body while decelerating forward progression after initial contact, which was consistent with its action to resist foot fall. After 3rd rocker, it was no longer able to support the body while promoting forward progression. Subtalar eversion was found to positively influence the plantarflexors' potential to accelerate the body COM propulsions.

The induced acceleration magnitudes of gastrocnemius and soleus were much greater in 1st rocker than in 2nd and 3rd rockers. While they are able to plantarflex the ankle by lowering the foot after initial-contact, they must overcome large inertial force to advance the tibia in 2nd and 3rd rockers. The changes arising from the additional subtalar inversion/eversion were more obvious in subtalar and ankle joints than in the more proximal joints, i.e. knee and hip. Since only 1 N force was applied in each muscle, the actual acceleration each muscle can induce is most likely much higher.

Similar to Kimmel and Schwartz [15], foot-ground joints were added under the foot to model the foot-floor contact. However, stance phase was divided into four sub-phases instead of Kimmel's three. General qualitative trends of the current findings agreed with his report. Rough transitions between sub-phases can be seen in the figures, mainly due to the rigid foot/ground contact model and the different DOFs allowed in the sub-phases. Unlike Kimmel's study, we used no data smoothing technique; the abrupt changes represented phase transition, e.g. after initial-contact, the floor blocked the foot from free motion, which was allowed before heel-

strike. Moreover, the interpretation was made at midpoints of each sub-phase, avoiding transitions. Sensitivity analyses have been performed to compare the effects of a ground-foot joint with three translational DOFs located at the moving COP and the ones used in the current study. Although the magnitudes of induced accelerations are slightly different between two contact models, the general trends in the observed gait and configurations of subtalar inversion and eversion were similar. The influence of medial and lateral COP shift and of different DOFs in the ground-foot joints was also evaluated. Slight deviations were found in joints' sagittal plane accelerations and the tibialis anterior was the most influenced muscle. Using non-linear springs may be better for more accurate analyses, however, the rigid contact model has been shown to approach a non-linear spring model over short time scales [28].

There are several study limitations. The subtalar inversion/ eversion configurations were manipulated from observed motion data. The variability of subtalar joint axes between subjects was not accounted for. Furthermore, only subtalar position, not joint orientation, was altered. Our intention was to focus on only one factor in the study. Also, the lack of individual subjects' muscle activation patterns and possible compensatory movements in response to modified subtalar angle limits the understanding of IAA results. Furthermore, the variability of results was ascertained to be largely attributable to participators' weight variations and small subject cohort. As noted earlier, IAA can be viewed as a theoretical prediction of accelerations; further experiments, e.g. using functional electrical stimulation [29,30], could determine real individual responses and correlate to IAA results. Also, IAA computation is prone to errors due to individual gait variability. model scaling accuracy, anthropometrical and biomechanical models, etc. Further investigations, for example with perturbation analysis may help to address how such errors can affect the results.

Subtalar inversion/eversion is a common gait deviation, but its influences on individual muscle functions are difficult to address because of the complexity of multi-joint dynamics. Our examination adapts IAA's ability to isolate the contributions of individual muscles with respect to a given factor. Excessive subtalar eversion can increase the dorsiflexor and plantarflexors function, while excessive inversion was found to have a smaller and opposite potential influence. More proximal joints were found less affected by subtalar angle deviations. Moreover, subtalar eversion acceleration can be generated by the ankle plantarflexors, where increasing plantarflexion potentials help to further evert subtalar joint in an excessive subtalar eversion position. Our findings were an essential step toward explaining the pathomechanics of excessive subtalar inversion/eversion and the consequences of clinical interventions.

Acknowledgments

The authors would like to acknowledge Peter Loan at MusculoGraphics, Inc., for his help with model modification, technical support and for his inspirational discussion. We also thank Åsa Bartonek and all participators in the data collecting. Funding for this project was generously provided by the Swedish Research Council and the Frimurare Barnhuset Foundation.

Conflict of interest

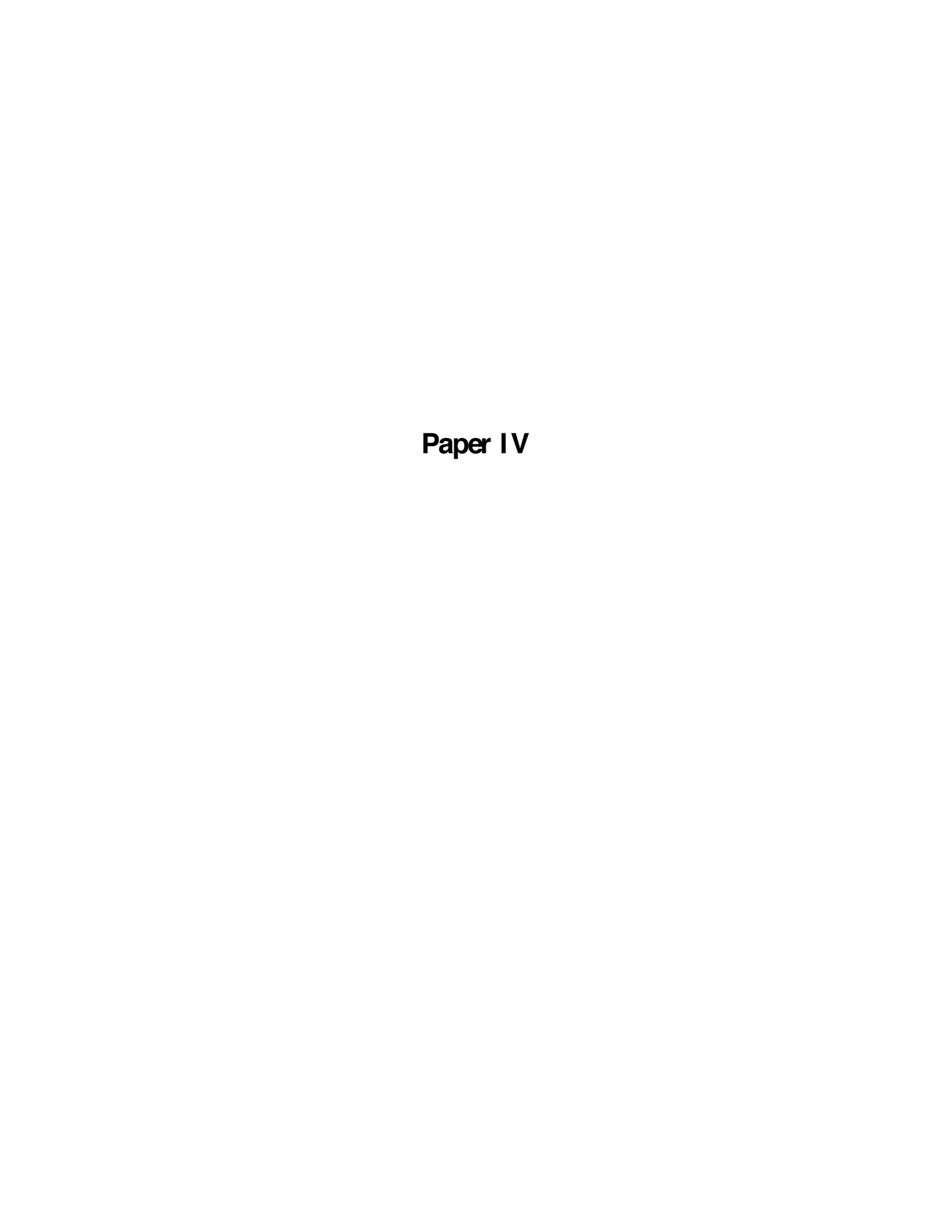
None declared.

References

- [1] Inman VT. The joints of the ankle. Baltimore: Williams & Wilkins; 1976.
- [2] Czerniecki JM. Foot and ankle biomechanics in walking and running. A review. Am J Phys Med Rehabil 1988;67:246–52.

- [3] Perry J. Anatomy and biomechanics of the hindfoot. Clin Orthop Relat Res 1983;177:9–15.
- [4] Perry J. Gait analysis: normal and pathological function. Thorofare: SLACK Inc; 1992.
- [5] DiGiovanni CW, Greisberg J. Foot and ankle: core knowledge in orthopaedics. Elsevier Mosby; 2007.
- [6] Hamill J, Knutzen KM. Biomechanical basis of human movement. Lippincott Williams & Wilkins; 2006.
- [7] Simon SR, Mann RA, Hagy JL, Larsen LJ. Role of the posterior calf muscles in normal gait. J Bone Joint Surg Am 1978;60:465–72.
- [8] Zajac FE, Gordon ME. Determining muscle's force and action in multi-articular movement. Exercise Sport Sci Rev 1989;187–230.
- [9] Neptune RR, Zajac FE, Kautz SA. Muscle force redistributes segmental power for body progression during walking. Gait Posture 2004;19: 194–205.
- [10] Schwartz M, Lakin G. The effect of tibial torsion on the dynamic function of the soleus during gait. Gait Posture 2003;17:113–8.
- [11] Hicks J, Arnold A, Anderson F, Schwartz M, Delp S. The effect of excessive tibial torsion on the capacity of muscles to extend the hip and knee during singlelimb stance. Gait Posture 2007;26:546–52.
- [12] Delp SL, Loan JP, Hoy MG, Zajac FE, Topp EL, Rosen JM. An interactive graphics-based model of the lower extremity to study orthopaedic surgical procedures. IEEE Trans Biomed Eng 1990;37:757–67.
- [13] Arnold AS, Salinas S, Asakawa DJ, Delp SL. Accuracy of muscle moment arms estimated from MRI-based musculoskeletal models of the lower extremity. Comput Aided Surg 2000;5:108–19.
- [14] Inc MG. SIMM 4.0 (Software for Interactive Musculoskeletal Modeling) user's manual. User Manual, Version 2004.
- [15] Kimmel SA, Schwartz M. A baseline of dynamic muscle function during gait. Gait Posture 2006;23:211–21.
- [16] Delp SL, Loan JP. A software system to develop and analyze models of the lower extremity. Comput Aided Surg 2005;5:108–11.

- [17] Stebbins J, Harrington M, Thompson N, Zavatsky A, Theologis T. Repeatability of a model for measuring multi-segment foot kinematics in children. Gait Posture 2006;23:399–400.
- [18] Yoon HK, Park KB, Roh JY, Park HW, Chi HJ, Kim HW. Extraarticular subtalar arthrodesis for pes planovalgus: An interim result of 50 feet in patients with spastic diplegia. Clin Orthop Surg 2010;2:13–21.
- [19] Hagman F. Can plantar pressure predict foot motion? Technical University Eindhoven, Eindhoven, 2005.
- [20] Perry J. Gait analysis: normal and pathological function. Slack Incorporated; 1992
- [21] Riley PO, Kerrigan DC. Kinetics of stiff-legged gait: induced acceleration analysis. IEEE Transac Rehabil Eng 1999;7:420–6.
- [22] Klein P, Mattys S, Rooze M. Moment arm length variations of selected muscles acting on talocrural and subtalar joints during movement: an in vitro study. J Biomech 1996;29:21–30.
- [23] Perry J, Hislop HJ. Principles of lower-extremity bracing. New York: Amer Physical Therapy Association; 1967.
- [24] Zatsiorsky VM. Kinetics of human motion. Champaign: Human Kinetics; 2002.
- [25] Liu MQ, Anderson FC, Pandy MG, Delp SL. Muscles that support the body also modulate forward progression during walking. J Biomech 2006;39:2623–30.
- [26] Kepple TM, Siegel KL, Stanhope SJ. Relative contributions of the lower extremity joint moments to forward progression and support during gait. Gait Posture 1997:6:1–8.
- [27] Gottschall JS, Kram R. Energy cost and muscular activity required for propulsion during walking. J Appl Physiol 2003;94:1766–72.
- [28] Anderson FC, Pandy MG. Individual muscle contributions to support in normal walking. Gait Posture 2003;17:159–69.
- [29] Stewart C, Postans N, Schwartz MH, Rozumalski A, Roberts A. An exploration of the function of the triceps surae during normal gait using functional electrical stimulation. Gait Posture 2007;26:482–8.
- [30] Hernandez A, Dhaher Y, Thelen DG. In vivo measurement of dynamic rectus femoris function at postures representative of early swing phase. J Biomech 2008;41:137–44.



A parametric study of the rigid foot-ground contact model: effects on induced angular accelerations of the lower limb joints in the stance-phase

Ruoli Wang¹, Elena M. Gutierrez-Farewik^{1,2}

¹ Department of Mechanics, Royal Institute of Technology, Sweden ² Department of Women's and Children's Health, Karolinska Institutet, Stockholm, Sweden

Reformatted version of submitted manuscript

Abstract

Determining individual contributions of muscles during movement using computational musculoskeletal models is an important and challenging problem. Induced acceleration analysis was introduced to investigate the relationship between individual muscle function and movement pattern. However, little evidence of the sensitivity of the computational results has limited the use of induced acceleration analysis. This paper described a parametric study on eight healthy adults to analysis how sensitive the muscle-induced joints' accelerations are to the parameters of the rigid foot-ground contact model. We evaluated induced accelerations from the gastrocnemius, soleus and tibialis anterior at the hip, knee, ankle and subtalar joints. We compared two types of models - a 'fixed joint' model with three fixed joints under the foot and a 'moving joint' model with one joint located along the moving center of pressure. The influences of different foot-ground contact joint constraints and locations of center of pressure were also investigated. Small differences were found in lower limb joints' sagittal plane accelerations computed by the two models. The non-sagittal plane muscle induced accelerations at all joints were more affected by center of pressure locations, though differently for different muscles and joints. Among all three muscles, the tibialis anterior was the one whose induced accelerations were affected by all three variations in foot-ground contact models, while the gastrocnemius' and soleus' induced accelerations were influenced trivially by the degreesof-freedom of constraint joint. Care should be taken in applying appropriate constraints and locations of the foot-ground contact joints, especially in investigations of muscle-induced joint accelerations in frontal and transverse planes.

Key words: rigid foot-ground contact model, musculoskeletal modeling, gait, muscle function, center of pressure

1. Introduction

Many researchers have used various approaches to find the contributions of individual muscles to the movement of body segments (Zajac et al., 2002), which are difficult to assess via traditional gait analysis techniques. Induced acceleration analysis (IAA) is a method for computing the accelerations produced by an application force or moment to a body or system of bodies (Schwartz and Lakin, 2003). Recently, the analysis has been used to assess roles of individual muscles and joint moments in providing body support and forward progression during walking (Kepple et al., 1997; Anderson and Pandy, 2003; Neptune et al., 2001). Researchers have studied the causes of pathological gait (Riley and Kerrigan, 1999; Goldberg et al., 2003), and suggested IAA is a useful tool for defining the link between patients' specific muscle impairments and their gait disability.

Performing sensitivity studies to ascertain the reliability of muscle functions computed from simulation is important. The foundation for generating simulation relies on computer-implemented musculoskeletal models which are constructed with assumptions, e.g. physiological properties and paths of muscles and tendons, inertial properties of body segments, the interaction of the body with ground, etc. (Zajac et al., 2002). The best approach to modeling foot-ground contact (FGC) is a widely-debated issue. The most prominent approaches have simplified foot-ground contact as a rigid contact, which occurs either at one joint with varying

rotational degrees of freedom (DOFs) moving instantaneously at the center of pressure (COP) (Schwartz and Lakin, 2003; Goldberg and Kepple, 2009; Hamner et al., 2010; Kepple et al., 1997) or at multiple joints distributed over the foot sole (Anderson and Pandy, 2003; Wang and Gutierrez-Farewik, 2011). Studies also exist which model the shoe sole and underlying soft tissue behavior during contact with a compliant contact model – multiple foot-floor interaction points using visco-elastic elements (Neptune et al., 2004a; Sasaki and Neptune, 2006).

In the rigid-contact model, locations and DOFs of FGC joints are key factors in validating the investigation of interest. In particular, the COP path is usually obtained forceplates. whose resolution frequency can considerably influence the accuracy of the COP path. A mediolateral shift of the COP during walking is often associated with the foot malalignment; the COP path tends to move medially in foot pronation and laterally in supination (Yoon et al., 2010). A recent study has reported that the number of foot-contact points and kinematic constraints affect simulated muscle functions, by examining muscles' contributions to the GRF (Dorn et al., 2011). However, the sensitivity of simulated muscle-induced joint angular accelerations to the location of the COP path and locations of FGC joints have not been investigated. The aim of this study was to determine the influences of location of the COP path and constraints of FGC joints on potential dynamic functions of the medial gastrocnemius, soleus and tibialis anterior in accelerating lower limb joints during the stance phase of gait.

2. Methods

2.1 Configuration data

Eight healthy adults were examined while walking at a self-selected speed, using an 8-camera motion capture system (Vicon MX40, Oxford, UK). Sixty-four reflective markers (9mm) were placed bilaterally on body landmarks based on a conventional full-body marker set (Vicon Plug-in-Gait), plus a multisegment foot model marker set (Stebbins et al., 2006). GRF and COP data were obtained from two forceplates (Kistler) at 1000Hz. Due to lack

of trailing limb forceplate data from leading leg initial contact to trailing leg toe-off, corresponding trailing limb forceplate data from the subsequent gait cycle was merged to yield a complete data set of the stance phase (Gutierrez-Farewik et al., 2006). Ethical approval for this study was obtained.

2.2 Musculoskeletal model and simulations

The generic model was described in a previous study (Wang and Gutierrez-Farewik, 2011). The model consisted of 28 rigid segments and 88 muscles. The pelvis could rotate and translate in 3D with respect to the ground. Hips were modeled as ball-and-socket joints, and knees as planar joints. The talocrural, subtalar, and metatarsophalangeal joints were modeled as hinge joints (Delp et al., 1990). The generic model was scaled to fit each subject based on tracked marker data. The inverse kinematics algorithm solved for joint kinematics differences minimized the between experimental and virtual marker positions. Dynamic inconsistency between measured ground reaction force (GRF) and the kinematics was resolved by applying small external forces and torques (i.e. residuals) to the torso and making small adjustments to the model's mass properties and kinematics (Delp et al., 2007). Computed muscle control (CMC) was utilized to determine a set of muscle excitations that produced a forward simulation of the subject's kinematics (Thelen and Anderson, 2006).

IAA was used to compute the contribution of the gastrocnemius, soleus and tibialis anterior on the lower limb joints' angular accelerations with different foot-ground contact models. The dynamic equations of motion were outlined by Zajac and Gordon (Zajac and Gordon, 1989) and detailed in a recent study (Hamner et al., 2010).

2.3 Foot-ground contact model

Two types of FGC models commonly used in published studies - 'fixed joint' and 'moving joint' - were evaluated in this study. The stance phase was divided into four sub-phases: initial-contact to foot-flat ('1st rocker'), foot-flat ('2nd rocker'), heel lift to toe-flat ('3rd rocker'), and toe-flat to foot-flat ('toe-off').

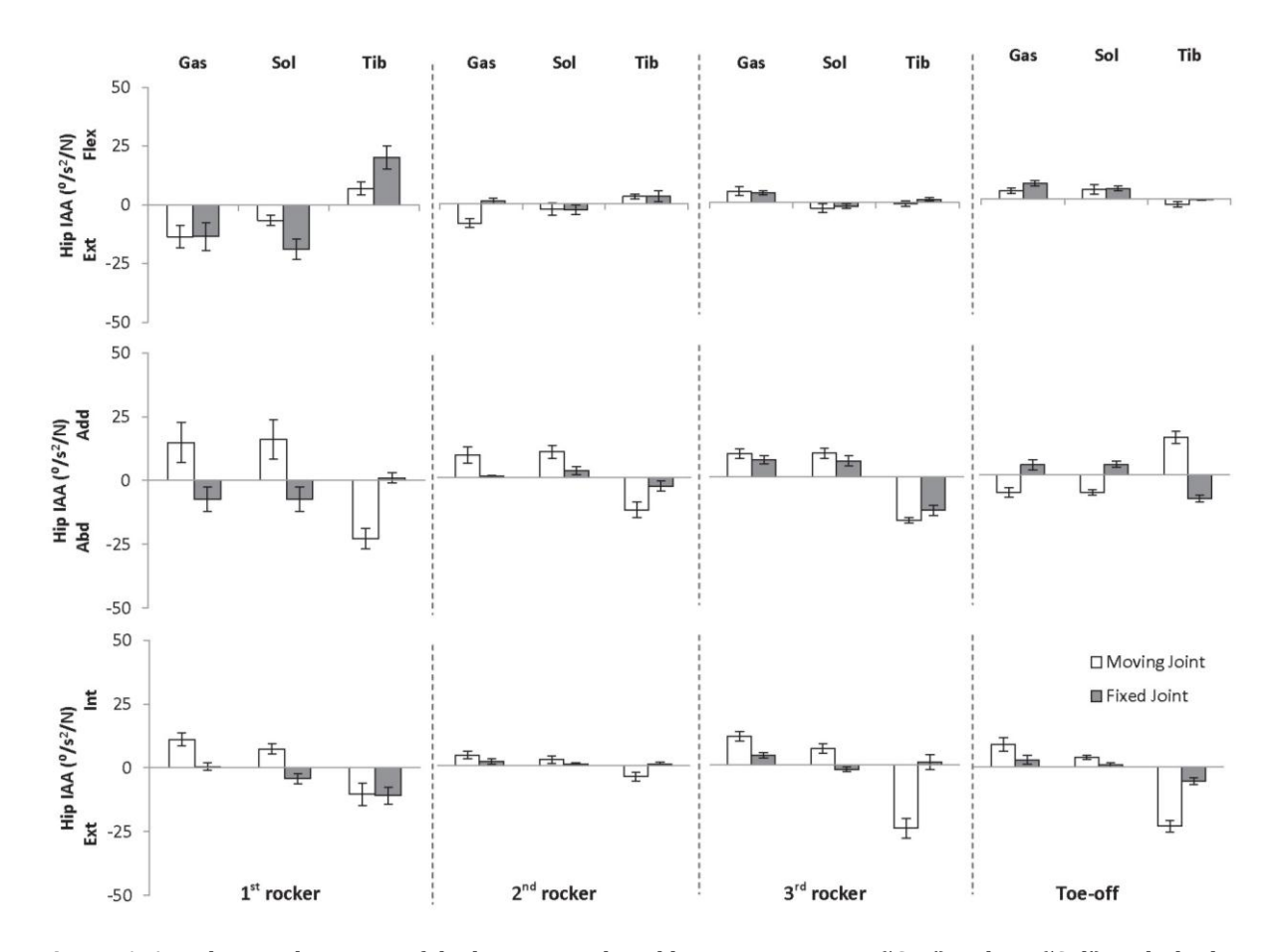


Figure 1. Angular accelerations of the hip joint induced by gastrocnemius ('Gas'), soleus ('Sol') and tibialis anterior ('Tib') in the 'moving joint' and 'fixed joint' foot ground contact model. Each bar represents the mean \pm 1 S.D. of each sub-phase of eight subjects. Dashed lines divide the stance phase into 4 sub-phases: 1st rocker, 2nd rocker, 3rd rocker and toe-off.

Each FGC model was added bilaterally in the linkage model. In the 'fixed joint' model, three FGC joints were created and served as constraints for the estimated COP during gait: under the heel ('GFH'), the third metatarsal ('GFM'), and hallux ('GFT'). Two set of constraints in the 'fixed joint' model were also evaluated. In the 'Simple DOF' constraint, the foot was completely fixed to the ground in the 2nd rocker. During the rest of the stance phase, 3 DOFs were allowed at the GFH, GFM and GFT joints. In the 'Multiple DOF' constraint, in the 1st rocker, 3 DOFs were allowed at GFH joint. In the 2nd rocker, the foot is completely fixed to the ground. In the 3rd rocker, only a sagittal DOF was allowed at the GFM joint. In toe-off, sagittal and transverse DOFs were allowed at the GFT joint (Appendix A).

In the 'moving joint' model, one joint with 3 rotational DOFs moved instantaneously along the recorded COP. In order to study the influences of the location of the COP, the lateral

and medial shift of the path of COP was modeled by moving foot-ground joints laterally or medially by 10% of the subject's foot width in the 'moving joint' model.

2.4 Comparisons

Three comparisons were evaluated in this study based on two FGC models (Section 2.3.).

2.4.1 Comparison 1

The muscle induced accelerations (MIAs) were compared in the 'fixed joint' and 'moving joint' models. In the 'fixed joint' model, FGC joints had 'Simple DOF' constraints.

2.4.2 Comparison 2

The MIAs were compared in the 'fixed joint' model with 'Multiple DOF' or 'Simple DOF' constraints.

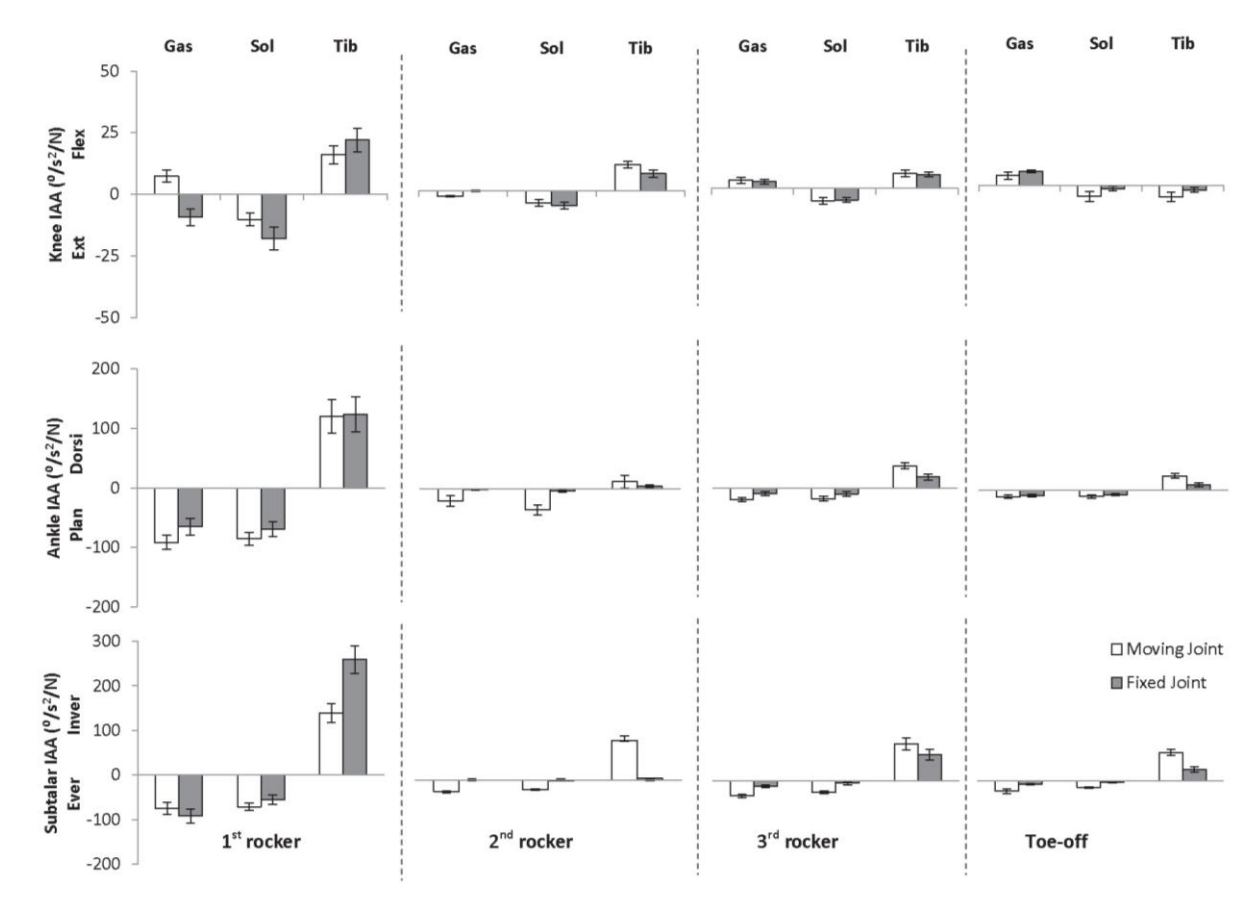


Figure 2. Angular accelerations of the knee, ankle, and subtalar joints induced by gastrocnemius ('Gas'), soleus ('Sol') and tibialis anterior ("Tib') in the 'moving joint' and 'fixed joint' foot ground contact model. Each bar represents the mean ± 1 S.D. of each sub-phase of eight subjects. Dashed lines divide the stance phase into 4 sub-phases: 1st rocker, 2nd rocker, 3rd rocker and toe-off.

2.4.3 Comparison 3

The MIAs were compared in the 'moving joint' model with lateral and medial shift of COP.

2.5 Data Analysis

In each comparison, the gastrocnemius, soleus and tibialis anterior's potential contributions to the hip, knee, ankle and subtalar joint angular accelerations were averaged throughout each sub-phase. In Comparison 3, the absolute mean differences were also quantified for each subject and averaged across all subjects to obtain a mean difference in each sub-phase.

3. Results

Inverse kinematics analysis of two FGC models tracked the measured joint angles with an RMS error of less than 3 degrees. The

superposition of contributions due to all forces (e.g. muscles, gravity and centrifugal forces) to the GRF were in agreement with measured GRF in the 'fixed joint' and 'moving joint' models (Appendix B).

3.1 Comparison 1

In general, the pattern of ankle muscles' potential function at the hip (sagittal plane), knee, ankle and subtalar joint were similar in the 'moving joint' and 'fixed joint' model (Figs 1-2). However, opposing accelerations can be found at the hip and knee. Opposing potentials were found in hip frontal and transverse plane rotations, e.g. soleus had potential to abduct and external rotate the hip in the 'fixed joint', but to adduct and internal rotate the hip in the 'moving joint' in the 1st rocker. Some magnitude discrepancies were also noticeable, in particular, in the tibialis anterior's induced accelerations.

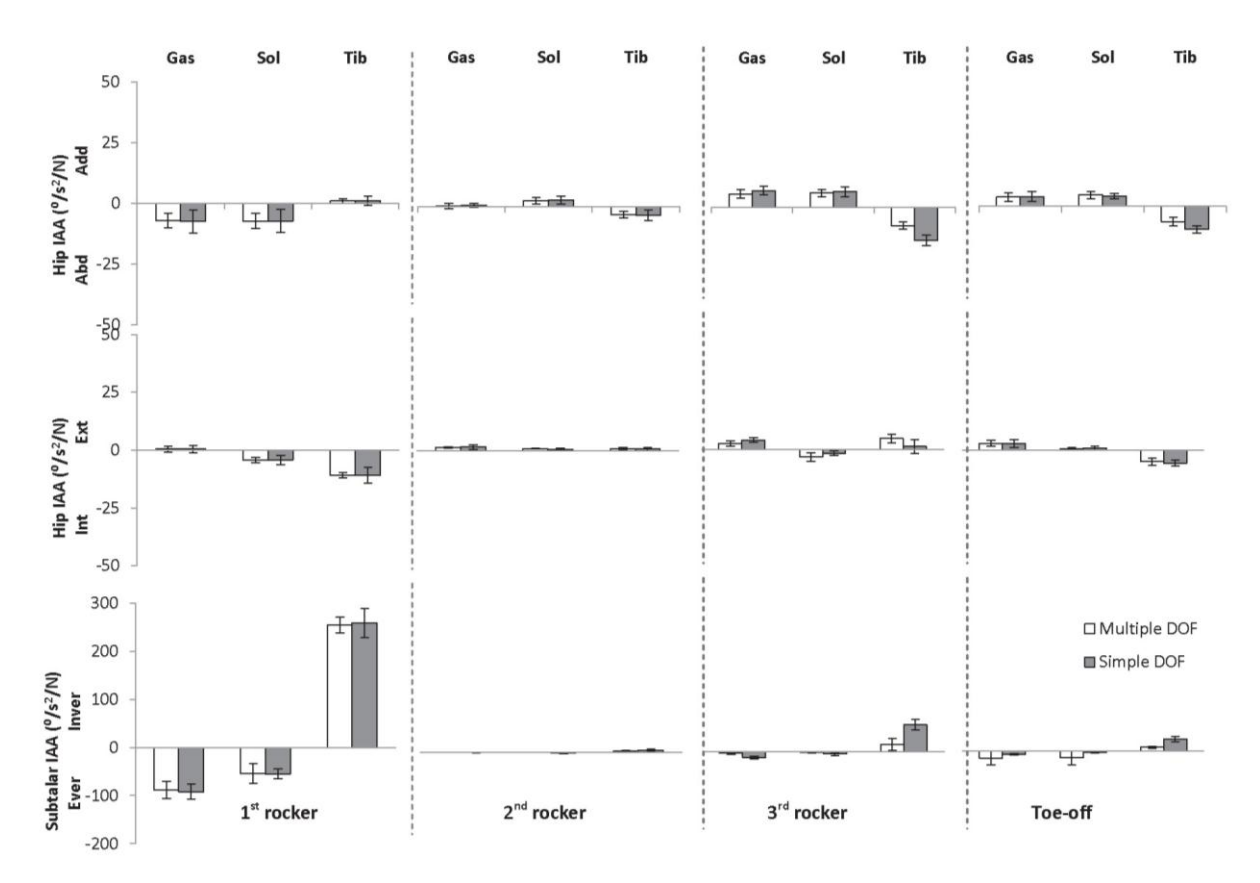


Figure 3. Non-sagittal plane joint accelerations at the hip and subtalar joints induced by gastrocnemius ('Gas'), soleus ('Sol') and tibialis anterior ('Tib') in the 'Multiple DOF' and 'Simple DOF' foot ground contact model. Each bar represents the mean \pm 1 S.D. of each sub-phase of eight subjects. Dashed lines divide the stance phase into 4 sub-phases: 1st rocker, 2nd rocker, 3rd rocker and toe-off.

3.2 Comparison 2

The gastrocnemius and soleus had very similar potentials to accelerate the hip in all three planes with the two types of constraints. The tibialis anterior induced less hip abduction acceleration in 'multiple DOF' after foot-flat (Fig 3). No obvious differences can be found in general trends of three muscles' potential to accelerate knee and ankle joints (Appendix C), except at the subtalar joint, less inversion acceleration was induced by tibialis anterior in the 'Multiple DOF' constraint in the 3rd rocker and toe-off.

3.3 Comparison 3

At the hip, very small effects can be found in ankle muscles' potentials to flex/extend the hip by shifting the COP; however, the muscles' potential functions in the frontal and transverse planes were more sensitive to COP shifting (Fig 4). In the frontal plane, the muscles' potential functions were more sensitive to the medial COP shift than the lateral shift, but the directions were consistent with the observed COP (Appendix D). In the transverse plane, the gastrocnemius and soleus had potentials to rotate the hip externally and the tibialis anterior to rotate hip internally when the COP was shifted medially. When the COP was shifted laterally, muscles' functions were consistent with the observed COP with some magnitude differences. At the ankle, the potential accelerations were more sensitive to the lateral COP shift (Fig 5). For instance, tibialis anterior increased its potential to dorsiflex the ankle, and the gastrocnemius and soleus increased their potentials to plantarflex the ankle. At the knee and subtalar joints, ankle muscles' potential were influenced inconsistently by the medial and lateral shift of the COP in each sub-phase; at the subtalar joint, the gastrocnemius and soleus were more sensitive to medial COP shift in the 1st rocker, but were more sensitive to lateral COP shift in the 3rd rocker and toe-off.

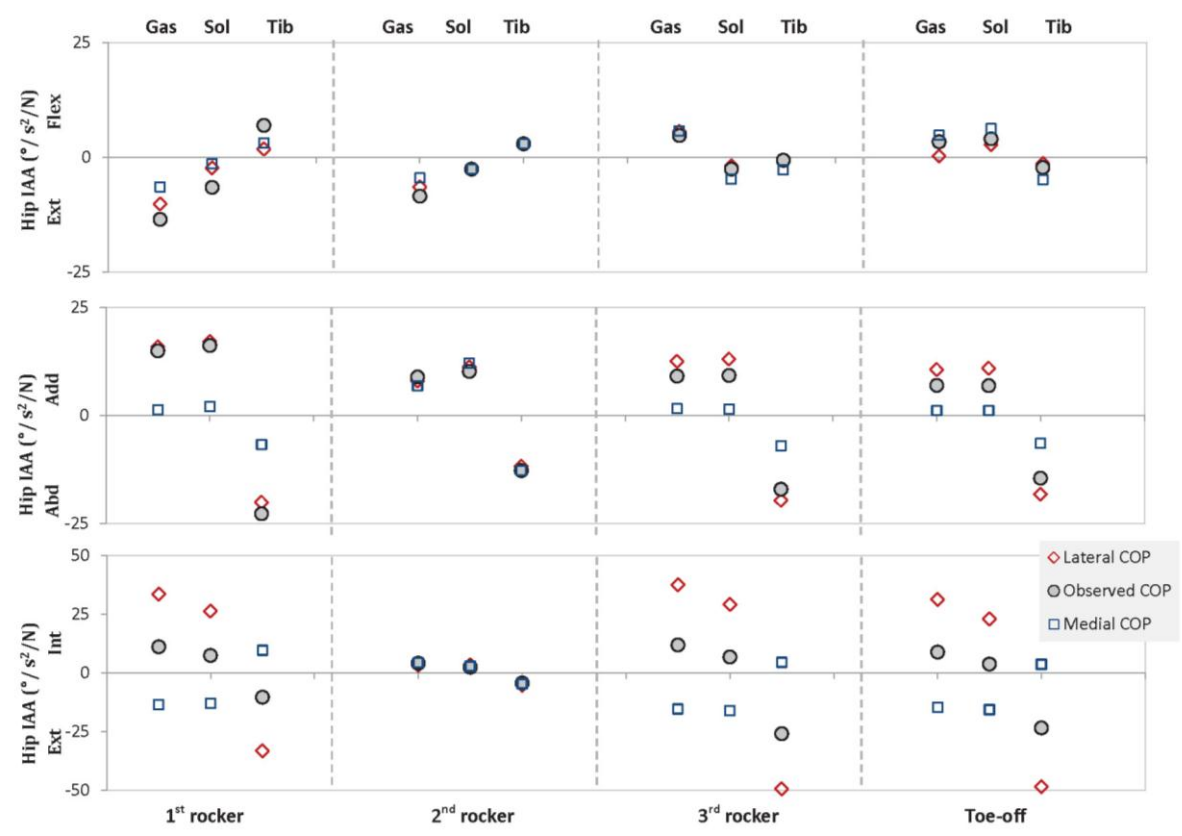


Figure 4. Angular accelerations of the hip joint induced by gastrocnemius ('Gas'), soleus ('Sol') and tibialis anterior ('Tib') in the 'moving joint' floor-foot contact model. Each mark represents the mean of each subphase of six subjects in the observed COP, and with COP shifted medially and laterally. Dash lines divided the stance phase into 4 sub-phases: 1st rocker, 2nd rocker, 3rd rocker and toe-off.

4. Discussion

The foot-ground model plays a particularly important role in IAA since only one Newton of muscle force and corresponding ground reaction force with constrained foot-ground contact are presented in the dynamic equations. Computed potential contributions of the gastrocnemius, soleus and tibialis anterior in the frontal and transverse plane joint accelerations were sensitive to the applied DOFs constraints and location of constraint forces, but with the latter one more influential.

The essential differences between FGC models were the ground reaction constraint force, given a prescribed configuration and applying a unit muscle force. The constraint force was further determined by its prescribed DOFs and the location of application. Comparison 1 is the consequence of the latter. In the current study, the qualitative trend of the 'moving joint' model, which is commonly used in rigid-contact modelling, agreed with previous reports. In addition to dorsiflexion potentials, knee flexion potential was observed in the 1st

rocker by the tibialis anterior, which has been attributed to shock absorption during weightacceptance (Perry, 1992). The soleus can plantarflex the ankle, and extend the hip and knee in mid-stance (Hicks et al., 2007; Schwartz and Lakin, 2003). Knee extension potential was found in part of the stance-phase in the gastrocnemius, corresponding to findings by Neptune et al., even though this opposes its anatomical classification (Neptune et al., 2004b). In comparison 1, qualitative trends in lower joints' sagittal plane MIAs were similar in the two FGC models, but more pronounced differences can be found in the hip frontal and transverse planes accelerations. The locations of reaction force application were assumed in the horizontal plane (ground), which can influence constraint forces in the frontal and transverse planes. In a recent study evaluating the FGC models' influence on predicted muscles contributions to the GRF, authors have also concluded that predicted muscle function in the medial-lateral plane are sensitive to the number of foot-contact points (Dorn et al., 2011).

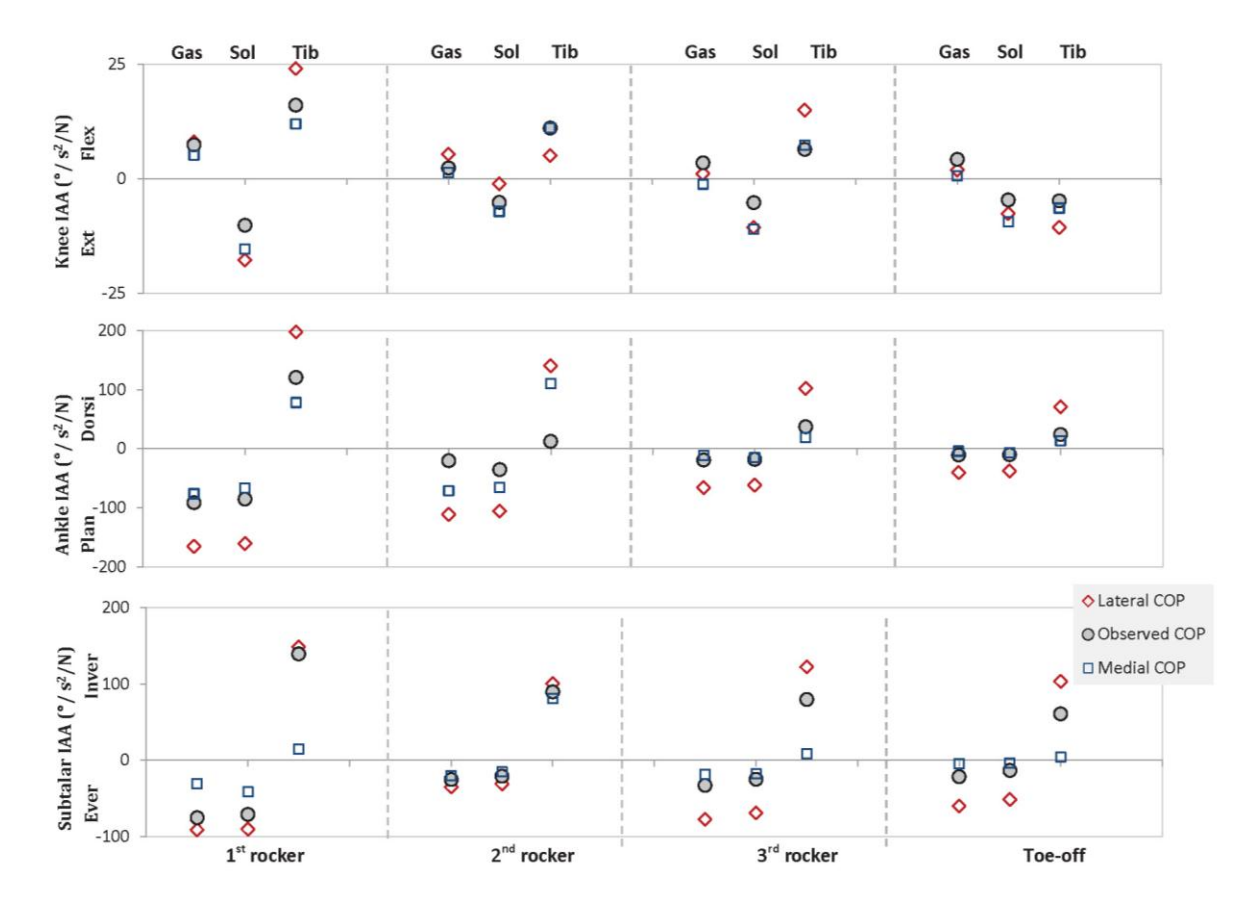


Figure 5. Angular accelerations of the knee, ankle and subtalar joints induced by gastrocnemius ('Gas'), soleus ('Sol') and tibialis anterior ('Tib') in the 'moving joint' floor-foot contact model. Each mark represents the mean of each sub-phase of eight subjects in the observed COP, and with COP shifted medially and laterally. Dash lines divided the stance phase into 4 sub-phases: 1st rocker, 2nd rocker, 3rd rocker and toe-off.

The 'Multiple DOF' and 'Simple DOF' constraints did not produce obvious deviations in the trends of muscles' acceleration potentials. A recent study has indicated that kinematic constraint in the frontal plane affects the model calculations of muscle contributions to the medial-lateral GRFs, and the transverse constraints have little effect (Dorn et al., 2011). In our study, the MIAs were almost identical in the 1st and 2nd rockers due to the same constraints. Only slight differences were found in gastrocnemius and soleus in accelerating joints after foot-flat. Compared to the 'Simple DOF' constraint, the frontal and transverse plane DOFs during 3rd rocker and the frontal plane rotation in toe-off were blocked in the 'Multiple DOF', which influenced the constraint forces in these two directions. The tibialis anterior was found more sensitive to variations in DOFs, which was probably associated with its secondary function to create subtalar inversion by adducting the calcaneus. In other words, its anatomical function made it able to

resist the reaction constraint forces in the frontal planes.

locations were found to have considerable effects on the potential ankle muscle functions. In a previous study, Kimmel concluded that moving the COP location had the smallest effect among changing the location of muscle origin, muscle insertion, joint center and COP (Kimmel, 2004). In contrast, non-sagittal plane MIAs at all joints were visibly affected by COP locations. Interestingly, MIA influences were inconsistent at each joint as well as in each sub-phase (Appendix D). For example, at the subtalar joint, muscles' potential functions were more sensitive to the medial COP shift during the 1st rocker, but they were more affected by the lateral shift after foot-flat. At the ankle. muscles' potential functions were sensitive to the lateral shift throughout the whole stance phase. The influences of COP path on muscle function were very complicated to predict even with a given muscle force, which was influenced by the location and direction of the joint axis, muscle moment arm, constraint reaction force and its moment arm. Nevertheless, most of these factors were not constant variables in the movement. Previous studies have reported that the gastrocnemius and soleus can switch moment directions depending on the position of the subtalar joint, while the tibialis anterior has a consistent inversion moment (Klein et al., 1996; Wang and Gutierrez-Farewik, 2011). When COP location was shifted, the moment arm of the foot-ground constraint force also depended on the relative position of the COP location and the joint axis. Moreover, the dynamic coupling effects must also to be taken into account, e.g. the large plantarflexion acceleration generated by the gastrocnemius and soleus at the ankle can also cause eversion acceleration in the subtalar joint (Wang and Gutierrez-Farewik, 2011).

Several limitations should be kept in mind. worthy to note that lack It electromyography data may affect the validity in the GRF superposition, although relative low superposition error was noticed in the study. A previous study has also indicated superposition error only quantifies the accuracy with which the various action forces sum to the total GRF; it does not verify the calculations of the contributions of the individual action forces themselves (Dorn et al., 2011). Consequently, only potential muscle function (acceleration per unit muscle force) was quantified in the study, which did not depend on the activation level of each muscle so as to exclude the potential uncertainties from predicted muscle activation. In addition, it is worth mentioning that the COP was only shifted only 10% foot width (an average of 8.5 mm) in Comparison 3. To which extent IAA results can be affected by realistic magnitudes may warrant future force investigations.

5. Conclusions

IAA has been used increasingly often to investigate the influences of gait deviations on individual muscle functions, which are difficult to address due to the complexity of multi-joint dynamics. However, lack of sensitivity analysis largely limits its validation and clinical applicability. Our study examined the effect of locations and constraints of FGC joints on the computed muscle functions. In general, non-sagittal plane potential muscle functions were

most influenced by FGC models. Ankle muscles' potential functions were influenced differently at each joint as well as in each sub-phase when COP location was shifted. Among all three muscles, tibialis anterior was the only one whose function was affected by both locations and DOFs in the FGC models; the gastrocnemius and soleus functions were influenced trivially by the DOFs of constraint joint. Care should be taken in applying appropriate constraints and locations of the FGC joints, especially in investigations of non-sagittal plane joint accelerations.

Acknowledgment

The authors would like to acknowledge Peter Loan at MusculoGraphics, Inc., for his help with model modification. We also thank Åsa Bartonek and all participators in the data collecting. Funding for this project was generously provided by the Swedish Research Council and Promobilia Foundation.

Conflict of Interest

No authors had any proprietary, financial, professional or other personal conflicts of interest that may have influenced this study.

Reference List

- Anderson, F. C., Pandy, M. G., (2003). Individual muscle contributions to support in normal walking. Gait Posture 17, 159-169.
- Delp, S. L., Anderson, F. C., Arnold, A. S., Loan, P., Habib, A., John, C. T., Guendelman, E., Thelen, D. G., (2007). OpenSim: open-source software to create and analyze dynamic simulations of movement. IEEE T Biomed Eng 54, 1940-1950.
- Delp, S. L., Loan, J. P., Hoy, M. G., Zajac, F. E., Topp, E. L., Rosen, J. M., (1990). An interactive graphics-based model of the lower extremity to study orthopaedic surgical procedures. IEEE T Biomed Eng 37, 757-767.
- Dorn, T. W., Lin, Y. C., Pandy, M. G., (2011). Estimates of muscle function in human gait depend on how foot-ground contact is modelled. Comp Methods Biomech Biomed Eng 1, 1-12.
- Goldberg, S. R., Kepple, T. M., (2009). Muscle-induced accelerations at maximum

- activation to assess individual muscle capacity during movement. Journal of biomechanics 42, 952-955.
- Goldberg, S. R., Ounpuu, S., Delp, S. L., (2003). The importance of swing-phase initial conditions in stiff-knee gait. J Biomech 36, 1111-1116.
- Gutierrez-Farewik, E. M., Bartonek, A., Saraste, H., (2006). Comparison and evaluation of two common methods to measure center of mass displacement in three dimensions during gait. Human movement science 25, 238-256.
- Hamner, S. R., Seth, A., Delp, S. L., (2010). Muscle contributions to propulsion and support during running. J Biomech 43, 2709-2716.
- Hicks, J., Arnold, A., Anderson, F., Schwartz, M., Delp, S., (2007). The effect of excessive tibial torsion on the capacity of muscles to extend the hip and knee during single-limb stance. Gait Posture 26, 546-552.
- Kepple, T. M., Siegel, K. L., Stanhope, S. J., (1997). Relative contributions of the lower extremity joint moments to forward progression and support during gait. Gait Posture 6, 1-8.
- Kimmel, S. A., (2004). Toward a clinical understanding of dynamic muscle function. University of Minnesota.
- Klein, P., Mattys, S., Rooze, M., (1996). Moment arm length variations of selected muscles acting on talocrural and subtalar joints during movement: an in vitro study. J Biomech 29, 21-30.
- Neptune, R. R., Kautz, S. A., Zajac, F. E., (2001). Contributions of the individual ankle plantar flexors to support, forward progression and swing initiation during walking. J Biomech 34, 1387-1398.
- Neptune, R. R., Zajac, F. E., Kautz, S. A., (2004a). Muscle force redistributes segmental power for body progression during walking. Gait & posture 19, 194-205
- Neptune, R. R., Zajac, F. E., Kautz, S. A., (2004b). Muscle force redistributes segmental power for body progression during walking. Gait Posture 19, 194-205.
- Perry, J., (1992). Gait analysis: normal and pathological function. SLACK Inc., Thorofare.

- Riley, P. O., Kerrigan, D. C., (1999). Kinetics of stiff-legged gait: induced acceleration analysis. IEEE Transac Rehabil Eng 7, 420-426.
- Sasaki, K., Neptune, R. R., (2006). Differences in muscle function during walking and running at the same speed. J Biomech 39, 2005-2013.
- Schwartz, M., Lakin, G., (2003). The effect of tibial torsion on the dynamic function of the soleus during gait. Gait Posture 17, 113-118.
- Stebbins, J., Harrington, M., Thompson, N., Zavatsky, A., Theologis, T., (2006). Repeatability of a model for measuring multi-segment foot kinematics in children. Gait Posture 23, 399-400.
- Thelen, D. G., Anderson, F. C., (2006). Using computed muscle control to generate forward dynamic simulations of human walking from experimental data. J Biomech 39, 1107-1115.
- Wang, R. L., Gutierrez-Farewik, E. M., (2011). The effect of subtalar inversion/eversion on the dynamic function of the tibialis anterior, soleus, and gastrocnemius during the stance phase of gait. Gait Posture 34, 29-35.
- Yoon, HK., Park, KB., Roh, JY., Park, HW., Chi, HJ., Kim, HW., (2010). Extraarticular Subtalar Arthrodesis for Pes Planovalgus: An Interim Result of 50 Feet in Patients with Spastic Diplegia. Clin Orthop Surg 2, 13-21.
- Zajac, F. E., Gordon, M. E., (1989). Determining muscle's force and action in multi-articular movement. Exercise Sport Sci Rev 187-230.
- Zajac, F. E., Neptune, R. R., Kautz, S. A., (2002). Biomechanics and muscle coordination of human walking. Part I: introduction to concepts, power transfer, dynamics and simulations. Gait Posture 16, 215-232.

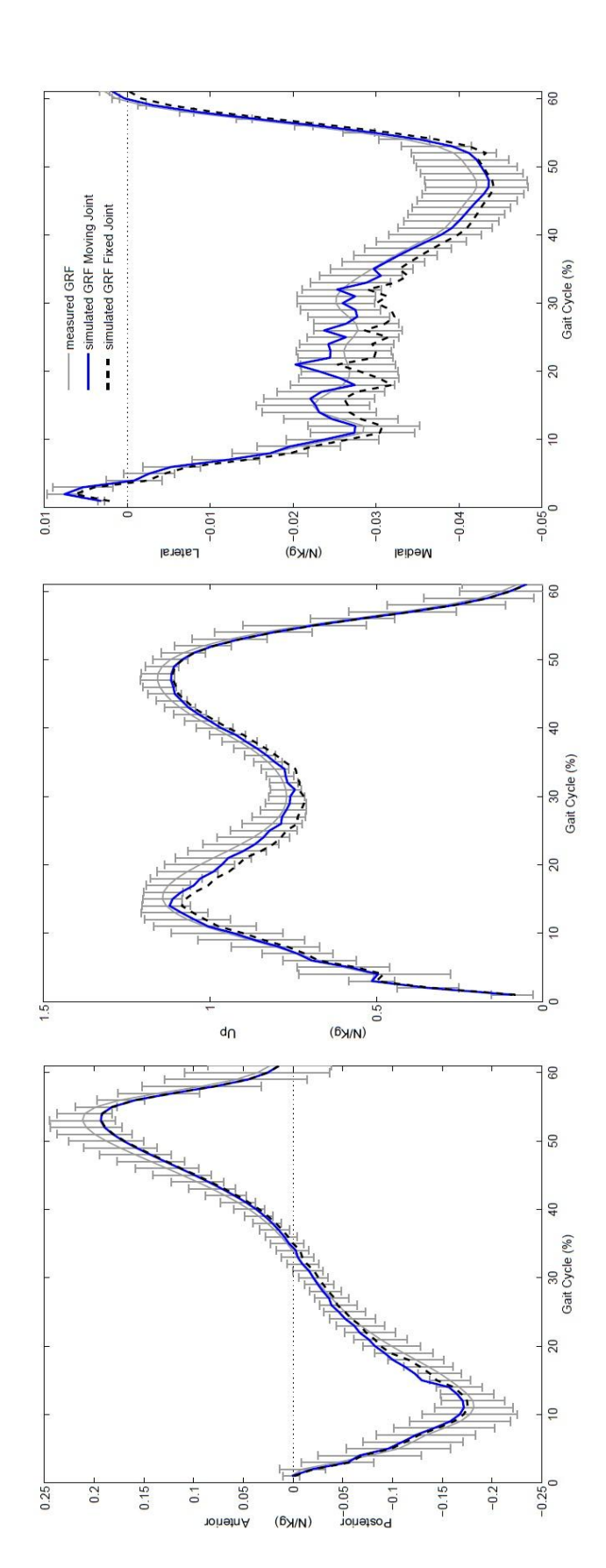
Appendix A

Three ground foot joints were fixed under the foot – at the posterior inferior point of the heel ('GFH'), the distal end of the third metatarsal ('GFM') and the distal end of the hallux ('GFT') in the 'fixed joint' model. In the 'Simple DOF' constraint, the foot was completely fixed to the ground in the 2nd rocker. During the rest of the stance phase, 3 DOFs were allowed at GFH, GFM and GFT joints. In the 'Multiple DOF' constraint, in the 1st rocker, 3 DOFs were allowed at GFH joint. In the 2nd rocker, the foot is completely fixed to the ground. In the 3rd rocker, only a sagittal DOF was allowed at the GFM joint. In toe-off, sagittal and transverse DOFs were allowed at the GFT joint.

Sub-phase		1 st rocker	2 nd rocker	3 rd rocker	Toe-off	
Ground-foot joint		GFH	GFH, GFM, GFT	GFM	GFT	
Rotational	Simple	3	0	3	3	
DOF	Multiple	3	0	1 (sagittal)	2 (sagittal&transverse)	
Locations relative to foot(top view)						

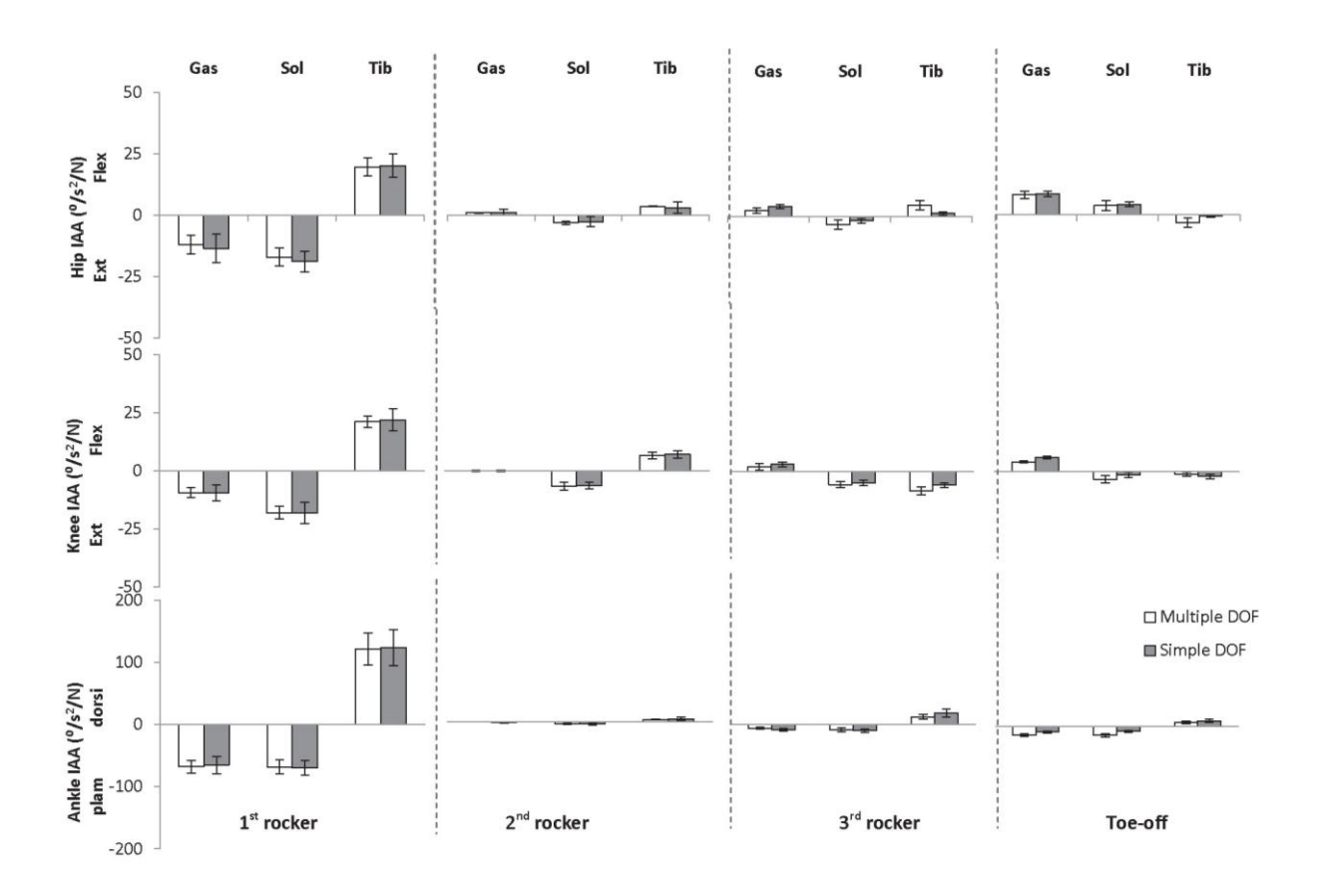
Appendix B

Comparison of measured ground reaction force and superposition of contributions of all force terms (muscles, gravity, centrifugal forces) to the ground reaction force in 'moving joint' and 'fixed joint' models. The grey line represented the mean ± 1 S.D. measured ground reaction force of six subjects. The blue line represented the mean superposition contributions to the ground reaction force in the 'moving joint'. The dash line represented the mean superposition contributions to the ground reaction force in the 'fixed joint' model.



Appendix C

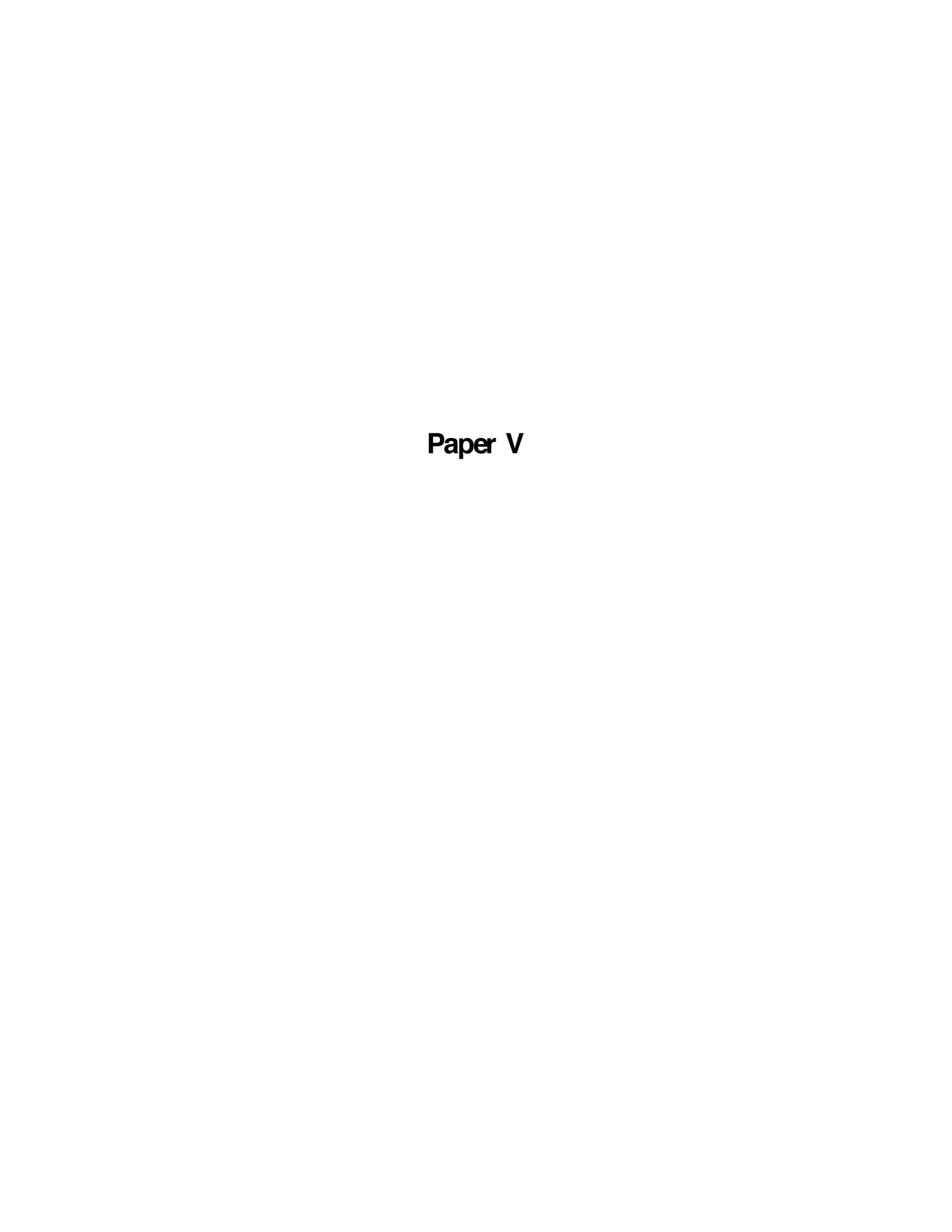
Sagittal plane angular accelerations of the hip, knee and subtalar joints induced by gastrocnemius ('Gas'), soleus ('Sol') and tibialis anterior ('Tib') in the 'Multiple DOF' and 'Simple DOF' foot ground contact model. Each bar represents the mean \pm 1 S.D. of each sub-phase of six subjects. Dashed lines divide the stance phase into 4 sub-phases: 1^{st} rocker, 2^{nd} rocker, 3^{rd} rocker and toe-off.



Appendix D

Absolute mean differences ± 1 S.D. between lateral shift of COP and observed COP (DiffL), and between medial shift of COP and observed COP (DiffM) in the 'moving joint' foot-ground contact model. Angular accelerations at each joint induced by gastrocnemius ('Gas'), soleus ('Sol') and tibialis anterior ('Tib') were averaged across all subjects in each sub-phase.

Mean difference (S.D) (°/S²/N)		subtalar inversion		ankle dorsiflexion		knee flexion		hip flexion		hip abduction		hip rotation	
		DiffL	DiffM	DiffL	DiffM	DiffL	DiffM	DiffL	DiffM	DiffL	DiffM	DiffL	DiffM
1^{st}	Gas	16.1	44.4	74.2	14.1	0.7	2.2	3.3	7.1	0.9	13.6	22.4	24.7
rocker		(9.1)	(8.6)	(23.6)	(21.9)	(1.8)	(2.7)	(1.2)	(1.7)	(1.5)	(1.2)	(2.5)	(1.8)
	Sol	19.4	29.5	74.9	18.2	7.6	5.2	4.2	5.1	0.9	14.1	18.9	20.4
		(8.9)	(8.6)	(22.3)	(21.9)	(1.9)	(2.5)	(0.8)	(1.3)	(1.4)	(1.2)	(1.9)	(1.5)
	Tib	9.1	125.1	77.1	42.2	8.1	4.1	5.2	3.8	2.6	15.9	22.9	19.9
		(12.8)	(11.2)	(24.2)	(22.9)	(2.6)	(2.9)	(1.1)	(1.4)	(1.7)	(1.3)	(3.2)	(1.5)
2^{st}	Gas	10.2	5.4	90.9	51.2	2.9	1.1	2.1	4.2	1.2	2.2	1.3	1.5
rocker		(5.8)	(5.6)	(11.7)	(9.7)	(1.4)	(1.9)	(1.2)	(1.2)	(1.1)	(0.8)	(1.7)	(1.3)
	Sol	9.7	6.1	69.9	30.3	4.2	2.4	0.1	0.3	1.9	2.7	1.5	1.4
		(5.9)	(4.9)	(10.1)	(8.9)	(1.4)	(1.9)	(0.8)	(0.9)	(1.2)	(0.9)	(1.6)	(1.1)
	Tib	10.9	9.2	128.2	98.4	5.1	0.8	0.9	0.6	1.7	0.5	1.8	0.7
		(9.9)	(11.5)	(10.2)	(8.9)	(2.1)	(2.2)	(1.3)	(1.1)	(1.6)	(1.2)	(2.4)	(2.2)
3 nd	Gas	44.5	14.1	46.5	7.4	2.4	2.2	0.8	0.9	3.4	7.6	25.7	27.3
rocker		(6.4)	(3.7)	(6.9)	(3.1)	(1.1)	(1.5)	(1.2)	(1.5)	(1.4)	(0.8)	(2.7)	(1.5)
	Sol	44.4	7.1	43.6	3.4	5.5	5.8	0.7	2.2	3.8	7.8	23.5	22.9
		(5.9)	(3.7)	(6.6)	(3.2)	(0.8)	(1.1)	(0.9)	(1.2)	(1.3)	(0.8)	(2.1)	(1.3)
	Tib	42.6	71.1	64.8	18.1	8.6	0.9	0.1	2.2	2.5	10.1	27.5	30.3
		(8.9)	(6.5)	(10.1)	(4.9)	(1.1)	(1.3)	(1.1)	(1.4)	(2.1)	(1.4)	(2.7)	(1.8)
toe-off	Gas	38.6	16.1	30.1	6.1	2.3	3.6	1.4	3.1	3.6	5.8	22.5	23.5
		(6.3)	(3.2)	(5.5)	(2.8)	(1.8)	(1.9)	(1.3)	(1.4)	(1.5)	(0.8)	(2.6)	(1.7)
	Sol	38.1	9.1	27.3	2.9	2.9	4.8	1.3	3.3	3.9	5.8	19.2	19.4
		(6.1)	(3.4)	(5.3)	(3.4)	(1.2)	(1.4)	(0.6)	(0.9)	(1.4)	(0.7)	(2.2)	(1.6)
	Tib	42.6	56.1	46.6	10.2	5.8	1.6	0.9	3.6	3.8	8.1	25.2	27.1
		(8.9)	(7.5)	(8.5)	(4.1)	(1.5)	(1.6)	(0.8)	(1.1)	(2.1)	(1.3)	(3.5)	(3.3)



Compensatory strategies in response to excessive muscle co-contraction at the ankle joint during walking

Ruoli Wang¹, Elena M. Gutierrez-Farewik^{1,2}

¹ KTH Mechanics, Royal Institute of Technology, Stockholm, Sweden ² Department of Women's and Children's Health, Karolinska Institutet, Stockholm, Sweden

Reformatted version of submitted manuscript

Abstract

It has been reported that excessive co-contraction is a cause of inefficient or abnormal movement in some neuromuscular pathologies. How synergistic muscles and proximal muscles (i.e. knee muscles) adapt to the co-contraction of ankle muscles is not well understood. The purpose of this study was to identify the necessary compensation strategies to overcome excessive antagonistic muscle cocontraction at the ankle joint and retain a normal walking pattern. Muscle-actuated simulation of normal walking and induced acceleration analysis were performed to quantify compensatory mechanisms of primary ankle and knee muscles in the presence of normal, medium and high levels of co-contraction of two antagonistic pairs (pair 1: gastrocnemius-tibialis anterior and pair 2: soleustibialis anterior) in single-limb stance and pre-swing phases. The study showed that if the cocontraction level increases, the nearby synergistic muscles can contribute most to compensation, e.g. with gastrocmemius-tibialis anterior co-contraction, the soleus will be the dominant contributor to ankle plantarflexion acceleration, and quadriceps and rectus femoris to knee extension acceleration. In contrast, with soleus-tibialis anterior co-contraction, the sartorius and hamstrings can provide important compensatory roles in knee accelerations. We also found that the ankle and knee muscles alone can provide sufficient compensation at the ankle joint, but hip muscles must be involved to generate sufficient knee moment. Our findings imply that subjects with a certain level of dorsiflexors/plantarflexor co-contraction can still perform normal walking. The compensatory mechanism can be useful in clinical interpretation of motion analyses, when secondary muscle cocontraction or other deficits may present simultaneously in subjects with motion disorders.

Keywords: gait analysis, muscle-actuated simulation, gastrocnemius, soleus, tibialis anterior

1. Introduction

Co-contraction, the concurrent activation of agonist and antagonist muscles (antagonistic pairs) across the same joint, occurs in many activities including posture control, walking, and running (Winter, 1990; Nagai et al., 2011; Falconer and Winter, 1985). In normal gait, antagonistic muscle pairs in the lower extremities contract in an alternating pattern with low durations of concurrent activity to generate sufficient joint moment (Grasso et al., 2000). The function of muscle co-contraction as joint stabilizing has been observed by Falconer and Winter (Falconer and Winter, 1985), who calculated a co-contraction value for ankle joint plantar- and dorsiflexors and found highest cocontraction values in the weight-acceptance phase and lowest in push-off and swing phases. In some gait disorders, e.g. spastic gait due to

central nervous system disorders, the temporal separation and magnitude differences of activities between agonist-antagonist muscles are frequently attenuated and motor control becomes poor (Dierick et al., 2002).

It has been reported that excessive cocontraction can cause inefficient or abnormal movement in some neuromuscular pathologies and is even associated with normal aging. Reduced plantarflexor moment was found on the non-paretic side in patients after stroke, attributable to excessive gastrocnemius-tibialis anterior co-contraction and involved in high energy cost of locomotion (Lamontagne et al., 2002). In persons with knee osteoarthritis, increased co-contraction during daily activities through increased hamstrings activity and reduced quadriceps activity has been interpreted as a compensatory adaptation to quadriceps weakness, pain and altered local joint

environment, e.g. loading distributions (Hortobaígyi et al., 2005; Sharma, 2001). Biceps femoris-vastus lateralis and gastrocnemiustibialis anterior co-contraction have been reported higher in elderly than in young subjects during stepping down (Hortobagyi and DeVita, 2000). Assessment of co-contraction is most often carried out by measuring muscle activity with electromyography (EMG) and quantified using indices (Frost et al., 1997; Hubley-Kozey et al., 2009), but there are limitations in the number of the muscles feasibly recordable, and the necessary compensation strategies to overcome excessive co-contraction are not possible to assess.

One of the mechanisms to generate normal walking is to regulate the whole-body angular momentum by muscle force generation operated by the central nervous system (Hogan, 1984). Due to muscle redundancy, various neuromotor strategies may exist to compensate for excessive muscle co-contraction, but this has not yet been studied. In addition, lower limb muscles can accelerate all joints and segments depending on the body configuration (Zajac et al., 2002). Muscle-actuated simulations provide a platform to investigate the causal relationship between muscle activation, muscle forces acting on the skeletal system, generated joint moments and movement pattern. For instance, compared to heel-toe walking, increased soleus gastrocnemius contributions to body support and forward propulsion were observed in early stance in toe-walking (Sasaki et al., 2008). A dynamic simulation study of crouch gait revealed that larger muscle force is needed to support body weight and propel the body single-limb stance forward in than unimpaired gait (Steele et al., 2010).

The goals of this study were to use computed muscle control and induced acceleration analysis to analyze dynamic muscle functions walking at a nominal speed and to identify the necessary compensatory mechanisms to overcome excessive cocontraction of gastrocnemius-tibialis anterior and soleus-tibialis anterior pairs and retain a normal walking pattern.

2. Methods

2.1. Musculoskeletal model

A generic musculoskeletal model with 14 segments, 23 degree-of-freedom and 96

musculotendon actuators was used to create the simulation. The head and torso were modeled as a single rigid body, which articulated with the pelvis via a ball-and-socket back joint. Each hip was modeled as a ball-and-socket joint, each knee as a hinge joint, and each ankle, subtalar and metatarsophalangeal joints as revolute joints (Arnold et al., 2010). Simulations of stance-phase were generated using OpenSim (Delp et al., 2007). The period from initial contact to contralateral toe-off (approximately the first 14% of the gait cycle) was not included in this study due to lack of bilateral force plate data.

2.2. Subjects

Nine healthy adults (5 females and 4 males, age: 30 ± 3 yrs, weight: 64 ± 11 kg, height: 1.68 ± 0.09m), were examined while walking at a self-selected speed, using an 8-camera motion capture system (Vicon MX40, Oxford, UK) and forceplates (Kistler, Winterthur, two Switzerland). Several trials were collected on each subject and motion was obtained by fitting the musculoskeletal model to tracked marker data from one representative trial. Sixty-four markers (9mm) were reflective placed bilaterally on bony landmarks based on a conventional full-body marker set (Vicon Plugin-Gait), plus a multi-segment foot model marker set (Stebbins et al., 2006). Surface EMG signals (Motion Laboratory System, Baton Rouge, LA) according to standardized electrode placement (www.seniam.org) were recorded from the biceps femoris long head (BFLH), rectus femoris (RF), medial gastrocnemius (GAS), soleus (SOL) and tibialis anterior (TA) bilaterally. Ethical approval for data collection obtained. Subjects participated with informed consent. EMG was sampled at 1000Hz, rectified and linear enveloped (2nd order bidirectional Butterworth filter with cutoff frequency at 6Hz). EMG for each muscle was normalized from zero to one based on maximum values of that muscle's activation over the whole gait cycle.

2.3. Dynamic simulation

The model was scaled to each subject based on the marker set (Wang and Gutierrez-Farewik, 2011). The inverse kinematics algorithm solved for joint kinematics that minimized the differences between experimental and virtual marker positions.

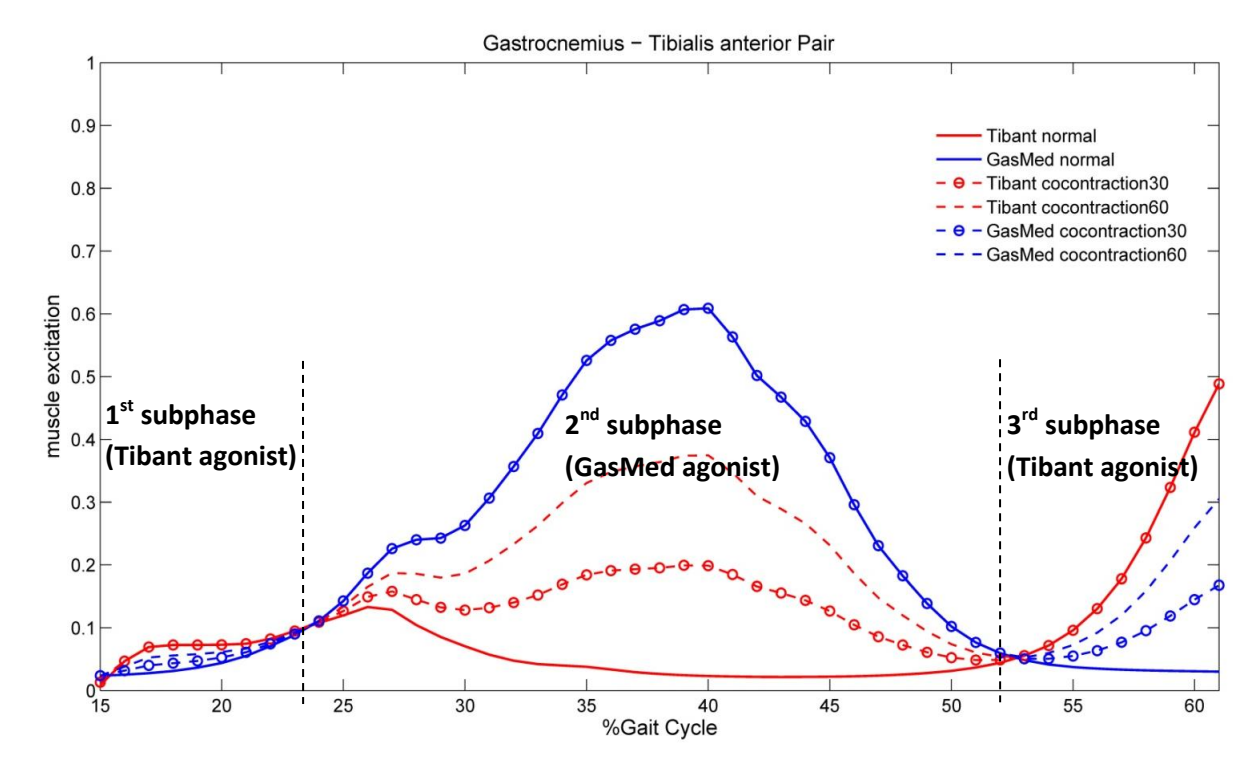


Figure 1: A sample calculation of co-contraction of the gastrocnemius-tibialis anterior pair. Excessive co-contractions (medium, high) were calculated based on computed muscle excitation in normal gait. The single-limb stance phase and pre-swing phase was divided into three sub-phases depending on which muscle served as agonist or antagonist. Muscle excitation is presented from 0 (no excitation) to 1 (fully excited) scale.

Dynamic inconsistency between the measured ground reaction forces (GRF) and the kinematics was resolved by applying small external forces and torques (i.e. residuals) to the torso and making small adjustments to the model's mass properties and kinematics (Delp et al., 2007). Computed muscle control (CMC) (Thelen and Anderson, 2006), with constraints on muscle excitation, was used to find a set of actuator excitations that would both track the experimental kinematics and be generally consistent with experimental EMG patterns. CMC solves a static optimization problem to resolve muscle redundancy by minimizing the sum of the square of muscle activations, while accounting for muscle activation and contraction dynamics (Crowninshield and Brand, 1981; Zajac and Gordon, 1989).

Induced acceleration analysis (IAA) was used to compute contributions of individual muscles to accelerations of ankle and knee joints using the simulated muscle forces from CMC. The dynamic equations of motion were outlined by Zajac and Gordon (Zajac and Gordon, 1989) and detailed in a recent study (Hamner et al., 2010). The foot-floor interaction was modeled as a rolling-on-surface joint which did not allow

slipping, twisting or penetrating the floor, as described in a recent study (Hamner et al., 2010).

2.4. Muscle co-contraction analyses

According to Falconer and Winter (Falconer and Winter, 1985), the agonist and antagonist muscle can be estimated using normalized EMG by defining the one with lesser activation as antagonist. Three co-contraction levels (normal, medium and high) of two ankle joint antagonistic pairs (pair 1: GAS-TA, pair 2: SOL-TA) were evaluated during normal gait. At the normal level, the excitations of antagonistic pairs were computed in CMC with experimental EMG constraints as described in Section 2.3. The co-contraction ratio γ was defined according to Eq.1:

 $\begin{aligned} Excitation_{cocontr,ant} &= Excitation_{normal,ant} \\ &+ \gamma (Excitation_{normal.ago} \\ &- Excitation_{normal.ant}) \end{aligned}$

where $Excitation_{cocontr,ant}$ is excitation of the antagonist muscle under medium or high level co-contraction, $Excitation_{normal,ant}$ is

excitation of the antagonist muscle under normal co-contraction, γ is the co-contraction ratio, $Excitation_{normal.ago}$ is excitation of the agonist muscle under normal co-contraction, and $Excitation_{normal.ant}$ is excitation of the antagonist muscle under normal co-contraction. A medium level of co-contraction was defined as $\gamma = 0.3$, and a high level as $\gamma = 0.6$, and were simulated by increasing the antagonist activity (Fig. 1).

In order to simulate the response of other muscles to the excessive co-contracted antagonistic pair, CMC and IAA were repeated after constraining excitations of the antagonistic pair at each co-contraction level.

2.5. Co-contraction Index

The co-contraction index (CI) was calculated in normal, medium and high levels of co-contraction using the computed excitations (Eq. 2) (Falconer and Winter, 1985).

$$CI = \frac{2I_{ant}}{I_{total}} \times 100\%$$
 (2)

Where I_{ant} is the area of the total antagonist activity, e.g. GAS-TA, calculated in accord with Eq 3.

$$I_{ant} = \int_{t1}^{t2} Excitation_{TA}(t)dt + \int_{t2}^{t3} Excitation_{GAS}(t)dt$$
(3)

Where t1 to t2 denotes the period during which the excitation of TA is less than GAS and t2 to t3 denotes the period during which excitation of GAS is less than TA. I_{total} is the integral of the sum of GAS and TA during the movement, calculated according to Eq. 4

$$I_{total} = \int_{t1}^{t3} (Excitation_{ago} + Excitation_{ant})(t)dt$$
(4)

2.6. Data analysis

Three sub-phases were identified according to the role of the agonist and antagonist muscle in each subject (Table 1). Contributions from primary ankle dorsiflexors/plantarflexors (GAS, SOL, TP: tibialis posterior; PL: peroneus longus; EDL: extensor digitorum longus; EHL: extensor hallucis longus) and knee flexors/extensors (HAMS: semimembranosus,

semitendinosus and BFLH combined; BFSH: biceps femoris short head; GRC: gracilis; SART: Sartorius; VAS: vastus medialis, vastus intermedius, and vastus lateralis combined; RF: rectus femoris) to knee and ankle angular accelerations were averaged throughout each sub-phase. In the SOL-TA pair, only data from the 2nd sub-phase was presented since not all subjects had a 1st sub-phase and the number of data points in the 3rd sub-phase was not always sufficient.

3. Results

The muscle-actuated simulation tracked joint angles and resultant joint moments (normalized by body weight) with an RMS error of less than 2 degrees and 0.05 Nm/kg (Fig. 2). To test the validity of the IAA, we verified that the sum of all contributions due to muscles, gravity, and velocity-related forces (centrifugal and Coriolis forces) were in agreement with accelerations of ankle and knee joint calculated from experimental data. The simulated muscle activation showed similar on-off patterns to the observed EMGs.

3.1. Co-contraction Index

At normal co-contraction, CI was 0.28 ± 0.08 (mean \pm S.D.) and 0.31 ± 0.07 in the GAS-TA and SOL-TA pairs, respectively. At medium and high co-contraction levels, CI in the GAS-TA pair increased to 0.58 ± 0.04 and 0.79 ± 0.02 , respectively, and in the SOL-TA pair, to 0.60 ± 0.03 and 0.80 ± 0.02 , respectively.

3.2. Gastrocnemius-tibialis anterior cocontraction pair

3.2.1. The 1st subphase

The 1st subphase is characterized by TA as agonist. At the ankle joint, the net effect of knee and ankle muscles was to accelerate the ankle (stance limb) into plantarflexion (Fig. 3). Ankle plantarflexors GAS and SOL contributed the most to plantarflexion acceleration, with most assistance from knee extensor RF. Other muscles decelerated ankle plantarflexion, including TA, TP, EDL, EHL, HAMS, GRC and VAS. When GAS-TA co-contraction was increased through increased excitation of GAS, GAS contributed more to plantarflexion acceleration.

Table 1: Agonist and antagonist muscle were determined in each sub-phase. The percent of each sub-phase was averaged in 9 subjects.

		SOL-TA		
	1 st subphase	2 nd subphase	3 rd subphase	2 nd subphase
percent of gait cycle (%)	15-25	26-52	53-61	30-55
Agonist	TA	GAS	TA	SOL
Antagonist	GAS	TA	GAS	TA

GAS: gastrocnemius median; TA: tibialis anterior; SOL: soleus

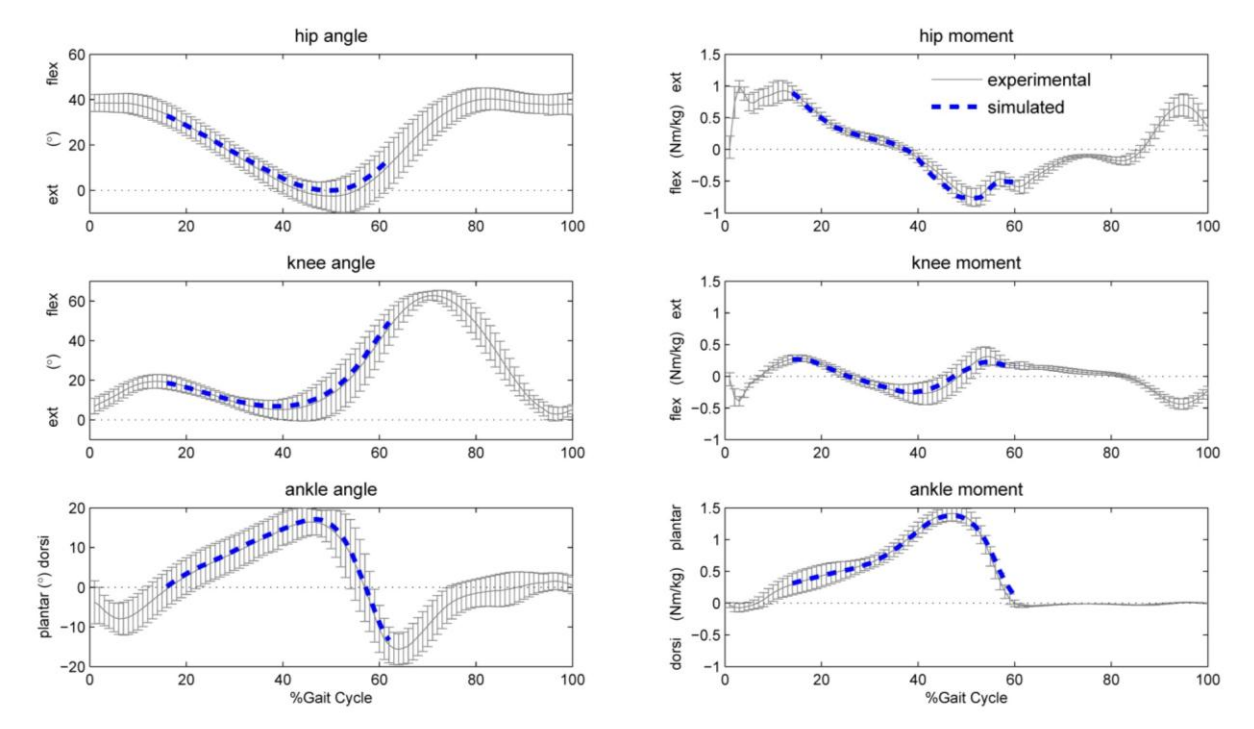


Figure 2: Comparison of simulated (blue dash line) and experimentally (black line) measured joint angles and moment. Experimental data are the 9 subjects' average± 1 S.D. for the gait cycle. Simulated data are the averaged value reproduced by simulation. The simulated joint angles and moments are only available for single-limb and pre-swing phase (15%-61% gait cycle).

The primary compensation was decreased SOL excitation, which resulted in a reduced contribution to plantarflexion acceleration. Some of the other muscles also compensated, e.g. knee extensor RF increased its excitation to contribute more to plantarflexion acceleration.

At the knee joint, the net effect of knee and ankle muscles was to accelerate the knee into extension (Fig. 4). The knee extensor VAS contributed most to the extension acceleration. Knee flexors (GAS, BFSH, GRC and SART) and ankle dorsiflexor TA decelerated knee flexion. Other muscles had very small contributions to knee flexion acceleration. When GAS -TA co-contraction was increased through increased excitation of GAS, GAS contributed

more to decelerating knee extension. The primary compensation was increased excitation of VAS, which led to a higher contribution to knee extension acceleration.

3.2.2. The 2nd subphase

The 2nd subphase is characterized by GAS as agonist. Similar to the 1st sub-phase, the net effect of knee and ankle muscles was to accelerate the ankle into plantarflexion primarily by GAS and SOL. Besides ankle dorsiflexors (TA, EDL and EHL), TP and HAMS decelerated ankle plantarflexion. Other knee muscles had very small contributions to ankle plantarflexion.

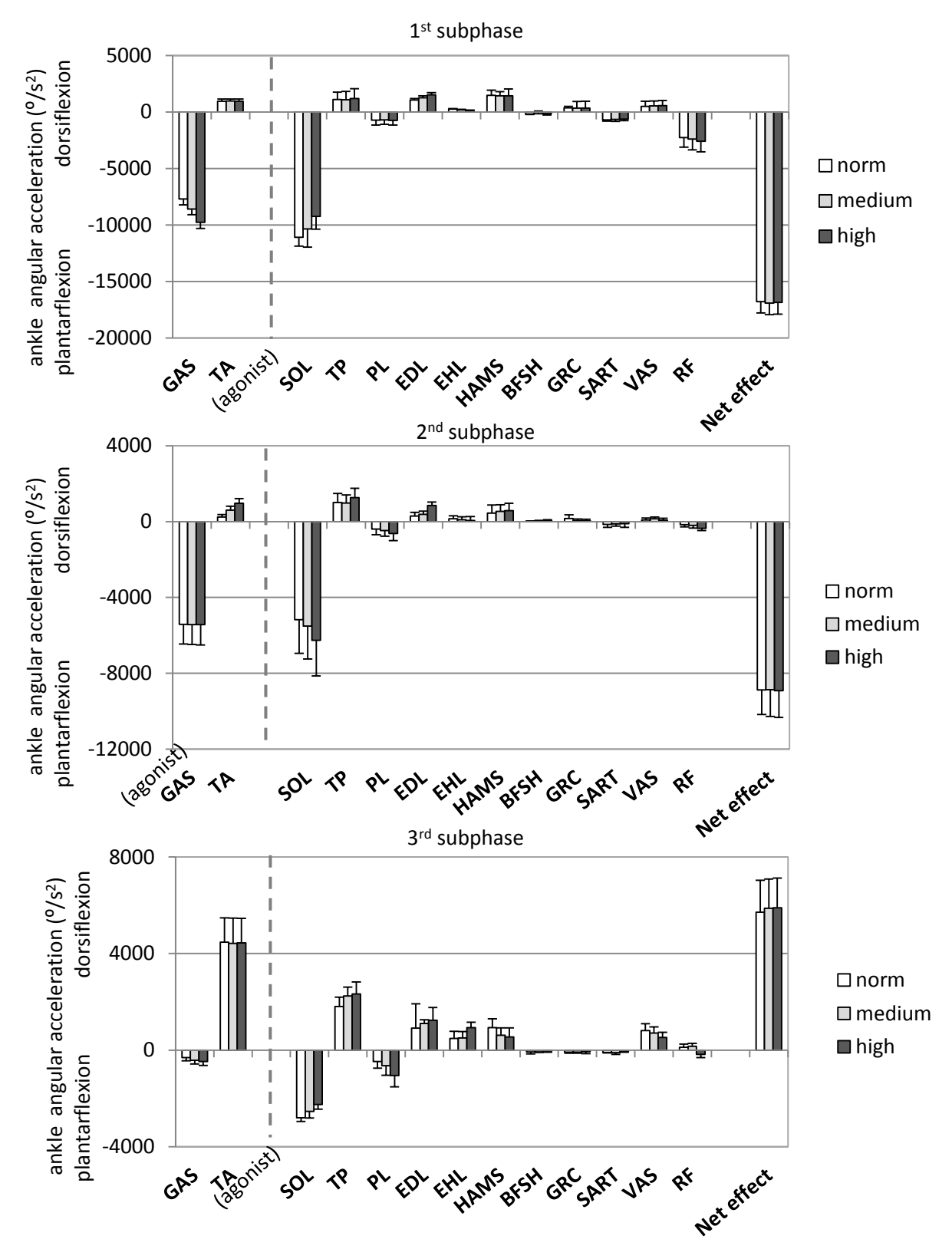


Figure 3: Contributions from primary ankle and knee muscle groups (grouped by anatomy function) to ankle dorsiflexion accelerations during $1^{\rm st}$, $2^{\rm nd}$ and $3^{\rm rd}$ sub-phases in the gastrocnemius-tibialis anterior pair. Each bar represented the mean \pm 1 S.D. of the 9 subjects in normal, medium and high co-contraction levels. The net effect is the summation from muscles' contribution (GAS: lateral gastrocnemius and medial gastrocnemius; TA: tibialis anterior; SOL: soleus; TP: tibialis posterior; PL: peroneus longus; EDL: extensor digitorum longus; EHL: extensor hallucis longus; HAMS: semimembranosus, semitendinosus and biceps femoris long head; BFSH: biceps femoris short head; GRC: gracilis; SART: sartorius; VAS: vastus medialis, vastus intermedius, and vastus lateralis; RF: rectus femoris). The excitation of agonist muscle is constrained to be the same when the excitation of the antagonist is increased.

The primary compensation was increased excitation of SOL, which led to a higher contribution to plantarflexion acceleration. Other ankle muscles also compensated, to a less extent, i.e. increased excitation of EDL and PL, which led to higher contribution to plantarflexion decelerating and acceleration respectively.

At the knee joint, the net effect of knee and ankle muscles was to accelerate the knee into extension primarily by knee extensors (VAS and RF), ankle dorsiflexor TB and ankle plantarflexor SOL. Knee flexors GAS, BFSH and SART decelerated knee extension. Other muscles had very small contributions to knee flexion. When GAS-TA co-contraction was increased through increased excitation of TA, TA contributed more to accelerate knee extension. The primary compensation was decreased extension acceleration by knee extensors, i.e. increased excitation of VAS and decreased excitation of RF, which led to the increased extension deceleration contribution decreased extension deceleration and contribution respectively. Decreased excitation of HAMs was also found, which led to the decreased extension acceleration contribution.

3.2.3. The 3rd subphase

The 3rd subphase is characterized by TA as agonist. At the ankle joint, the net effect of knee and ankle muscles was to accelerate the ankle into dorsiflexion primarily by TA. Other ankle dorsiflexors (EDL and EHL), knee flexor HAMS and knee extensor VAS also contributed to dorsiflexion acceleration. Except TP, ankle plantarflexors GAS, SOL and PL contributed to dorsiflexion deceleration. When GAS-TA cocontraction was increased through increased excitation of GAS, GAS contributed slightly more to plantarflexion deceleration. primary compensation was decreased excitation of SOL and increased excitation of TP, which led to the decreased dorsiflexion deceleration contribution increased acceleration and contribution.

At the knee joint, the net effect of knee and ankle muscles was to accelerate the knee into extension primarily by knee extensor (VAS and RF). Knee flexor (GAS, BFSH and SART) and ankle dorsiflexors (TA) contributed to knee extension deceleration. When GAS-TA co-contraction was increased through increased excitation of GAS, compensations were mostly

found in knee flexors (HAMS and SART) and extensors (VAS and RF).

3.3. Soleus-tibialis anterior co-contraction pair

The 2nd sub-phase is characterized by SOL as agonist. At the ankle joint, when SOL-TA co-contraction was increased through increased excitation of TA, TA contributed more to decelerate plantarflexion. The primary compensation was increased excitation of GAS, which led to increased plantarflexion acceleration contribution (Fig. 5).

At the knee joint, when SOL-TA cocontraction was increased through increased excitation of TA, TA contributed more to accelerate knee extension. The primary compensation was increased excitation of GAS and SART, which led to higher knee extension deceleration contribution. Knee extensors also compensated i.e. increased excitation of VAS and decreased excitation of RF, which led to increased knee extension acceleration and decreased extension acceleration contribution respectively.

4. Discussion

In this study, we created the first muscleactuated simulation to analyze muscles' compensation strategies responding to increased co-contraction from two antagonistic pairs (GAS-TA and SOL-TA), which provides insights into how individual muscles can contribute to joint angular accelerations during the single-support and pre-swing phases of gait. Results of this simulation indicate that with a y = 0.6(dorsiflexors/plantarflexor co-contraction, one can still perform normal walking through other means; the dynamic equations of motions can be fully satisfied under relatively high levels of muscle co-contraction. It is worth noting that the dynamic simulations failed to track normal joint kinematics and GRF in most of the subjects when the co-contraction ratio γ was higher than 0.6, indicating that normal walking would no longer be possible.

From a purely mechanical point of view, muscle co-contraction is an inefficient utilization of muscle forces, does not contribute to the useful work output of muscles, and requires higher metabolic costs. Nevertheless, it has been documented that antagonist muscle co-contraction occurs in nominal physiological

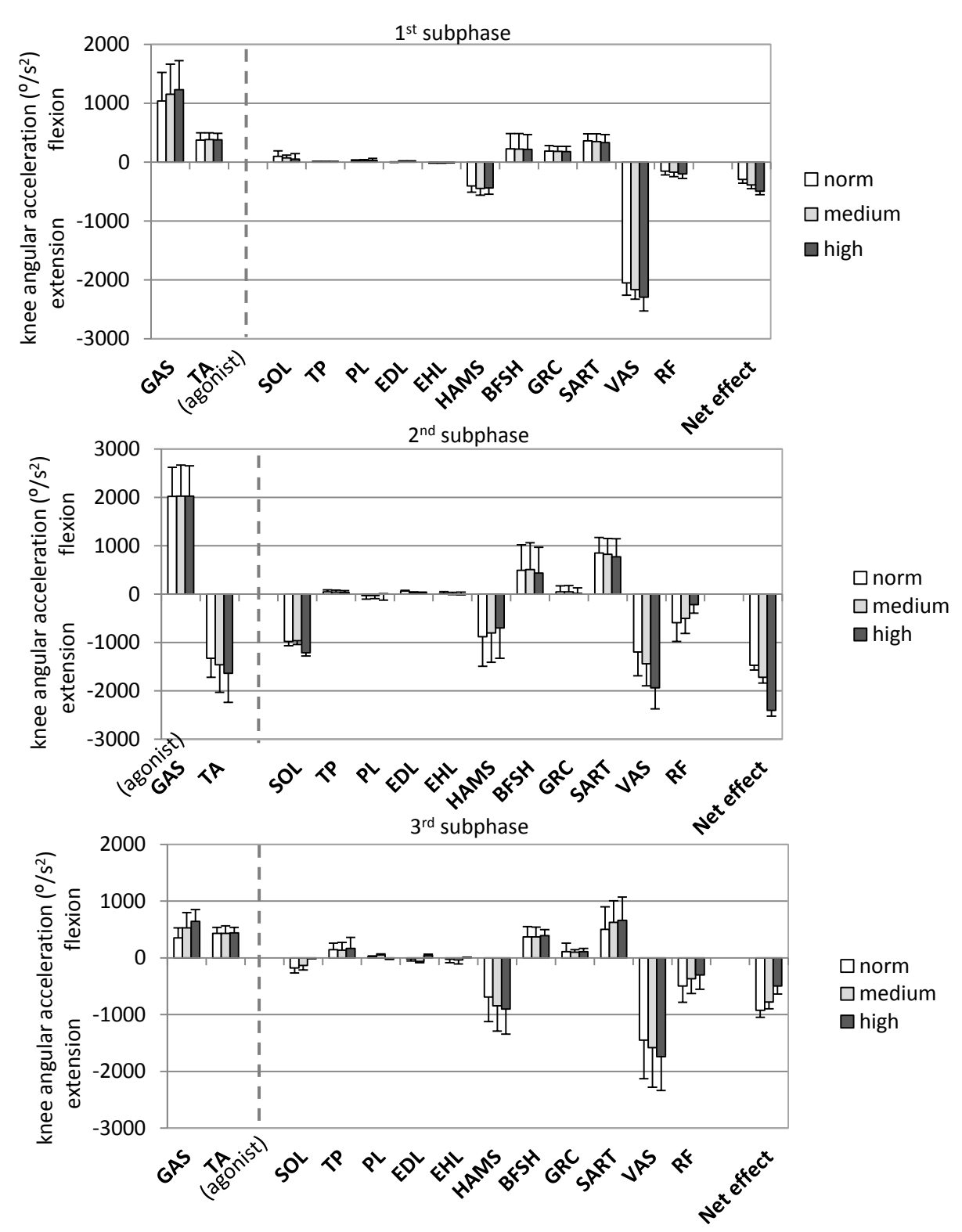


Figure 4: Contributions from primary ankle and knee muscle groups (grouped by anatomy function) to knee flexion accelerations during 1^{st} , 2^{nd} and 3^{rd} sub-phases in the gastrocnemius-tibialis anterior pair. Each bar represented the mean \pm 1 S.D. of the 9 subjects in normal, medium and high co-contraction level. The net effect is the summation from muscles' contribution (GAS: lateral gastrocnemius and medial gastrocnemius; TA: tibialis anterior; SOL: soleus; TP: tibialis posterior; PL: peroneus longus; EDL: extensor digitorum longus; EHL: extensor hallucis longus; HAMS: semimembranosus, semitendinosus and biceps femoris long head; BFSH: biceps femoris short head; GRC: gracilis; SART: sartorius; VAS: vastus medialis, vastus intermedius, and vastus lateralis; RF: rectus femoris). The excitation of agonist muscle is constrained to be the same when the excitation of the antagonist is increased.

conditions e.g. ankle plantarflexors/dorsiflexors in gait. Although we used a slightly different sub-phase definition, we found comparable CI as Falconer and Winter's in normal gait (Falconer and Winter, 1985). The highest CI was found during mid-stance, reflecting the large demands for ankle stability in body-weight support and control of shank advancement over the fixed foot. The relatively low CI in the preswing phase was consistent with the role of the plantarflexors in propulsion along the path of the progression. Stability is no longer a prime pre-requisite as the weight shifts to the contralateral limb. Significantly higher SOL-TA CI value has been observed in older adults than in young adults in gait, which indicates changes in the control of dynamic movement to cope with age-associated decline in stability (Nagai et al., 2011).

IAA has been used in previous angular to compute joint investigations and body center of mass accelerations accelerations induced by individual muscles. Our simulation showed that the GAS and SOL were primarily responsible for accelerating the ankle into plantarflexion during single-support, while TA was responsible for accelerating the ankle into dorsiflexion in pre-swing. At the knee joint, knee extensors (VAS and RF) contributed most to knee extension acceleration. Two major plantarflexors, SOL and GAS (also a knee had opposite effects flexor). on acceleration in both single-stance and pre-swing While SOL contributed to knee extension, GAS generated flexion acceleration. These findings were consistence with previous simulation studies, which have indicated that synergistic actions of muscles can vary over the joint (Steele et al., 2010; Fox and Delp, 2010; Jonkers et al., 2002). Interestingly a counterintuitive knee extension function has been reported from the HAMS. Although the HAMs are usually considered as a hip extensor and knee flexor, knee extension function was found in the support phase in running, which was interpreted as a mechanism to synchronize hip and knee extension and as related to the knee angle (Wiemann and Tidow, 1995).

Understanding how individual muscles contribute to joint accelerations can help to clarify the neurological control strategies by means of muscle excitation patterns to overcome excessive muscle co-contraction. The changes in individual muscles' contributions also depend on changes in interaction between

the neurological system and the mechanical demands of gait (Dierick et al., 2002). When increased co-contraction in the GAS-TA pair was simulated, the nearby synergistic muscles contributed most to compensation, wherein SOL the dominant contributor to plantarflexion acceleration, and VAS and RF to knee extension acceleration regardless whether GAS or TA was the antagonist muscle. Compensation could also be found in the antagonist muscle group, e.g. EDL in the 2nd subphase at ankle joint. Least alterations were noticed in remote joint muscles, with the only exception that considerable compensations can be found from SOL in the 2nd subphase at the knee joint. In the SOL-TA pair, at the ankle joint, GAS was the largest compensator. At the knee joint, larger knee extension deceleration from SART and acceleration from HAMS were noticed, which were different compared to GAS-TA pair.

Hypothetically, the net joint accelerations provided by all the muscles should be approximately constant under different cocontraction levels, since joint angles/moments remain the same in the simulations. In our study, the net acceleration of the ankle joint from ankle and knee muscles was generally unchanged increased antagonistic muscle cowhen contraction was simulated, but increased at the knee joint. This indicates that ankle and knee muscles alone are able to compensate for increased co-contraction at the ankle joint and generate sufficient ankle moment. However, at the knee joint, hip muscles must also be involved, which agrees with recent findings that hip flexors also have important contributions to knee angular acceleration (Fox and Delp, 2010). Previous simulation studies have performed analyses of compensatory mechanisms in response to some other pathological conditions. Jonkers et al. (Jonkers et al., 2003) used forward simulations and optimization to determine compensatory strategies during stance resulting from SOL and GAS exclusion. Similar to the present study, they found that SOL and GAS played an important role in compensating for one another. Goldberg and Neptune (Goldberg and Neptune, 2007) studied compensatory mechanisms necessary to overcome muscle weakness and regain normal walking by analyzing total work of individual muscles. They stated that the ankle plantarflexors SOL and GAS were able to compensate for most of the major muscle groups.

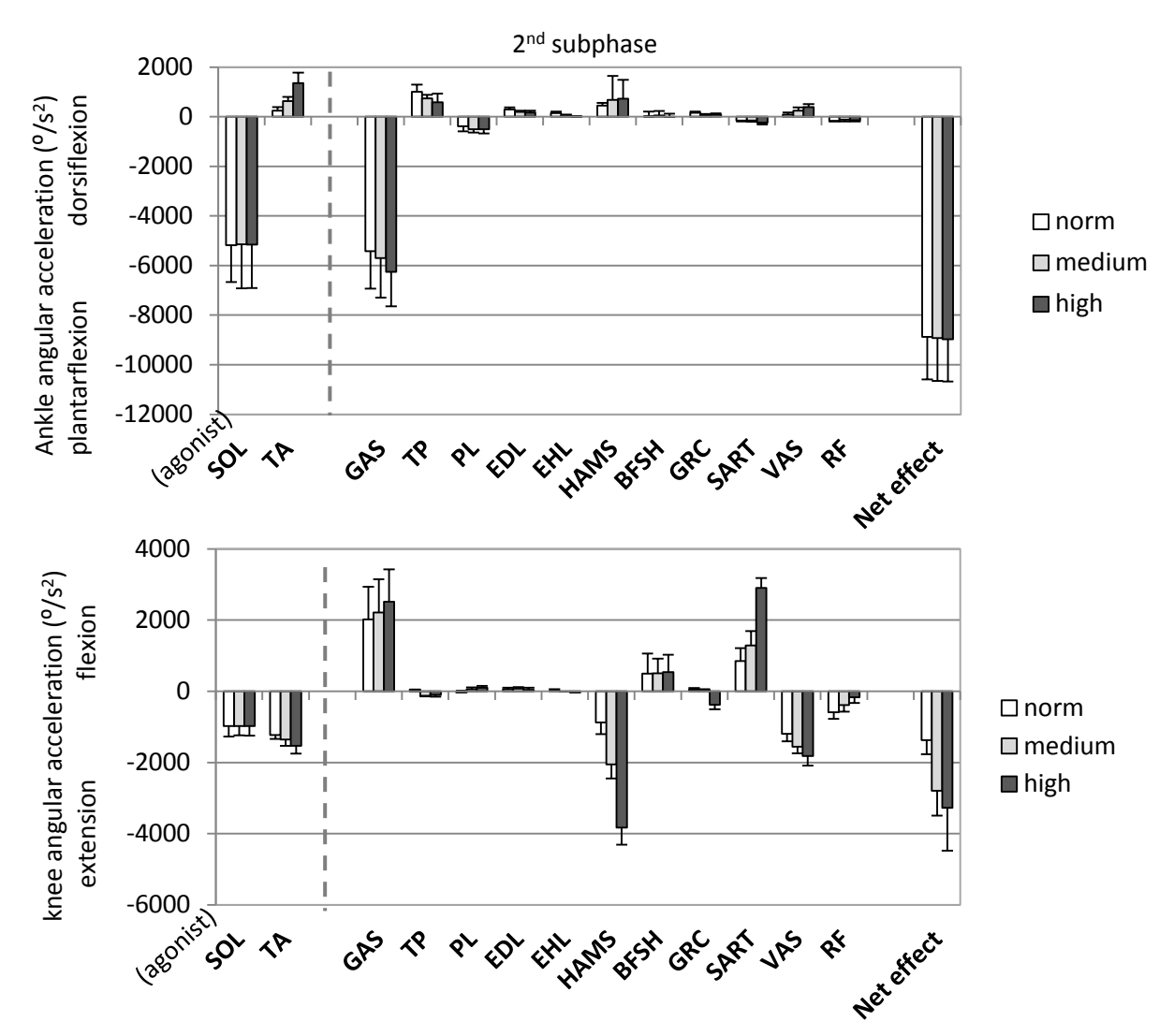


Figure 5: Contributions from primary ankle and knee muscle groups (grouped by anatomy function) to ankle dorsiflexion accelerations and knee flexion acceleration in the 2^{nd} sub-phase in the soleus-tibialis anterior pair. Each bar represented the mean \pm 1 S.D. of the 9 subjects in normal, medium and high co-contraction levels. The net effect is the summation from muscles' contribution (GAS: lateral gastrocnemius and medial gastrocnemius; TA: tibialis anterior; SOL: soleus; TP: tibialis posterior; PL: peroneus longus; EDL: extensor digitorum longus; EHL: extensor hallucis longus; HAMS: semimembranosus, semitendinosus and biceps femoris long head; BFSH: biceps femoris short head; GRC: gracilis; SART: sartorius; VAS: vastus medialis, vastus intermedius, and vastus lateralis; RF: rectus femoris). The excitation of agonist muscle is constrained to be the same when the excitation of the antagonist is increased.

In our study, comparable conclusions can be found at the ankle joint, but knee muscles were found to play important roles in compensating for increased ankle plantarflexor/dorsiflexor co-contraction.

Our results should be interpreted in light of several limitations. First, the accuracy of muscle forces estimated from dynamic simulations is a challenge. Our simulation tracked the experimental kinematics and joint moments closely. However, due to lack of maximum voluntary contractions (MVC) data from all subjects, we could not directly compare the magnitude of the EMG with the estimated activation in nominal gait. We tested

the impact of constraining activations to match the normalized EMG using available MVC and found that resulting alterations in muscle activations did not impact the conclusion of the study. Second, the co-contraction of antagonistic pairs was manipulated by a defined scheme, which probably does not always represent the excitation patterns in different co-contracted populations. The conclusions of the study can be extended to subjects with pathologies affecting motor control of gait by careful examination of muscle co-contraction patterns.

5. Conclusion

This study identified how redundancy in muscle contributions to ankle and knee angular accelerations during walking allows the nervous system to compensate for specific antagonistic muscle co-contraction. Although plantarflexors play an important role in compensation at ankle joint, compensatory mechanisms at the knee joint can mostly be provided by knee muscles. The results of this study can help to clarify how muscles can provide compensation to co-contraction at the ankle joint in patient populations with motion disorders affecting motor control of walking. It be informative also for clinical interpretation of motion analyses in persons with motion disorders, when secondary muscle co-contraction or deficits may simultaneously.

Conflict of interest statement

We declare no financial or personal relationships with other people or organisations that could influence this work.

Acknowledgments

Funding for this project was generously provided by the Swedish Research Council and Stiftelsen Promobilia. The authors would like to thank the subjects for participating and Natalia Kosterina for her help in data collection. The authors would also like to thank Dr. Ayman Habib at Stanford University for his technical support.

Reference List

- Arnold, E. M., Ward, S. R., Lieber, R. L., Delp, S. L., (2010). A model of the lower limb for analysis of human movement. Ann Bio Eng 38, 269-279.
- Crowninshield, R. D., Brand, R. A., (1981). A physiologically based criterion of muscle force prediction in locomotion. J Biomech 14, 793-801.
- Delp, S. L., Anderson, F. C., Arnold, A. S., Loan, P., Habib, A., John, C. T., Guendelman, E., Thelen, D. G., (2007). OpenSim: open-source software to create and analyze dynamic simulations of movement. IEEE T Biomed Eng 54, 1940-1950.
- Dierick, F., Domicent, C., Detrembleur, C., (2002). Relationship between antagonistic

- leg muscles co-contractions and body centre of gravity mechanics in different level gait disorders. J Electromyogr Kines 12, 59-66.
- Falconer, K., Winter, D. A., (1985). Quantitative assessment of co-contraction at the ankle joint in walking. Electromyogr Clin Neurophysiol 25, 135-149.
- Fox, M. D., Delp, S., (2010). Contributions of muscles and passive dynamics to swing initiation over a range of walking speeds. J Biomech 43, 1450-1455.
- Frost, G., Dowling, J., Dyson, K., Bar-Or, O., (1997). Cocontraction in three age groups of children during treadmill locomotion. J Electromyogr Kines 7, 179-186.
- Goldberg, E. J., Neptune, R. R., (2007). Compensatory strategies during normal walking in response to muscle weakness and increased hip joint stiffness. Gait Posture 25, 360-367.
- Grasso, R., Zago, M., Lacquaniti, F., (2000). Interactions between posture and locomotion: motor patterns in humans walking with bent posture versus erect posture. J Neurophysiol 83, 288-300.
- Hamner, S. R., Seth, A., Delp, S. L., (2010). Muscle contributions to propulsion and support during running. J Biomech 43, 2709-2716.
- Hogan, N., (1984). Adaptive control of mechanical impedance by coactivation of antagonist muscles. IEEE T Automat Contr 29, 681-690.
- Hortobagyi, T., DeVita, P., (2000). Muscle pre-and coactivity during downward stepping are associated with leg stiffness in aging. J Electrom Kinesio 10, 117-126.
- Hortobaígyi, T., Westerkamp, L., Beam, S., Moody, J., Garry, J., Holbert, D., DeVita, P., (2005). Altered hamstring-quadriceps muscle balance in patients with knee osteoarthritis. Clin Biomech 20, 97-104.
- Hubley-Kozey, C. L., Hill, N. A., Rutherford, D. J., Dunbar, M. J., Stanish, W. D., (2009). Co-activation differences in lower limb muscles between asymptomatic controls and those with varying degrees of knee osteoarthritis during walking. Clin Biomech 24, 407-414.
- Jonkers, I., Spaepen, A., Papaioannou, G., Stewart, C., (2002). An EMG-based, muscle driven forward simulation of

- single support phase of gait. J Biomech 35, 609-619.
- Jonkers, I., Stewart, C., Spaepen, A., (2003). The study of muscle action during single support and swing phase of gait: clinical relevance of forward simulation techniques. Gait Posture 17, 97-105.
- Lamontagne, A., Malouin, F., Richards, C. L., Dumas, F., (2002). Mechanisms of disturbed motor control in ankle weakness during gait after stroke. Gait Posture 15, 244-255.
- Nagai, K., Yamada, M., Uemura, K., Yamada, Y., Ichihashi, N., Tsuboyama, T., (2011). Differences in muscle coactivation during postural control between healthy older and young adults. Arch.Gerontol.Geriatr. 53, 338-343.
- Sasaki, K., Neptune, R. R., Burnfield, J. M., Mulroy, S. J., (2008). Muscle compensatory mechanisms during ablebodied toe walking. Gait Posture 27, 440-446.
- Sharma, L., (2001). Local factors in osteoarthritis. Curr Opin Rheumatol 13, 441-446.
- Stebbins, J., Harrington, M., Thompson, N., Zavatsky, A., Theologis, T., (2006). Repeatability of a model for measuring multi-segment foot kinematics in children. Gait Posture 23, 399-400.
- Steele, K. M., Seth, A., Hicks, J. L., Schwartz, M. S., Delp, S. L., (2010). Muscle contributions to support and progression during single-limb stance in crouch gait. J Biomech 43, 2099-2105.
- Thelen, D. G., Anderson, F. C., (2006). Using computed muscle control to generate forward dynamic simulations of human walking from experimental data. J Biomech 39, 1107-1115.
- Wang, R. L., Gutierrez-Farewik, E. M., (2011). The effect of subtalar inversion/eversion on the dynamic function of the tibialis anterior, soleus, and gastrocnemius during the stance phase of gait. Gait Posture 34, 29-35.
- Wiemann, K., Tidow, G., (1995). Relative activity of hip and knee extensors in sprinting-implications for training. New Stud Athlet 10, 29-49.
- Winter, D. A., (1990). Biomechanics and Motor Control of Human Movement. John Wiley & Sons, Inc., New Jersy.

- Zajac, F. E., Gordon, M. E., (1989). Determining muscle's force and action in multi-articular movement. Exercise Sport Sci Rev 187-230.
- Zajac, F. E., Neptune, R. R., Kautz, S. A., (2002). Biomechanics and muscle coordination of human walking. Part I: introduction to concepts, power transfer, dynamics and simulations. Gait Posture 16, 215-232.